

CausalCompass: Evaluating the Robustness of Time-Series Causal Discovery in Misspecified Scenarios

Huiyang Yi
Southeast University
Nanjing, China
yihuiyang@seu.edu.cn

Duxin Chen*
Southeast University
Nanjing, China
chendx@seu.edu.cn

Xiaojian Shen
Jilin University
Changchun, China
shenxj22@mails.jlu.edu.cn

He Wang
Southeast University
Nanjing, China
wanghe91@seu.edu.cn

Yonggang Wu
Southeast University
Nanjing, China
wuyg@seu.edu.cn

Wenwu Yu
Southeast University
Nanjing, China
wwyu@seu.edu.cn

Abstract

Causal discovery from time series is a fundamental task in machine learning. However, its widespread adoption is hindered by a reliance on untestable causal assumptions and by the lack of robustness-oriented evaluation in existing benchmarks. To address these challenges, we propose CausalCompass, a flexible and extensible benchmark suite designed to assess the robustness of time-series causal discovery (TSCD) methods under violations of modeling assumptions. To demonstrate the practical utility of CausalCompass, we conduct extensive benchmarking of representative TSCD algorithms across eight assumption-violation scenarios. Our experimental results indicate that no single method consistently attains optimal performance across all settings. Nevertheless, the methods exhibiting superior overall performance across diverse scenarios are almost invariably deep learning-based approaches. We further provide hyperparameter sensitivity analyses to deepen the understanding of these findings. We also find, somewhat surprisingly, that NTS-NOTEARS relies heavily on standardized preprocessing in practice, performing poorly in the vanilla setting but exhibiting strong performance after standardization. Finally, our work aims to provide a comprehensive and systematic evaluation of TSCD methods under assumption violations, thereby facilitating their broader adoption in real-world applications. The code and datasets are available at <https://github.com/huiyang-yi/CausalCompass>.

CCS Concepts

- Mathematics of computing → Causal networks; Time series analysis; • General and reference → Evaluation.

*Corresponding author.

Permission to make digital or hard copies of all or part of this work for personal or classroom use is granted without fee provided that copies are not made or distributed for profit or commercial advantage and that copies bear this notice and the full citation on the first page. Copyrights for components of this work owned by others than the author(s) must be honored. Abstracting with credit is permitted. To copy otherwise, or republish, to post on servers or to redistribute to lists, requires prior specific permission and/or a fee. Request permissions from permissions@acm.org.

Conference'17, Washington, DC, USA

© 2026 Copyright held by the owner/author(s). Publication rights licensed to ACM. ACM ISBN 978-x-xxxx-xxxx-x/YYYY/MM
<https://doi.org/10.1145/nnnnnnnn.nnnnnnn>

Keywords

Time-Series Causal Discovery, Benchmark, Assumption Violations, Robustness

ACM Reference Format:

Huiyang Yi, Xiaojian Shen, Yonggang Wu, Duxin Chen, He Wang, and Wenwu Yu. 2026. CausalCompass: Evaluating the Robustness of Time-Series Causal Discovery in Misspecified Scenarios. In . ACM, New York, NY, USA, 58 pages. <https://doi.org/10.1145/nnnnnnnn.nnnnnnn>

1 Introduction

Many scientific applications of time-series analysis rely on understanding the underlying causal relationships [55]. Owing to cost, risk, and ethical constraints, randomized controlled trials are frequently infeasible. Consequently, inferring causal relationships directly from purely observational time-series data, known as time-series causal discovery (TSCD), plays a critical role in addressing causal questions concerning intervention and counterfactual [48–50, 62].

TSCD primarily encompasses constraint-based, noise-based, score-based, topology-based, Granger causality-based, and deep learning-based approaches, all of which typically rest on untestable causal assumptions [27, 50]. Constraint-based methods (e.g., PCMCi [56]) recover causal graphs via conditional independence tests under the faithfulness assumption. Noise-based methods (e.g., VARLiNGAM [34]) impose specific assumptions on functional forms and noise distributions in structural equation models, exploiting asymmetries between causal and anticausal directions to identify causal structure. Score-based methods (e.g., DYNOTEARs [47]) infer causal relationships by defining a scoring function to evaluate and rank candidate causal graphs. Topology-based methods (e.g., CCM [64] and TSCI [6]) leverage Takens' state-space reconstruction theory [66] to infer causality. Granger causality (GC)-based methods (e.g., LGC [3]) identify causal relationships by testing whether one time series improves the prediction of another, with classical GC being limited to linear settings [28]. Recently, given that the core principle of GC is highly compatible with neural networks (NNs), deep learning-based methods (e.g., cMLP [67] and cLSTM [67]) have been proposed, leveraging the expressive capacity of deep NNs for nonlinear Granger causal discovery [13].

Beyond the various assumptions of the aforementioned methods, causal sufficiency and no measurement error assumptions are also commonly required [50, 80]. In practice, real-world data rarely

satisfy all such assumptions, and these assumptions are inherently difficult to test effectively, thereby constraining the application of TSCD in practical scenarios [50]. Although certain studies have acknowledged the complexity of real-world data and developed causal discovery algorithms tailored to nonstationarity [1, 22, 24, 30, 32, 41, 57, 81], latent confounders [7, 14, 19, 25, 31, 40, 44, 72], mixed data [8, 10, 16, 36, 52, 68, 71, 78], measurement error [17, 37, 73, 74, 79, 80], and missing data [12, 13, 21, 23, 33, 69, 70, 76, 77], when algorithms are applied to real-world data, the true data-generating mechanisms remain unknown, rendering these purpose-built algorithms still inadequately applicable. Consequently, the robustness of TSCD algorithms under violations of model assumptions is of paramount importance.

Prior research [38] argued that the widespread application of causal models required a paradigm shift from scientific perfectionism toward scientific pragmatism, prioritizing practical utility. Building on this perspective, the work [51] further identified the key obstacle to transforming the research community's mindset lay in the lack of robustness assessment in current evaluation frameworks, noting that evaluations on datasets strictly adhering to all requisite assumptions severely overestimated method reliability, and underscoring that robustness evaluation was essential for the widespread adoption of causal models. Those studies [43] and [75] benchmarked causal discovery algorithms in i.i.d. settings under violations of model assumptions, yet did not consider the ubiquitous time-series data in real-world applications and related TSCD works. Those works [26] and [27] respectively reviewed progress in causal discovery for i.i.d. and time-series settings, but lacked experimental support. Prior work [20] benchmarked only constraint-based methods among TSCD approaches, with benchmark datasets relying solely on a limited number of manually specified structural equation models, offering no flexible parameter configurations and considering only a restricted range of assumption-violation scenarios. Recent work [2] benchmarked TSCD methods under varying degrees of assumption violations. However, the vanilla data considered only linear settings, precluding a fair evaluation of nonlinear methods, and it also neglected representative topology-based and deep learning-based approaches.

Our study conducts an extensive empirical evaluation of both classical and cutting-edge TSCD methods under violations of modeling assumptions. The vanilla data considered encompass both linear and nonlinear settings, ensuring a fair comparison across different approaches. We evaluate representative constraint-based, noise-based, score-based, topology-based, Granger causality-based, and deep learning-based methods, covering the broadest range of method categories considered in the existing literature and enabling a comprehensive assessment of TSCD. Notably, our work fills a critical gap in the literature by providing the first systematic evaluation of deep learning-based methods under diverse misspecified scenarios. Given their practical potential, assessing the robustness of deep learning-based approaches is of particular importance. Our contributions are summarized as follows:

- We conduct large-scale experiments on six major categories of mainstream TSCD algorithms across eight substantially different scenarios involving violations of modeling assumptions. In total,

our evaluation comprises over 110,000 experimental runs across eleven distinct TSCD algorithms.

- Our results reveal that, overall, the best-performing methods across diverse scenarios are almost invariably deep learning-based approaches. We further provide hyperparameter sensitivity analyses to deepen the understanding of method performance. In addition, we find that NTS-NOTEARS is highly sensitive to standardized preprocessing in practice. Given the robustness exhibited by deep learning-based methods under misspecified settings, conducting more in-depth investigations into these approaches holds significant value.
- We introduce the CausalCompass benchmark suite, which supports both linear and nonlinear vanilla models and encompasses eight misspecified scenarios, including mixed data, nonstationarity, standardization, trends and seasonality, latent confounders, min–max normalization, measurement error, and missing data. The benchmark offers flexible parameter configurations and strong extensibility. Through this contribution, we aim to advance the understanding of the performance limits of TSCD algorithms, foster the development of more robust TSCD methods, and ultimately promote the broader adoption of TSCD in practice.

2 Preliminaries

Consider a D -dimensional time series denoted by $\mathbf{X} = \{\mathbf{x}_{1:T,i}\}_{i=1}^D$, where each sample vector $\mathbf{x}_t = (x_{t,1}, x_{t,2}, \dots, x_{t,D})^\top$ corresponds to the observations of D variables at time index $t \in \{1, \dots, T\}$. Assume that the causal dependencies among these variables follow a structural causal model \mathcal{M} [48] of the form:

$$x_{t,i} = f_i(Pa(x_{t,i}), u_{t,i}), \quad \forall i = 1, \dots, D, \quad (1)$$

where $Pa(x_{t,i})$ denote the parents of $x_{t,i}$, $f_i : \mathbb{R}^{|Pa(x_{t,i})|+1} \rightarrow \mathbb{R}$ is the causal structure function, and $u_{t,i}$ represents the independent noise variable.

The task of TSCD is to recover the underlying temporal dependency structure among variables [50]. In general, two types of causal graphs can be inferred: the summary causal graph \mathcal{G}_{SCG} and the window causal graph \mathcal{G}_{WCG} [27].

For the summary causal graph, each vertex corresponds to one temporal variable. Formally, the vertex set is $\{X_1, \dots, X_D\}$, where $X_i = \{x_{t,i}\}_{t=1}^T$ denotes the temporal process of the i -th variable. An edge $X_p \rightarrow X_q$ is included in \mathcal{G}_{SCG} if and only if there exists at least one time index t and a lag τ such that $x_{t-\tau,p}$ has a causal influence on $x_{t,q}$, where $\tau \geq 0$ is allowed for $p \neq q$ and $\tau > 0$ is required for $p = q$ [4].

For the window causal graph, we consider a fixed temporal window of size τ_{max} . The vertex set contains all variable-time instances within this window, that is, $\{x_{t,i}, x_{t+1,i}, \dots, x_{t+\tau_{max},i}\}$ for each variable $i \in \{1, \dots, D\}$. A directed edge $x_{t-l,p} \rightarrow x_{t,q}$ is present in \mathcal{G}_{WCG} if and only if $x_{t-l,p}$ has a causal influence on $x_{t,q}$, where $0 \leq l \leq \tau_{max}$ is allowed for $p \neq q$ and $0 < l \leq \tau_{max}$ is required for $p = q$ [4].

Table 1: Summary of the assumptions associated with each algorithm and the types of causal graphs they are designed to recover. Each cell indicates whether an algorithm explicitly supports (✓) or does not support (✗) the specific condition listed in the corresponding row. “Summary” and “window” refer to the summary causal graph and the window causal graph, respectively. The table format is adapted from [43].

	VAR	LCC	VARLINGAM	PCMCI	DYNOTEARS	NTS-NOTEARS	TSCI	cMLP	cLSTM	CUTS	CUTS*
Gaussian noise	✓	✓	✗	✓	✓	✓	✗	✓	✓	✓	✓
Linear mechanisms	✓	✓	✓	✓	✓	✗	✗	✗	✗	✗	✗
Nonlinear mechanisms	✗	✗	✗	✓	✗	✓	✓	✓	✓	✓	✓
Latent confounders	✗	✗	✗	✗	✗	✗	✗	✗	✗	✗	✗
Measurement error	✗	✗	✗	✗	✗	✗	✗	✗	✗	✗	✗
Nonstationary effects	✗	✗	✗	✗	✗	✗	✗	✗	✗	✗	✗
Missing mechanisms	✗	✗	✗	✗	✗	✗	✗	✗	✓	✓	✓
Mixed data effects	✗	✗	✗	✗	✗	✗	✗	✗	✗	✗	✗
Z-score standardization	✗	✗	✗	✗	✗	✗	✗	✗	✗	✗	✗
Min-max normalization	✗	✗	✗	✗	✗	✗	✗	✗	✗	✗	✗
Trend and seasonality	✗	✗	✗	✗	✗	✗	✗	✗	✗	✗	✗
Output	Summary	Summary	Window	Window	Window	Window	Summary	Window	Summary	Window	Window

3 Experimental Design

In this section, we introduce the vanilla model, the assumption-violation scenarios, the evaluated causal discovery methods, the algorithm hyperparameters, and the evaluation metrics.

3.1 Vanilla Model

Most causal discovery methods rely on unverifiable assumptions, and this work examines their performance under assumption violations. We therefore begin by introducing the vanilla models for both linear and nonlinear settings, followed by the various assumption-violation scenarios.

Linear vanilla model. In linear settings, we consider a vector autoregressive (VAR) model, following the settings of [67]:

$$\mathbf{x}_t = \sum_{l=1}^{\tau_{\max}} \mathbf{A}_l \mathbf{x}_{t-l} + \mathbf{u}_t, \quad (2)$$

where \mathbf{A}_l denotes the sparse coefficient matrix for time lag l , τ_{\max} is the maximum lag, and $\mathbf{u}_t = (u_{t,1}, u_{t,2}, \dots, u_{t,D})^\top$ is a jointly independent zero-mean Gaussian noise vector with covariance matrix $\Omega = \text{cov}(\mathbf{u}_t) = \text{diag}(\sigma_1^2, \dots, \sigma_D^2)$. We refer to this setting as the linear vanilla model, since it aligns with the assumptions adopted by the majority of linear benchmark methods (see Table 1).

Nonlinear vanilla model. In nonlinear settings, we consider the Lorenz-96 model, following the settings of [67]:

$$\frac{\partial \mathbf{x}_{t,i}}{\partial t} = -\mathbf{x}_{t,i-1} (\mathbf{x}_{t,i-2} - \mathbf{x}_{t,i+1}) - \mathbf{x}_{t,i} + F, \quad 1 \leq i \leq D \quad (3)$$

where $\mathbf{x}_{t,0} = \mathbf{x}_{t,D}$, $\mathbf{x}_{t,-1} = \mathbf{x}_{t,D-1}$, $\mathbf{x}_{t,D+1} = \mathbf{x}_{t,1}$, and F denotes the magnitude of the external forcing (a larger F corresponds to a more chaotic system [35]). We refer to this setting as the nonlinear vanilla model, since it aligns with the assumptions adopted by the majority of nonlinear benchmark methods (see Table 1).

To eliminate the potential influence of Gaussian noise in the vanilla model on the experimental results, we also consider the vanilla model with non-Gaussian noise (see Appendix H).

3.2 Model Assumption Violation Scenarios

We define eight distinct assumption-violation scenarios, each of which can be applied to both the linear vanilla and nonlinear vanilla model to generate datasets that exhibit specific assumption violations.

Measurement error model. Causal discovery algorithms commonly assume that variables are observed without measurement error [17, 58, 80]. However, measurement noise is almost inevitable during real-world data acquisition. To account for this effect, we define the observation mechanism as

$$\hat{X}_i = X_i + \epsilon_i, \quad \forall i = 1, \dots, D, \quad (4)$$

where $X_i = \{x_{t,i}\}_{t=1}^T$ is generated from the linear vanilla model (2) or nonlinear vanilla model (3). ϵ_i denotes a zero-mean Gaussian noise term independent of X_i , with variance given by $\text{Var}(\epsilon_i) = \alpha \cdot \text{Var}(X_i)$ for $\alpha \in \{0.4, 0.6, 0.8, 1.0, 1.2\}$.

Nonstationary model. Most TSCD methods typically rest on the assumption of stationarity, namely that the underlying structural causal model remains invariant over time [1, 24, 32]. However, real-world data often exhibit pronounced nonstationary behavior. Following the setting in [32], the form of nonstationarity we consider refers to scenarios in which the underlying causal generative process remains fixed, while the variance of the noise terms evolves smoothly over time. The observed data are generated as:

$$x_{t,i}^{\text{NS}} = f_i(Pa(x_{t,i})) + \omega_{t,i} u_{t,i}, \quad \forall i = 1, \dots, D, \quad (5)$$

where $f_i(\cdot)$ represents the deterministic causal mechanism for variable i (either the VAR dynamics in (2) or the Lorenz-96 dynamics in (3)), $u_{t,i} \sim \mathcal{N}(0, \sigma_i^2)$ is the base-level independent noise, and $\omega_{t,i}$ is the time-varying scaling parameter generated by sampling from a Gaussian process. Specifically, we sample $\log \omega_i = (\log \omega_{1,i}, \dots, \log \omega_{T,i})^\top \sim \mathcal{GP}(m \cdot \mathbf{1}_T, v^2 K(\mathbf{t}, \mathbf{t}))$, where $\mathbf{1}_T$ denotes a T -dimensional vector of ones, m controls the average log-scale noise level, v controls the magnitude of variance fluctuations, and $K(\mathbf{t}, \mathbf{t}) \in \mathbb{R}^{T \times T}$ is the covariance matrix with entries

$$(K)_{ij} = \exp\left(-\frac{(t_i - t_j)^2}{2\ell^2}\right), \quad (6)$$

where ℓ is the kernel width. The actual scaling parameter is computed as $\omega_{t,i} = \exp(\log \omega_{t,i})$ to ensure positivity. In Appendix F, we additionally investigate a nonstationary setting where the coefficients of the linear vanilla model are allowed to vary over time.

Latent confounders model. The causal sufficiency assumption ensures that no unobserved confounders exist between any pair of observed variables [50]. However, in real-world applications, it is often impossible to guarantee that all relevant factors have been measured [43]. Let $\mathbf{L} = \{L_i\}_{i=1}^D$ denote a collection of latent confounding variables. For each pair of observed nodes, we sample a Bernoulli random variable $C \sim \text{Bernoulli}(\zeta)$. Whenever $C = 1$, a variable from \mathbf{L} is randomly selected to serve as a latent common cause. In the linear setting, we introduce cross-lag confounders [40], where the latent confounders \mathbf{L} follow a VAR process. In the non-linear setting, we introduce contemporaneous confounders [40], where \mathbf{L} evolves according to the Lorenz-96 mechanism. The parameter $\zeta \in \{0.1, 0.3, 0.5, 0.7, 0.9\}$ controls the number of confounding links present in the causal graph.

Z-score standardization model. The work [53] observed that in i.i.d. causal discovery settings, methods based on continuous optimization, such as NOTEARS [82] and GOLEM [45], exhibit a substantial performance drop when applied to standardized data. This behavior is attributed to the fact that these methods exploit high variance-sortability in the data, which is removed by standardization [53]. As argued in [53], standardization can therefore serve as a diagnostic tool to assess whether such methods genuinely recover causal structure, rather than relying on variance-sortability shortcuts. In i.i.d. data, standardization is typically performed across samples, whereas in time-series data it is applied across the temporal dimension, and these two procedures are inherently different [24]. Consequently, the conclusions of [53] cannot be directly extrapolated to time-series data. To date, no studies have explicitly pointed out how standardization influences TSCD, even though many TSCD methods (NTS-NOTEARS [65], CUTS [13], CUTS+ [12]) in practice directly adopt standardized data and report only the results under such preprocessing. This gap highlights the importance of understanding the role of standardization in TSCD. The data-generation mechanism considered is:

$$\overline{X}_i = \frac{X_i - \mathbb{E}[X_i]}{\sqrt{\text{Var}(X_i)}}, \quad \forall i = 1, \dots, D, \quad (7)$$

where $\mathbb{E}[X_i]$ and $\text{Var}(X_i)$ are the mean and variance of X_i , respectively. The standardized data are used as the algorithm inputs, while the ground-truth causal graph remains identical to that of the original vanilla data.

Mixed data model. Most causal discovery methods assume that time-series data consist solely of continuous-valued variables [10]. However, in many real-world scenarios, the collected data typically contain both discrete and continuous variables, a setting commonly referred to as mixed data [10, 16, 36, 68, 71, 78]. Thus, ensuring that algorithms maintain robustness in the presence of mixed data is of considerable importance. We follow the procedure in [10] to generate mixed data by applying min–max normalization to the continuous-valued data produced by (2) and (3), thereby mapping them into the range $[0, 1]$ as $\tilde{X}_i = \min\text{-}\max(X_i)$. We then randomly select $D \times \beta$ variables for discretization, where $\beta \in \{0.1, 0.3, 0.5, 0.7, 0.9\}$. The discrete variables are generated as

follows:

$$x_{t,i}^{\text{DV}} = \begin{cases} 1 & \text{if } \tilde{x}_{t,i} > 0.5 \\ 0 & \text{if } \tilde{x}_{t,i} \leq 0.5 \end{cases} \quad (8)$$

Here, $x_{t,i}^{\text{DV}}$ denotes the value of the i -th variable at time t after discretization.

Min–max normalization model. In TSCD, it remains unclear which normalization strategy is appropriate [24]. Nevertheless, the existing work [10] adopts min–max normalization when generating mixed data, which motivates the need to evaluate the robustness of causal discovery methods under normalization settings. In this work, the data-generation mechanism we consider is:

$$\tilde{X}_i = \frac{X_i - \min(X_i)}{\max(X_i) - \min(X_i)}, \quad \forall i = 1, \dots, D, \quad (9)$$

where \tilde{X}_i denotes the normalized temporal process of the i -th variable.

Missing model. Missing data are pervasive in real-world time-series applications, and performing causal inference directly in the presence of such gaps can lead to substantial estimation errors [12, 13, 33, 54]. It is therefore crucial that causal discovery algorithms be capable of handling incomplete observations. In this work, we adopt the Missing Completely At Random (MCAR) mechanism [69], where each entry is independently removed according to a Bernoulli distribution with probability $\gamma \in \{0.1, 0.2, 0.3, 0.4, 0.5\}$. Since most benchmark methods considered in our study cannot operate directly on datasets containing missing values, we impute the missing entries using zero-order hold interpolation [12, 13] before applying causal discovery.

Trend and seasonality model. Real-world time series frequently exhibit deterministic trends and periodic seasonal fluctuations [9, 15]. Following the setup in [20], we augment the vanilla data-generating process by adding a trend component together with a seasonal component. The observed process is defined as:

$$x_{t,i}^{\text{TS}} = x_{t,i} + \text{trend}_{t,i} + \text{season}_{t,i}, \quad 1 \leq i \leq D, \quad (10)$$

where $x_{t,i}$ denotes the value generated by the linear vanilla model (2) or nonlinear vanilla model (3). The trend component introduces a variable-specific linear drift:

$$\text{trend}_{t,i} = \frac{\rho t i}{2}, \quad (11)$$

where ρ controls the strength of the trend. The seasonal component incorporates two harmonics with variable-specific phase shifts:

$$\text{season}_{t,i} = \eta \sin\left(\frac{2\pi t}{P} + \phi_i\right) + \frac{\eta}{2} \cos\left(\frac{4\pi t}{P} + \phi_i\right), \quad (12)$$

where P denotes the seasonal period, η specifies the overall seasonal magnitude, and $\phi_i = \frac{2\pi i}{D}$ induces distinct phase shifts across variables.

3.3 Data Generation

We generate datasets for each scenario using the number of nodes $D \in \{10, 15\}$, time-series lengths $T \in \{500, 1000\}$, and forcing constants $F \in \{10, 40\}$. For each experimental configuration and modeling setting, we further sample data under 5 different random seeds to ensure statistical reliability.

3.4 Methods

We evaluate 11 well-established TSCD algorithms, covering Granger causality-based (VAR [4], LGC [3]), constraint-based (PCMCI [56]), noise-based (VARLINGAM [34]), score-based (DYNOTEAR [47], NTS-NOTEARS [65]), topology-based (TSCI [6]), and deep learning-based (cMLP [67], cLSTM [67], CUTS [13], CUTS+ [12]) approaches. To the best of our knowledge, the breadth of benchmark methods considered in this study constitutes one of the most comprehensive collections of methods in current robustness benchmarking research [20]. For a more detailed introduction to the various methods, see the Appendix A.

3.5 Hyperparameter Settings

In practice, the underlying causal structure of real-world datasets is typically unknown, making it difficult to determine optimal hyperparameters for different algorithms. To ensure a fair comparison, we follow the default or recommended hyperparameter configurations provided in the official implementations of each method, and conduct an exhaustive hyperparameter search to obtain the best performance [4, 6, 10, 12, 13, 56, 65, 67]. A detailed description of the hyperparameter search ranges is provided in Appendix C.

3.6 Evaluation Metrics

Following the settings in [10, 29, 42], we evaluate performance using areas under receiver operating characteristic (AUROC [5]) and precision-recall (AUPRC [18]) curves. Consistent with prior studies [42, 63], our evaluation considers only the off-diagonal entries of the adjacency matrix, excluding self-causal links that are typically the easiest to infer. We report results under the configuration achieving the best AUPRC. Higher AUROC and AUPRC values indicate more accurate recovery of the target causal graph.

4 Critical Experimental Results and Insights

In this section, we first present the experimental results under model assumption violations introduced in Section 3.2 and draw conclusions by comparing them with the results obtained in the vanilla scenario. We further provide sensitivity analyses of various methods with respect to hyperparameters (Section 4.2) to ensure a comprehensive understanding of their performance characteristics. Due to space constraints, the main text primarily discusses the linear 10-node case with $T = 1000$ and the nonlinear 10-node case with $T = 1000$ and $F = 10$ (Table 2.1, 2.2, 3.1, 3.2), while similar conclusions hold for different numbers of nodes, time series lengths, and external forcing intensities (see Appendix I and L). For a concise and intuitive presentation of the results, Figure 1 summarizes the outcomes for these two settings. For each scenario, we generate datasets using 5 different random seeds and report the mean and standard deviation of evaluation metrics across these 5 trials. To ensure fair comparison among methods, we determine each method's hyperparameters as optimal values relative to the specific dataset. Recognizing that optimal hyperparameters are typically unknown in practical applications [39], we additionally select for each causal discovery method a single hyperparameter configuration that maximizes average performance across all scenarios (see Appendix J and M). Since the principal conclusions drawn from these two hyperparameter selection strategies are essentially identical, we

discuss only the results obtained under optimal hyperparameters in the main text.

4.1 Current Methods' Performance in Misspecified Scenarios

Our experiments demonstrate that no single method achieves optimal performance across all scenarios, yet the methods exhibiting superior performance overall across various scenarios are almost invariably deep learning-based approaches. In this work, robustness refers to a model's ability to perform well under violations of modeling assumptions, consistent with the interpretations in [43] and [75].

Latent confounders, measurement error, missing, mixed data, and nonstationary models. Figure 1 shows that under confounded ($\zeta = 0.5$), measurement error ($\alpha = 1.2$), mixed data ($\beta = 0.5$), missing ($\gamma = 0.4$), and nonstationary scenarios (linear: $m = 1, v = 1$; nonlinear with $F = 10$: $m = 2.5, v = 2.0$; nonlinear with $F = 40$: $m = 3.5, v = 2.0$), the best-performing methods are predominantly deep learning-based approaches. The severity of model assumption violations can be flexibly controlled through the corresponding parameters. In the main text, we report results under a representative parameter setting, and we additionally consider experiments under varying levels of measurement error (see Appendix D), nonstationarity (see Appendix E), and confounding (see Appendix G). The results indicate that, overall, method performance generally degrades as the severity of model assumption violations increases, while the best-performing methods are predominantly deep learning-based approaches.

Z-score standardization model. In the linear settings of Table 2.2 and the nonlinear settings of Table 3.2, we observe that NTS-NOTEARS and CUTS exhibit notable performance improvements under standardization. In particular, although NTS-NOTEARS performs poorly in the vanilla setting, its performance improves substantially once standardization is applied. DYNOTEAR shows improved performance in the nonlinear settings reported in Table 3.2, while its performance remains unchanged in the linear 10-node case with $T = 1000$ and degrades in the remaining linear settings. In the nonlinear $F = 40$ scenario of Table 3.2, among the deep learning-based methods, cMLP, CUTS, and CUTS+ all exhibit performance improvements, while cLSTM shows performance degradation. Apart from these cases, the performance of most methods remains largely unchanged under standardization. It is particularly noteworthy that continuous optimization methods in the time-series settings (DYNOTEAR, NTS-NOTEARS) do not consistently exhibit the performance degradation observed for continuous optimization methods in the i.i.d. settings. Instead, they may even exhibit performance improvements. This observation helps explain why the original implementation of NTS-NOTEARS adopts standardized preprocessing, and our results further highlight its strong reliance on standardization. Nevertheless, not all time-series data are standardized in real-world applications, making it crucial to understand the impact of standardization on continuous optimization methods.

Min-max normalization model. In the linear settings of Table 2.1, NTS-NOTEARS exhibits performance improvements under min-max normalization, whereas both CUTS and CUTS+ show

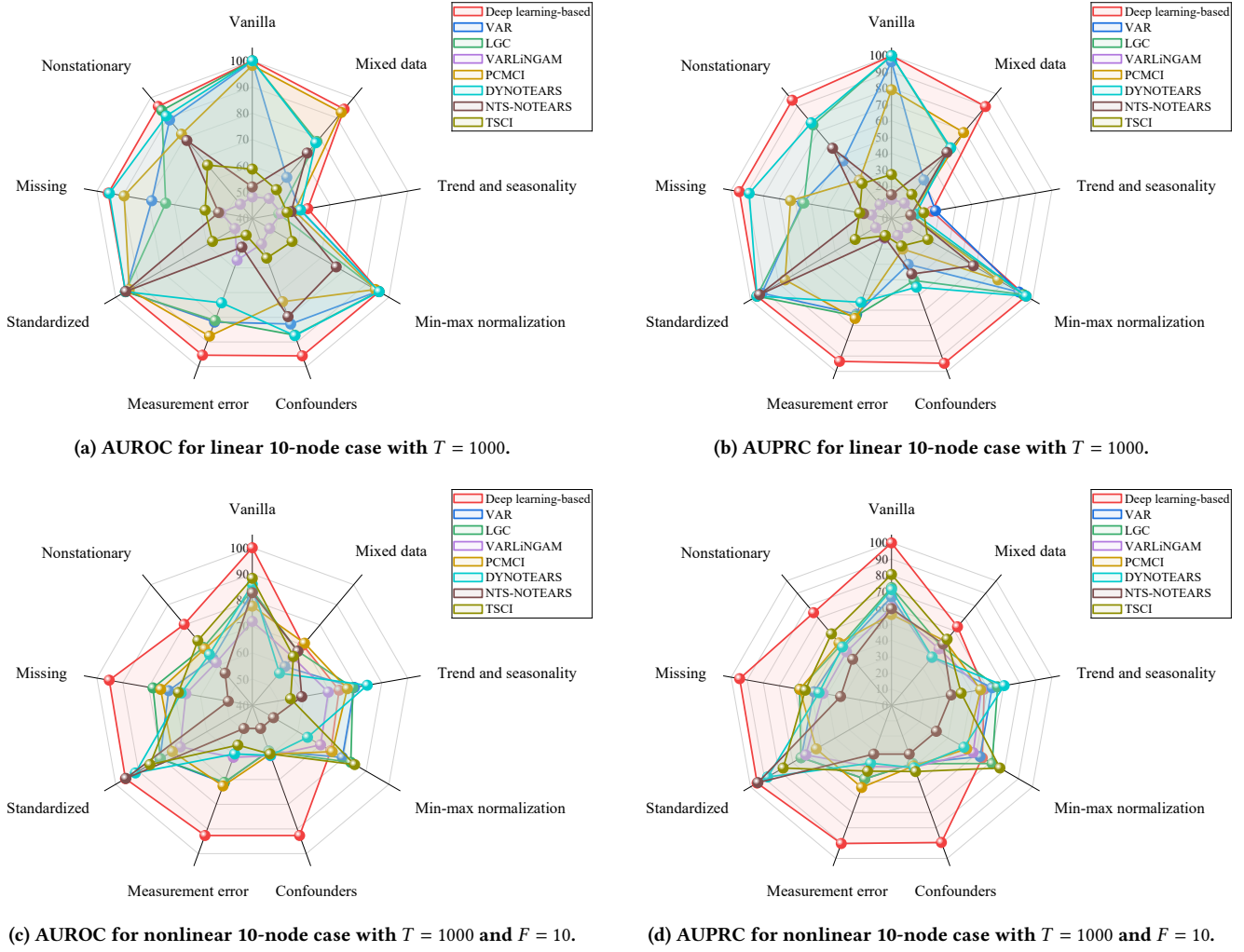


Figure 1: Experimental results under the linear and nonlinear settings across the vanilla scenario and eight assumption violation scenarios. AUROC and AUPRC (the higher the better) are evaluated over 5 trials for the 10-node case with $T = 1000$. For the deep learning-based methods, we present only the optimal results.

pronounced performance degradation. In the nonlinear settings of Table 3.1, all deep learning-based methods (cMLP, cLSTM, CUTS, and CUTS+) experience substantial performance declines, and both DYNOTEAR and NTS-NOTEARS also deteriorate under the $F = 10$ condition. Apart from these cases, the performance of most methods remains largely unchanged under min-max normalization. Overall, under min-max normalization, we observe that the performance of Granger causality-based, constraint-based, noise-based, and topology-based methods remains largely unchanged, whereas the performance of deep learning-based and score-based methods can vary across certain settings.

Trend and seasonality model. We generate trend and seasonality data with $\rho = 0.01$, $\eta = 0.5$, and $P = 12$. In the linear settings of Table 2.1, the performance of all methods deteriorates markedly under the influence of trend and seasonality. In the nonlinear settings of Table 3.1, the performance of nonlinear methods

generally deteriorates substantially, whereas the performance of linear methods remains largely unchanged.

4.2 Hyperparameter Sensitivity Analysis

Motivations. In real-world applications, the ground truth graph is typically unknown, which makes principled hyperparameter selection difficult. Consequently, investigating the performance of different methods across a range of hyperparameter configurations is of crucial importance.

Results. For each scenario, we report the mean and standard deviation of the evaluation metrics for each method under different hyperparameter settings (see Appendix K and N). The mean reflects the overall performance of a method, while the standard deviation quantifies its sensitivity to hyperparameter choices. The results indicate that deep learning-based methods continue to exhibit superior overall performance (mean values). However, in linear settings,

Table 2.1: Linear Setting, 10-node case with $T = 1000$ (Part I).

10 nodes	Vanilla		Mixed data		Trend and seasonality		Min–max normalization	
	AUROC↑	AUPRC↑	AUROC↑	AUPRC↑	AUROC↑	AUPRC↑	AUROC↑	AUPRC↑
VAR	99.7±0.3	96.3±4.4	62.0±2.4	32.4±4.3	60.0±3.1	28.8±5.6	99.6±0.5	94.8±6.7
LGC	100.0±0.0	100.0±0.0	81.2±5.5	58.4±6.5	51.0±2.0	12.8±3.5	99.8±0.2	98.1±3.6
VARLiNGAM	48.2±5.5	11.8±0.8	50.7±6.1	12.9±3.8	52.1±4.5	15.4±6.8	48.2±5.5	11.8±0.8
PCMCI	98.2±0.9	79.1±8.8	96.7±1.9	72.2±5.8	57.6±2.0	12.8±0.5	98.2±0.9	79.1±8.8
DYNOTEARNS	100.0±0.0	100.0±0.0	80.5±5.0	59.3±10.4	60.0±7.9	15.6±4.0	100.0±0.0	100.0±0.0
NTS-NOTEARS	52.0±3.9	14.6±7.1	75.0±3.1	55.5±5.6	56.2±5.1	12.6±1.3	79.7±12.8	60.9±21.3
TSCI	58.8±6.7	27.0±9.3	55.4±9.2	20.3±10.3	54.5±10.4	21.1±9.0	58.8±6.7	27.0±9.3
cMLP	99.9±0.0	99.8±0.3	98.3±2.4	94.1±4.5	50.7±3.5	18.2±3.4	99.9±0.0	99.8±0.3
cLSTM	100.0±0.0	100.0±0.0	98.5±0.8	90.8±3.2	63.1±10.6	26.4±11.7	100.0±0.0	100.0±0.0
CUTS	96.8±1.3	80.8±8.9	51.6±9.4	21.5±10.7	49.6±11.7	20.9±11.7	52.8±4.6	17.3±4.6
CUTS+	100.0±0.0	100.0±0.0	74.5±6.0	45.8±9.0	56.0±6.1	18.7±5.3	94.3±4.0	73.3±11.1

Table 2.2: Linear Setting, 10-node case with $T = 1000$ (Part II).

10 nodes	Latent confounders		Measurement error		Standardized		Missing		Nonstationary	
	AUROC↑	AUPRC↑	AUROC↑	AUPRC↑	AUROC↑	AUPRC↑	AUROC↑	AUPRC↑	AUROC↑	AUPRC↑
VAR	86.0±2.7	31.4±4.0	85.2±8.9	65.6±18.8	99.7±0.3	96.3±4.4	81.8±10.5	58.3±21.7	92.7±2.6	48.4±10.9
LGC	90.9±3.3	42.5±7.3	84.5±7.4	66.9±17.4	100.0±0.0	100.0±0.0	76.0±5.8	57.3±10.3	97.7±2.2	78.6±19.1
VARLiNGAM	51.1±3.3	11.7±0.7	58.2±5.1	13.7±1.8	48.2±5.5	11.8±0.8	53.1±9.0	13.0±3.9	47.6±5.7	11.6±0.9
PCMCI	76.3±2.2	21.0±1.4	91.3±6.0	68.5±11.9	98.2±0.9	79.1±8.8	93.3±4.5	66.0±14.7	85.1±5.9	32.2±9.5
DYNOTEARNS	91.1±6.2	47.1±10.8	76.8±9.3	57.4±17.1	100.0±0.0	100.0±0.0	99.4±0.4	93.0±6.3	94.8±5.8	80.4±16.9
NTS-NOTEARS	82.8±8.4	38.0±10.9	52.5±4.9	13.0±3.8	99.8±0.2	98.1±3.6	54.0±7.9	18.2±14.2	81.7±19.2	59.0±29.9
TSCI	57.3±8.8	18.9±2.3	47.3±6.1	11.7±2.0	58.8±6.7	27.0±9.3	59.6±4.9	20.8±3.8	68.5±11.3	29.4±11.7
cMLP	99.8±0.3	99.2±1.4	84.1±9.8	58.4±16.6	100.0±0.0	100.0±0.0	90.8±3.4	75.9±5.5	81.8±22.1	67.2±38.9
cLSTM	99.9±0.1	99.2±0.8	99.6±0.1	97.9±0.8	100.0±0.0	100.0±0.0	99.8±0.2	98.6±1.9	99.4±0.5	95.8±5.0
CUTS	83.9±10.2	58.3±17.3	90.1±7.1	64.6±14.9	100.0±0.0	100.0±0.0	76.7±11.6	49.4±15.2	98.6±1.9	93.8±8.9
CUTS+	93.1±5.2	67.1±20.5	99.4±0.3	96.0±2.9	99.9±0.0	99.8±0.3	99.9±0.0	99.4±0.4	99.9±0.1	99.4±0.6

Table 3.1: Nonlinear Setting, 10-node case with $T = 1000$ and $F = 10$ (Part I).

10 nodes	Vanilla		Mixed data		Trend and seasonality		Min–max normalization	
	AUROC↑	AUPRC↑	AUROC↑	AUPRC↑	AUROC↑	AUPRC↑	AUROC↑	AUPRC↑
VAR	83.3±3.6	66.6±5.6	60.8±4.2	40.2±3.4	82.5±2.4	65.7±3.8	82.6±2.8	65.8±4.8
LGC	83.8±2.6	72.4±4.5	69.0±5.4	49.7±8.4	81.8±2.3	69.3±3.8	86.6±1.0	74.8±2.7
VARLiNGAM	72.0±1.9	60.3±2.7	65.8±4.2	47.6±4.7	71.6±2.6	58.7±5.2	72.3±1.8	60.7±2.6
PCMCI	77.8±4.9	55.9±6.1	73.3±3.6	54.0±4.4	79.5±3.5	58.2±5.4	77.8±4.9	55.9±6.1
DYNOTEARNS	86.1±2.1	71.2±3.4	57.3±2.9	40.7±4.0	87.8±1.7	73.6±1.6	66.1±0.6	53.8±2.2
NTS-NOTEARS	82.9±1.4	59.5±2.0	69.0±2.2	51.7±3.8	60.6±4.0	39.0±2.6	50.0±0.0	33.3±0.0
TSCI	88.4±1.7	80.5±2.2	66.2±3.0	55.7±3.8	55.9±6.2	45.5±9.1	88.4±1.7	80.5±2.2
cMLP	99.9±0.0	99.9±0.0	59.6±5.5	43.5±4.2	51.2±1.0	46.1±1.5	54.8±3.7	39.0±3.2
cLSTM	100.0±0.0	99.9±0.0	59.6±3.9	49.3±3.3	76.1±2.7	60.5±5.3	49.8±3.2	36.9±0.8
CUTS	98.3±1.1	97.5±1.6	65.5±3.3	53.6±5.6	46.3±2.2	41.9±5.5	67.0±7.3	51.8±8.5
CUTS+	99.9±0.0	99.9±0.1	72.3±2.0	66.1±4.4	49.2±1.0	35.2±2.4	77.1±2.0	67.5±3.5

deep learning-based methods tend to show relatively high standard deviations, whereas in nonlinear settings, their standard deviations are generally much lower. This suggests that deep learning-based methods require more careful hyperparameter tuning in linear scenarios, while their performance is comparatively more stable in

nonlinear settings. Although these findings are influenced by the chosen hyperparameter search space, our configurations follow the recommendations or default settings in prior work and involve an

Table 3.2: Nonlinear Setting, 10-node case with $T = 1000$ and $F = 10$ (Part II).

10 nodes	Latent confounders		Measurement error		Standardized		Missing		Nonstationary	
	AUROC↑	AUPRC↑	AUROC↑	AUPRC↑	AUROC↑	AUPRC↑	AUROC↑	AUPRC↑	AUROC↑	AUPRC↑
VAR	59.8±9.5	39.7±5.9	73.8±3.4	50.3±3.8	83.6±4.1	67.1±6.5	74.8±2.3	50.7±2.2	65.1±14.9	48.3±14.6
LGC	60.0±9.6	39.9±6.0	73.5±3.9	50.3±4.4	83.5±3.2	67.3±5.0	81.3±2.6	60.1±3.4	71.1±14.4	50.7±12.8
VARLiNGAM	61.9±2.7	42.4±2.7	62.6±5.8	41.8±4.4	74.0±2.9	63.7±4.0	67.6±3.5	44.7±2.8	63.0±12.6	45.1±10.8
PCMCI	61.3±7.1	41.5±6.0	75.1±5.6	56.2±7.9	77.8±4.9	55.9±6.1	78.1±3.3	59.9±5.7	70.3±13.2	52.6±14.0
DYNOTEARNS	61.8±2.9	42.7±3.8	61.1±1.9	39.5±1.3	95.3±2.8	92.1±4.4	69.5±3.7	47.4±3.9	67.3±16.9	49.2±17.6
NTS-NOTEARS	50.0±0.0	33.3±0.0	50.0±0.0	33.3±0.0	99.8±0.3	99.3±1.2	50.0±0.0	33.3±0.0	57.3±13.0	38.9±10.5
TSCI	61.1±6.2	45.3±3.6	57.3±6.0	45.0±6.1	88.4±1.7	80.5±2.2	70.7±4.1	56.4±4.6	74.7±11.5	60.2±15.6
cMLP	66.5±7.6	52.0±10.3	57.7±1.5	42.4±1.5	99.8±0.2	99.7±0.3	82.2±2.4	70.7±5.3	73.8±22.8	65.4±29.6
cLSTM	91.7±1.9	86.8±1.4	77.5±2.3	69.2±2.7	99.8±0.1	99.6±0.2	96.4±0.7	94.9±1.1	75.4±22.4	67.2±28.9
CUTS	78.5±7.6	57.8±10.1	63.8±2.6	55.0±2.1	100.0±0.0	99.9±0.0	89.7±3.3	86.3±5.4	70.7±22.9	62.8±27.7
CUTS+	96.7±3.7	93.9±7.4	96.7±2.1	94.6±3.1	100.0±0.0	99.9±0.0	99.5±0.4	99.2±0.6	83.4±19.3	78.0±24.9

exhaustive hyperparameter exploration (see Appendix C). Consequently, our results remain instructive for real-world applications of TSCD.

4.3 Summary, Explanation and Implications for Practice

Based on the summarized results across all scenarios and configurations (see Appendix B), as well as results obtained with dataset-specific optimal hyperparameters (see Appendix I and L), hyperparameters selected by average performance (see Appendix J and M), different levels of assumption violations (see Appendix D, E, and G), and non-Gaussian noise (see Appendix H), we observe that deep learning-based methods exhibit superior overall performance. Hyperparameter sensitivity analyses (Section 4.2) further indicate that deep learning methods exhibit higher sensitivity to hyperparameter choices in linear settings, whereas their performance is comparatively more stable in nonlinear settings. The summarized results in Table 6 indicate that, under assumption violation scenarios, deep learning-based methods exhibit a larger relative advantage in AUPRC than in AUROC. Given that AUPRC is more sensitive to the introduction of spurious causal edges in sparse causal graph recovery, this observation suggests that deep learning approaches are relatively less prone to producing spurious causal edges when assumptions are violated. A possible explanation is that neural networks possess greater function approximation capacity, enabling them to better accommodate unmodeled factors without explicitly introducing additional causal edges, thereby exhibiting stronger robustness in causal graph recovery. In practice, violations of model assumptions are inevitable, rendering the robustness of methods critically important. Considering the robust characteristics of deep learning-based approaches, they possess tremendous potential in practical applications. We further observe that NTS-NOTEARS relies heavily on standardized preprocessing, performing poorly in the vanilla setting but achieving strong performance after standardization. Existing work [46, 53] has provided theoretical explanations for the performance degradation of continuous optimization methods under standardization in i.i.d. settings. In contrast, our empirical results reveal that, in time-series settings, the continuous optimization method NTS-NOTEARS consistently exhibits performance

gains under standardization. Establishing a rigorous theoretical explanation for this phenomenon is an important direction for future research. Our findings also suggest that TSCD methods respond differently to Z-score standardization and min–max normalization. We recommend reporting results under vanilla, standardized, and min–max normalized settings when developing TSCD algorithms, as this practice can provide practitioners with clearer insights into the effects of preprocessing choices and ultimately facilitate the broader adoption of TSCD methods.

5 Conclusion

This work evaluates the performance of eleven mainstream time-series causal discovery methods under eight misspecified scenarios. The methods considered include constraint-based, noise-based, score-based, topology-based, Granger causality-based, and deep learning-based approaches. Our experimental results demonstrate that no single method achieves optimal performance across all scenarios, yet the methods exhibiting superior performance overall across various scenarios are almost invariably deep learning-based approaches. We further provide hyperparameter sensitivity analyses to gain deeper insight into method performance. In particular, we find that NTS-NOTEARS relies heavily on standardized preprocessing in practice, performing poorly in the vanilla setting but exhibiting strong performance after standardization is applied. Given the robustness displayed by deep learning-based methods in our benchmark, further in-depth investigation of these approaches is of substantial importance. To facilitate reproducible and fair evaluation, we release CausalCompass, a flexible and extensible benchmark suite designed for long-term applicability. Our benchmark evaluates TSCD algorithms across diverse scenarios that reflect realistic data complexities, thereby improving understanding of their practical applicability, supporting more informed decision-making by practitioners, and ultimately promoting the broader adoption of TSCD methods. Finally, while this work focuses on TSCD algorithms, assessing the robustness of event sequence causal discovery in misspecified scenarios also represents an important direction for future research.

References

- [1] Wasim Ahmad, Maha Shadaydeh, and Joachim Denzler. 2024. Regime Identification for Improving Causal Analysis in Non-stationary Timeseries. *arXiv preprint arXiv:2405.02315* (2024).
- [2] Anonymous. 2025. TCD-Arena: Assessing Robustness of Time Series Causal Discovery Methods Against Assumption Violations. <https://openreview.net/forum?id=MtdrOCLAGY>. Under review as a conference paper at ICLR 2026.
- [3] Andrew Arnold, Yan Liu, and Naoki Abe. 2007. Temporal causal modeling with graphical granger methods. In *Proceedings of the 13th ACM SIGKDD international conference on Knowledge discovery and data mining*, 66–75.
- [4] Charles K Assaad, Emilie Devijver, and Eric Gaussier. 2022. Survey and evaluation of causal discovery methods for time series. *Journal of Artificial Intelligence Research* 73 (2022), 767–819.
- [5] Andrew P Bradley. 1997. The use of the area under the ROC curve in the evaluation of machine learning algorithms. *Pattern recognition* 30, 7 (1997), 1145–1159.
- [6] Kurt Butler, Daniel Waxman, and Petar Djuric. 2024. Tangent space causal inference: Leveraging vector fields for causal discovery in dynamical systems. *Advances in Neural Information Processing Systems* 37 (2024), 120078–120102.
- [7] Ruichu Cai, Feng Xie, Clark Glymour, Zhifeng Hao, and Kun Zhang. 2019. Triad constraints for learning causal structure of latent variables. In *Advances in Neural Information Processing Systems*, Vol. 32.
- [8] Zhanrui Cai, Dong Xi, Xuan Zhu, and Runze Li. 2022. Causal discoveries for high dimensional mixed data. *Statistics in Medicine* 41, 24 (2022), 4924–4940.
- [9] Chris Chatfield and Haipeng Xing. 2019. *The analysis of time series: an introduction with R*. Chapman and hall/CRC.
- [10] Jiawei Chen and Chunhui Zhao. 2025. Addressing information asymmetry: Deep temporal causality discovery for mixed time series. *IEEE Transactions on Pattern Analysis and Machine Intelligence* (2025).
- [11] Ricky TQ Chen, Yulia Rubanova, Jesse Bettencourt, and David K Duvenaud. 2018. Neural ordinary differential equations. *Advances in neural information processing systems* 31 (2018).
- [12] Yuxiao Cheng, Lianglong Li, Tingxiong Xiao, Zongren Li, Jinli Suo, Kunlun He, and Qionghai Dai. 2024. Cuts+: High-dimensional causal discovery from irregular time-series. In *Proceedings of the AAAI Conference on Artificial Intelligence*. 11525–11533.
- [13] Yuxiao Cheng, Runzhao Yang, Tingxiong Xiao, Zongren Li, Jinli Suo, Kunlun He, and Qionghai Dai. 2023. Cuts: Neural causal discovery from irregular time-series data. *arXiv preprint arXiv:2302.07458* (2023).
- [14] Tianjiao Chu, Clark Glymour, and Greg Ridgeway. 2008. Search for Additive Nonlinear Time Series Causal Models. *Journal of Machine Learning Research* 9, 5 (2008).
- [15] STL Cleveland. 1990. A seasonal-trend decomposition procedure based on Loess (with discussion). *J. Off. Stat* 6, 3 (1990).
- [16] Ruifei Cui, Perry Groot, and Tom Heskes. 2016. Copula PC algorithm for causal discovery from mixed data. In *Joint European conference on machine learning and knowledge discovery in databases*. Springer, 377–392.
- [17] Haoyue Dai, Peter Spirtes, and Kun Zhang. 2022. Independence testing-based approach to causal discovery under measurement error and linear non-Gaussian models. *Advances in Neural Information Processing Systems* 35 (2022), 27524–27536.
- [18] Jesse Davis and Mark Goadrich. 2006. The relationship between Precision-Recall and ROC curves. In *Proceedings of the 23rd international conference on Machine learning*, 233–240.
- [19] Doris Entner and Patrik O Hoyer. 2010. On causal discovery from time series data using FCI. *Probabilistic graphical models* 16 (2010).
- [20] Muhammad Hasan Ferdous, Enam Hossain, and Md Osman Gani. 2025. Time-graph: Synthetic benchmark datasets for robust time-series causal discovery. In *Proceedings of the 31st ACM SIGKDD Conference on Knowledge Discovery and Data Mining* V. 2, 5425–5435.
- [21] Ronja Foraita, Julianne Friemel, Kathrin Günther, Thomas Behrens, Jörn Bullerdiek, Rolf Nimzyk, Wolfgang Ahrens, and Vanessa Didelez. 2020. Causal discovery of gene regulation with incomplete data. *Journal of the Royal Statistical Society Series A: Statistics in Society* 183, 4 (2020), 1747–1775.
- [22] Daigo Fujiwara, Kazuki Koyama, Keisuke Kiritsoshi, Tomomi Okawachi, Tomonori Izumitani, and Shohei Shimizu. 2023. Causal discovery for non-stationary nonlinear time series data using just-in-time modeling. In *Conference on Causal Learning and Reasoning*. PMLR, 880–894.
- [23] Erdun Gao, Ignavier Ng, Mingming Gong, Li Shen, Wei Huang, Tongliang Liu, Kun Zhang, and Howard Bondell. 2022. MissDAG: Causal discovery in the presence of missing data with continuous additive noise models. In *Advances in Neural Information Processing Systems*, Vol. 35. 5024–5038.
- [24] Tian Gao, Songtao Lu, Junkyu Lee, Elliot Nelson, Debarun Bhattacharjya, Yue Yu, and Miao Liu. 2025. Meta-D2AG: Causal Graph Learning with Interventional Dynamic Data. In *The Thirty-ninth Annual Conference on Neural Information Processing Systems*.
- [25] Andreas Gerhardus and Jakob Runge. 2020. High-recall causal discovery for autorelated time series with latent confounders. *Advances in neural information processing systems* 33 (2020), 12615–12625.
- [26] Clark Glymour, Kun Zhang, and Peter Spirtes. 2019. Review of causal discovery methods based on graphical models. *Frontiers in Genetics* 10 (2019), 524.
- [27] Chang Gong, Chuzhe Zhang, Di Yao, Jingping Bi, Wenbin Li, and Yongjun Xu. 2024. Causal discovery from temporal data: An overview and new perspectives. *Comput. Surveys* 57, 4 (2024), 1–38.
- [28] Clive WJ Granger. 1969. Investigating causal relations by econometric models and cross-spectral methods. *Econometrica: journal of the Econometric Society* (1969), 424–438.
- [29] Benjamin Herdeanu, Juan Nathaniel, Carla Roesch, Jatan Buch, Gregor Ramien, Johannes Haux, and Pierre Gentine. 2025. CausalDynamics: A large-scale benchmark for structural discovery of dynamical causal models. *arXiv preprint arXiv:2505.16620* (2025).
- [30] Biwei Huang, Kun Zhang, Mingming Gong, and Clark Glymour. 2019. Causal discovery and forecasting in nonstationary environments with state-space models. In *International conference on machine learning*. PMLR, 2901–2910.
- [31] Biwei Huang, Kun Zhang, and Bernhard Schölkopf. 2015. Identification of Time-Dependent Causal Model: A Gaussian Process Treatment. In *IJCAI*. 3561–3568.
- [32] Biwei Huang, Kun Zhang, Jiji Zhang, Joseph Ramsey, Ruben Sanchez-Romero, Clark Glymour, and Bernhard Schölkopf. 2020. Causal discovery from heterogeneous/nonstationary data. *Journal of Machine Learning Research* 21, 89 (2020), 1–53.
- [33] Antti Hyttinen, Sergey Plis, Matti Järvisalo, Frederick Eberhardt, and David Danks. 2016. Causal discovery from subsampled time series data by constraint optimization. In *Conference on Probabilistic Graphical Models*. PMLR, 216–227.
- [34] Aapo Hyvärinen, Kun Zhang, Shohei Shimizu, and Patrik O Hoyer. 2010. Estimation of a structural vector autoregression model using non-Gaussianity. *Journal of Machine Learning Research* 11, 5 (2010).
- [35] Alireza Karimi and Mark R Paul. 2010. Extensive chaos in the Lorenz-96 model. *Chaos: An interdisciplinary journal of nonlinear science* 20, 4 (2010).
- [36] Samantha Kleinberg. 2011. A logic for causal inference in time series with discrete and continuous variables. In *IJCAI Proceedings-International Joint Conference on Artificial Intelligence*, Vol. 22. 943.
- [37] Yang Liu, Anthony C Constantinou, and Zhigao Guo. 2022. Improving Bayesian network structure learning in the presence of measurement error. *Journal of Machine Learning Research* 23, 324 (2022), 1–28.
- [38] Joshua Loftus. 2024. Position: The causal revolution needs scientific pragmatism. *arXiv preprint arXiv:2406.02275* (2024).
- [39] Damian Machlanski, Spyridon Samothrakis, and Paul S Clarke. 2024. Robustness of algorithms for causal structure learning to hyperparameter choice. In *Causal Learning and Reasoning*. PMLR, 703–739.
- [40] Daniel Malinsky and Peter Spirtes. 2018. Causal structure learning from multivariate time series in settings with unmeasured confounding. In *Proceedings of 2018 ACM SIGKDD workshop on causal discovery*. PMLR, 23–47.
- [41] Sarah Mameche, Lénaïg Cornanguer, Urmi Ninad, and Jilles Vreeken. 2025. SPACETIME: Causal Discovery from Non-Stationary Time Series. In *Proceedings of the AAAI Conference on Artificial Intelligence*, Vol. 39. 19405–19413.
- [42] Rūriks Marcinkevičs and Julia E Vogt. 2021. Interpretable models for granger causality using self-explaining neural networks. *arXiv preprint arXiv:2101.07600* (2021).
- [43] Francesco Montagna, Atalanti Mastakouri, Elias Eulig, Nicoletta Noceti, Lorenzo Rosasco, Dominik Janzing, Bryon Aragam, and Francesco Locatello. 2023. Assumption violations in causal discovery and the robustness of score matching. In *Advances in Neural Information Processing Systems*, Vol. 36.
- [44] Meike Nauta, Doina Bucur, and Christin Seifert. 2019. Causal discovery with attention-based convolutional neural networks. *Machine Learning and Knowledge Extraction* 1, 1 (2019), 19.
- [45] Ignavier Ng, AmirEmad Ghassami, and Kun Zhang. 2020. On the role of sparsity and DAG constraints for learning linear DAGs. In *Advances in Neural Information Processing Systems*, Vol. 33. 17943–17954.
- [46] Ignavier Ng, Biwei Huang, and Kun Zhang. 2024. Structure learning with continuous optimization: A sober look and beyond. In *Causal Learning and Reasoning*. PMLR, 71–105.
- [47] Roxana Pamfil, Nisara Sriwattanaworachai, Shaan Desai, Philip Pilgerstorfer, Konstantinos Georgatzis, Paul Beaumont, and Bryon Aragam. 2020. DYNOTEARS: Structure learning from time-series data. In *International Conference on Artificial Intelligence and Statistics*. PMLR, 1595–1605.
- [48] Judea Pearl. 2009. *Causality*. Cambridge university press.
- [49] Judea Pearl and Dana Mackenzie. 2018. *The Book of Why: The New Science of Cause and Effect*. Basic books.
- [50] Jonas Peters, Dominik Janzing, and Bernhard Schölkopf. 2017. *Elements of Causal Inference: Foundations and Learning Algorithms*. The MIT Press.
- [51] Audrey Poisot, Panayiotis Panayiotou, Alessandro Leite, Nicolas Chesneau, Özgür Şimşek, and Marc Schoenauer. 2025. Position: Causal machine learning requires rigorous synthetic experiments for broader adoption. *arXiv preprint arXiv:2508.08883* (2025).

[52] Vineet K Raghu, Joseph D Ramsey, Alison Morris, Dimitrios V Manatakos, Peter Sprites, Panos K Chrysanthis, Clark Glymour, and Panayiotis V Benos. 2018. Comparison of strategies for scalable causal discovery of latent variable models from mixed data. *International journal of data science and analytics* 6, 1 (2018), 33–45.

[53] Alexander Reisach, Christof Seiler, and Sebastian Weichwald. 2021. Beware of the simulated DAG! causal discovery benchmarks may be easy to game. In *Advances in Neural Information Processing Systems*, Vol. 34. 27772–27784.

[54] Jakob Runge. 2018. Causal network reconstruction from time series: From theoretical assumptions to practical estimation. *Chaos: An Interdisciplinary Journal of Nonlinear Science* 28, 7 (2018).

[55] Jakob Runge, Andreas Gerhardus, Gherardo Varando, Veronika Eyring, and Gustau Camps-Valls. 2023. Causal inference for time series. *Nature Reviews Earth & Environment* 4, 7 (2023), 487–505.

[56] Jakob Runge, Peer Nowack, Marlene Kretschmer, Seth Flaxman, and Dino Sejdinovic. 2019. Detecting and quantifying causal associations in large nonlinear time series datasets. *Science advances* 5, 11 (2019), eaau4996.

[57] Agathe Sadeghi, Achintya Gopal, and Mohammad Fesanghary. 2025. Causal discovery from nonstationary time series. *International Journal of Data Science and Analytics* 19, 1 (2025), 33–59.

[58] Richard Scheines and Joseph Ramsey. 2017. Measurement error and causal discovery. In *CEUR workshop proceedings*, Vol. 1792. 1.

[59] Shohei Shimizu, Patrik O Hoyer, Aapo Hyvärinen, Antti Kerminen, and Michael Jordan. 2006. A linear non-Gaussian acyclic model for causal discovery. *Journal of Machine Learning Research* 7, 10 (2006).

[60] Ali Shojaie and Emily B Fox. 2022. Granger causality: A review and recent advances. *Annual Review of Statistics and Its Application* 9, 1 (2022), 289–319.

[61] Peter Spirtes and Clark Glymour. 1991. An algorithm for fast recovery of sparse causal graphs. *Social science computer review* 9, 1 (1991), 62–72.

[62] Peter Spirtes, Clark Glymour, and Richard Scheines. 2001. *Causation, Prediction, and Search*. MIT press.

[63] Gideon Stein, Maha Shadaydeh, Jan Blunk, Niklas Penzel, and Joachim Denzler. 2025. CausalRivers—Scaling up benchmarking of causal discovery for real-world time-series. *arXiv preprint arXiv:2503.17452* (2025).

[64] George Sugihara, Robert May, Hao Ye, Chih-hao Hsieh, Ethan Deyle, Michael Fogarty, and Stephan Munch. 2012. Detecting causality in complex ecosystems. *science* 338, 6106 (2012), 496–500.

[65] Xiangyu Sun, Oliver Schulte, Guiliang Liu, and Pascal Poupart. 2021. Nts-notears: Learning nonparametric dbns with prior knowledge. *arXiv preprint arXiv:2109.04286* (2021).

[66] Floris Takens. 2006. Detecting strange attractors in turbulence. In *Dynamical Systems and Turbulence, Warwick 1980: proceedings of a symposium held at the University of Warwick 1979/80*. Springer, 366–381.

[67] Alex Tank, Ian Covert, Nicholas Foti, Ali Shojaie, and Emily B Fox. 2021. Neural granger causality. *IEEE Transactions on Pattern Analysis and Machine Intelligence* 44, 8 (2021), 4267–4279.

[68] Michail Tsagris, Giorgos Borboudakis, Vincenzo Lagani, and Ioannis Tsamardinos. 2018. Constraint-based causal discovery with mixed data. *International journal of data science and analytics* 6, 1 (2018), 19–30.

[69] Ruibo Tu, Cheng Zhang, Paul Ackermann, Karthika Mohan, Hedvig Kjellström, and Kun Zhang. 2019. Causal discovery in the presence of missing data. In *The 22nd International Conference on Artificial Intelligence and Statistics*. PMLR, 1762–1770.

[70] Yuhao Wang, Vlado Menkovski, Hao Wang, Xin Du, and Mykola Pechenizkiy. 2020. Causal discovery from incomplete data: a deep learning approach. *arXiv preprint arXiv:2001.05343* (2020).

[71] Wei Wenjuan, Feng Lu, and Liu Chunchen. 2018. Mixed causal structure discovery with application to prescriptive pricing. In *Proceedings of the 27th International Joint Conference on Artificial Intelligence*. 5126–5134.

[72] Feng Xie, Ruichu Cai, Biwei Huang, Clark Glymour, Zhifeng Hao, and Kun Zhang. 2020. Generalized independent noise condition for estimating latent variable causal graphs. In *Advances in Neural Information Processing Systems*, Vol. 33. 14891–14902.

[73] Yaqin Yang, AmirEmad Ghassami, Mohamed Nafea, Negar Kiyavash, Kun Zhang, and Ilya Shpitser. 2022. Causal discovery in linear latent variable models subject to measurement error. *Advances in Neural Information Processing Systems* 35 (2022), 874–886.

[74] Yaqin Yang, Mohamed Nafea, Negar Kiyavash, Kun Zhang, and AmirEmad Ghassami. 2024. Causal Discovery in Linear Models with Unobserved Variables and Measurement Error. *arXiv preprint arXiv:2407.19426* (2024).

[75] Huiyang Yi, Yanyan He, Duxin Chen, Mingyu Kang, He Wang, and Wenwu Yu. 2025. The Robustness of Differentiable Causal Discovery in Misspecified Scenarios. In *The Thirteenth International Conference on Learning Representations*.

[76] Alessio Zanga, Alice Bernasconi, Peter JF Lucas, Hanny Pijnenborg, Casper Reijnen, Marco Scutari, and Anthony C Constantinou. 2025. Federated causal discovery with missing data in a multicentric study on endometrial cancer. *Journal of biomedical informatics* (2025), 104877.

[77] Alessio Zanga, Alice Bernasconi, Peter JF Lucas, Hanny Pijnenborg, Casper Reijnen, Marco Scutari, and Fabio Stella. 2023. Causal discovery with missing data in a multicentric clinical study. In *International Conference on Artificial Intelligence in Medicine*. Springer, 40–44.

[78] Yan Zeng, Shohei Shimizu, Hidetoshi Matsui, and Fuchun Sun. 2022. Causal discovery for linear mixed data. In *Conference on Causal Learning and Reasoning*. PMLR, 994–1009.

[79] Hongbing Zhang, Kezhou Chen, Nankai Lin, Aimin Yang, Zhifeng Hao, and Zhengming Chen. 2025. Conditional independent test in the presence of measurement error with causal structure learning. In *Proceedings of the Thirty-Fourth International Joint Conference on Artificial Intelligence*. 9112–9120.

[80] Kun Zhang, Mingming Gong, Joseph Ramsey, K. Batmanghelich, Peter Spirtes, and Clark Glymour. 2018. Causal Discovery with Linear Non-Gaussian Models under Measurement Error: Structural Identifiability Results. In *Conference on Uncertainty in Artificial Intelligence*. <https://api.semanticscholar.org/CorpusID:54058643>

[81] Kun Zhang, Biwei Huang, Jiji Zhang, Clark Glymour, and Bernhard Schölkopf. 2017. Causal discovery from nonstationary/heterogeneous data: Skeleton estimation and orientation determination. In *IJCAI: Proceedings of the Conference*, Vol. 2017. 1347.

[82] Xun Zheng, Bryon Aragam, Pradeep K Ravikumar, and Eric P Xing. 2018. DAGs with NO TEARS: Continuous optimization for structure learning. In *Advances in Neural Information Processing Systems*, Vol. 31.

A Benchmark Methods

A.1 VAR

A standard approach to Granger causal discovery in multivariate time series is based on the VAR model [3]. If the lagged terms of a source variable receive non-negligible coefficients in the regression equation of a target variable, the source is considered to Granger-cause the target. Conversely, if all corresponding lagged coefficients are effectively zero, no Granger causal influence is inferred [60]. In practice, a threshold hyperparameter is introduced to filter the estimated coefficients before constructing the Granger causal graph. We refer to a publicly available VAR implementation from https://github.com/cloud36/graphical_granger_methods.

A.2 LGC

Lasso Granger Causality (LGC [3]) is a linear Granger causality approach that augments the VAR model with a Lasso penalty term, enabling the identification of sparse temporal causal relationships. We use a publicly available implementation of LGC from https://github.com/cloud36/graphical_granger_methods.

A.3 VARLiNGAM

VARLiNGAM [34] is a temporal extension of LiNGAM [59]. It first fits a vector autoregressive model via least squares estimation and then applies LiNGAM to the resulting residuals to recover the instantaneous causal graph. Subsequently, the instantaneous causal structure is used to reparameterize the lagged causal coefficients of the vector autoregressive model, yielding a structural vector autoregressive (SVAR) model. We use the implementation of the VARLiNGAM algorithm described in [4], available at https://github.com/ckassaa/causal_discovery_for_time_series.

A.4 PCMCI

PCMCI [56] is a constraint-based TSCD that extends the PC [61] algorithm to multivariate time series. It first performs variable selection to reduce the dimensionality of the conditioning sets, and then employs the momentary conditional independence (MCI) test

to address the inflated false positive rate induced by strong autocorrelations. The method outputs a window causal graph representing time-lagged causal dependencies. We use the implementation of the PCMC algorithm in Tigramite python package, available at <https://github.com/jakobrunge/tigramite>.

A.5 DYNOTEARNS

DYNOTEARNS [47] is a score-based temporal extension of NOTEARS [82] that casts causal discovery as a continuous constrained optimization problem. It simultaneously estimates instantaneous and lagged causal effects in linear settings and produces a window causal graph. A smooth acyclicity constraint is imposed to guarantee that the instantaneous causal structure forms a directed acyclic graph (DAG). We use the implementation of the DYNOTEARNS algorithm in the CausalNex python package, available at <https://github.com/mckinsey/causalnex>.

A.6 NTS-DYNOTEARNS

NTS-NOTEARS [65] is a score-based nonlinear extension of DYNOTEARNS. To address the limitation of multilayer perceptrons in exploiting temporal ordering information, it adopts one-dimensional convolutional neural networks to model nonlinear dependencies in time series. The method jointly estimates instantaneous and lagged causal effects, adopts an optimization framework similar to DYNOTEARNS, supports the incorporation of prior knowledge as additional constraints, and outputs a window causal graph. DYNOTEARNS and NTS-NOTEARS are also referred to as continuous optimization based methods, which constitute a subclass of score-based TSCD approaches [27]. We use the implementation of the NTS-NOTEARS algorithm provided by the authors, available at <https://github.com/xiangyu-sun-789/NTS-NOTEARS>.

A.7 TSCI

Tangent Space Causal Inference (TSCI [6]) is based on the idea that nonlinear dynamical systems can be locally approximated by linear dynamics in sufficiently small neighborhoods. Leveraging this property, TSCI conducts causal inference by analyzing the tangent spaces of the underlying data manifold. Concretely, it models the dynamics of each variable as a continuous vector field, which can be learned using neural ordinary differential equations [11] or Gaussian processes. Causal relationships are then assessed by applying Convergent Cross Mapping (CCM [64]) in local tangent spaces, evaluating whether the reconstructed state space of one variable can reliably predict another. This approach is designed for causal discovery in deterministic dynamical systems. We use the implementation of the TSCI algorithm provided by the authors, available at <https://github.com/KurtButler/tangentspaces>.

A.8 NGC

Neural Granger Causality (NGC [67]) refers to a class of deep learning-based nonlinear Granger causal discovery methods that

capture multivariate time series dependencies through neural architectures with sparsified input structures. The framework can be implemented using component-wise MLP (cMLP [67]) or component-wise LSTM (cLSTM [67]), and identifies Granger causality by imposing structural sparsity penalties. While the cMLP yields a window causal graph, the cLSTM is restricted to producing a summary causal graph. We use the implementations of the cMLP and cLSTM algorithms provided by the authors, available at <https://github.com/iancovert/Neural-GC>.

A.9 CUTS

CUTS [13] is a deep learning-based TSCD method tailored for irregular time series data. It employs an iterative two-module framework that jointly performs data imputation and causal structure learning in a mutually enhancing manner. Specifically, the first stage leverages a delayed supervision graph neural network to infer latent data from high-dimensional, irregularly sampled time series with complex distributions. The second stage applies sparsity-inducing regularization to the imputed data in order to recover causal relationships between variables. We use the implementation of the CUTS algorithm provided by the authors, available at <https://github.com/jarrycyx/UNN>.

A.10 CUTS+

CUTS+ extends the CUTS framework by integrating a two-stage coarse-to-fine search strategy with a message-passing graph neural network. This design allows the method to handle causal discovery in high-dimensional time series with irregular sampling. In the first stage, lightweight Granger causality tests are used to pre-select candidate parents for each variable, substantially reducing the search space. In the second stage, a graph neural network jointly imputes missing or unevenly sampled observations and learns a sparse causal graph through a penalized reconstruction loss with temporal encoding. The alternating optimization between imputation and structure learning enables CUTS+ to remain scalable while maintaining strong performance under missing-data scenarios. We use the implementation of the CUTS+ algorithm provided by the authors, available at <https://github.com/jarrycyx/UNN>.

B Summary of Methods' Performance

In Table 6, we present a comprehensive summary of methods' performance across diverse scenarios and configurations. The results indicate that deep learning-based approaches demonstrate superior performance, with CUTS+ achieving the best overall performance.

Table 6: Summary of methods' performances across all scenarios and configurations. The reported results are the mean and standard deviation of the metrics across different time series lengths, external forcing intensities, vanilla scenarios and misspecified scenarios.

Method	D (Nodes)	AUROC	AUPRC
VAR	10	71.73±14.55	48.91±17.62
	15	72.17±12.91	40.74±17.99
LGC	10	74.49±15.09	55.00±20.04
	15	72.52±13.44	45.50±19.83
VARLiNGAM	10	59.34±9.67	34.91±17.88
	15	59.01±8.86	27.99±12.53
PCMCI	10	74.60±13.91	51.13±16.93
	15	74.23±12.77	44.58±17.52
DYNOTEARNS	10	73.90±16.60	56.14±22.91
	15	73.34±14.64	46.46±22.23
NTS-NOTEARS	10	62.68±17.23	42.50±22.96
	15	59.92±15.68	30.78±21.51
TSCI	10	63.30±12.72	42.76±19.76
	15	63.01±14.07	35.35±19.50
cMLP	10	74.62±21.08	63.66±27.41
	15	73.44±19.47	52.85±29.81
cLSTM	10	81.61±19.76	73.91±26.04
	15	80.05±18.68	63.18±29.06
CUTS	10	72.40±19.64	57.75±25.45
	15	69.55±18.32	46.64±26.85
CUTS+	10	84.10±17.92	75.07±24.98
	15	82.53±16.87	67.17±27.26

C Hyperparameter Search Ranges

To ensure a fair comparison among methods, we follow the default or recommended hyperparameter settings provided in the official code repositories of the benchmark methods and further tune the hyperparameters to achieve optimal performance wherever possible. The hyperparameter search ranges are summarized in Table 7. The meanings of hyperparameters are as follows:

- τ_{max} : pre-defined maximum lag for capturing temporal dependencies in time series;
- α : significance level for statistical tests (used in PCMCI);
- *threshold*: threshold value for pruning weak causal connections (used in VAR, LGC, and VARLiNGAM);

- w_{thre} : threshold for edge weights to determine the presence of causal relationships (used in DYNOTEARNS and NTS-NOTEARS);
- $\lambda, \lambda_1, \lambda_2, \lambda_a, \lambda_w$: regularization parameters;
- θ, fnn_tol : specific hyperparameters of TSCI;
- *input step, batch size, weight decay*: hyperparameters of CUTS and CUTS+;
- *lr*: learning rate.

D Table Results under Different Levels of Measurement Error

Tables 8–10 report results under measurement error with $\alpha = 1.2$ and $\alpha = 10.0$. Larger values of α indicate stronger measurement error. The results indicate that, overall, method performance generally degrades as the severity of model assumption violations increases, while the best-performing methods across these settings are predominantly deep learning-based approaches. Considering that NTS-NOTEARS exhibits relatively slow runtime in certain settings and does not impact our main conclusions, we do not report its results in Appendices D–G.

E Table Results under Different Levels of Nonstationarity

Tables 11–16 present results under different levels of nonstationarity. We consider both moderate nonstationarity (linear: $m = 1, v = 1$; nonlinear with $F = 10$: $m = 2.5, v = 2.0$; nonlinear with $F = 40$: $m = 3.5, v = 2.0$) and stronger nonstationarity (linear: $m = 1.8, v = 1.5$; nonlinear with $F = 10$: $m = 4.2, v = 0.3$; nonlinear with $F = 40$: $m = 5.2, v = 0.3$). The results indicate that, overall, method performance generally degrades as the degree of nonstationarity increases, while the best-performing methods across these settings are predominantly deep learning-based approaches.

F Table Results under Time-Varying Coefficient Nonstationarity

In the main text, we consider nonstationarity induced by time-varying noise variance. Building on this setting, we further investigate a nonstationary scenario in which the coefficients of the linear vanilla model also vary over time. Table 17 reports the results under coefficient nonstationarity with $\sigma_{TV} = 0.3$ and $\sigma_{TV} = 1.0$. The parameter σ_{TV} controls the strength of coefficient nonstationarity, with larger values corresponding to stronger nonstationarity. The results indicate that, overall, method performance generally degrades as the degree of nonstationarity increases, while the best-performing methods across these settings are predominantly deep learning-based approaches.

G Table Results under Different Levels of Confounding

Table 18 reports the results under latent confounding with $\rho = 0.5$ and $\rho = 0.9$. Larger values of ρ correspond to stronger latent confounding. The results indicate that, overall, method performance generally degrades as the severity of model assumption violations increases, while the best-performing methods across these settings are predominantly deep learning-based approaches.

Table 7: Hyperparameter settings of benchmark methods.

Method	Linear Settings		Nonlinear Settings	
VAR	$\tau_{max} = \{3, 5\}$, $threshold = \{0, 0.01, 0.05, 0.1, 0.3\}$			
LGC	$\tau_{max} = \{3, 5\}$, $threshold = \{0, 0.01, 0.05, 0.1, 0.3\}$			
VARLiNGAM	$\tau_{max} = \{3, 5\}$, $threshold = \{0, 0.01, 0.05, 0.1, 0.3\}$			
PCMCI	$\tau_{max} = \{3, 5\}$, $\alpha = \{0.01, 0.05, 0.1\}$			
DYNOTEARS	$\tau_{max} = \{3, 5\}$, $w_{thre} = \{0.01, 0.05, 0.1, 0.3\}$, $\lambda_a = \{0.001, 0.01, 0.1\}$, $\lambda_w = \{0.001, 0.005, 0.01\}$			
NTS-NOTEARS	$\tau_{max} = \{3\}$, $w_{thre} = \{0.01, 0.05, 0.1, 0.3, 0.5\}$, $\lambda_1 = \{0.001, 0.01, 0.1\}$, $\lambda_2 = \{0.001, 0.005, 0.01\}$		$\tau_{max} = \{1\}$, $w_{thre} = \{0.1, 0.3, 0.5\}$, $\lambda_1 = \{(0.001, 0.1)\}$, $\lambda_2 = \{0.01\}$	
TSCI	$\theta = \{0.4, 0.5, 0.6\}$, $fnn_tol = \{0.005, 0.01\}$			
cMLP	$\lambda = \{1e-4, 5e-3, 0.05\}$, $lr = \{0.01, 0.1\}$		$\lambda = \{1e-4, 5e-3, 0.05\}$, $lr = \{5e-4, 0.001\}$	
cLSTM	$\lambda = \{1e-4, 5e-3, 0.05\}$, $lr = \{0.01, 0.1\}$		$\lambda = \{1e-4, 5e-3, 0.05\}$, $lr = \{5e-4, 0.001\}$	
CUTS	$input step = \{1, 3, 5, 10\}$, $batch size = \{32, 128\}$, $weight decay = \{0, 0.001, 0.003\}$			
CUTS+	$input step = \{1, 3, 5, 10\}$, $batch size = \{32, 128\}$, $weight decay = \{0, 0.001, 0.003\}$			

Table 8: Linear setting under measurement error with $\alpha = 1.2$ and $\alpha = 10.0$ ($T = 1000$).

10 nodes	Vanilla		ME ($\alpha = 1.2$)		ME ($\alpha = 10.0$)	
	AUROC \uparrow	AUPRC \uparrow	AUROC \uparrow	AUPRC \uparrow	AUROC \uparrow	AUPRC \uparrow
VAR	99.7 \pm 0.3	96.3 \pm 4.4	85.2 \pm 8.9	65.6 \pm 18.8	60.9 \pm 5.6	14.6 \pm 2.3
LGC	100.0\pm0.0	100.0\pm0.0	84.5 \pm 7.4	66.9 \pm 17.4	55.6 \pm 5.0	17.9 \pm 6.8
VARLiNGAM	48.2 \pm 5.5	11.8 \pm 0.8	58.2 \pm 5.1	13.7 \pm 1.8	50.2 \pm 2.4	12.8 \pm 3.5
PCMCI	98.2 \pm 0.9	79.1 \pm 8.8	91.3 \pm 6.0	68.5 \pm 11.9	66.3 \pm 7.5	19.8 \pm 5.6
DYNOTEARS	100.0\pm0.0	100.0\pm0.0	76.8 \pm 9.3	57.4 \pm 17.1	64.5 \pm 10.4	18.8 \pm 6.2
TSCI	58.8 \pm 6.7	27.0 \pm 9.3	47.3 \pm 6.1	11.7 \pm 2.0	58.3 \pm 4.8	17.3 \pm 4.2
cMLP	99.9 \pm 0.0	99.8 \pm 0.3	84.1 \pm 9.8	58.4 \pm 16.6	53.5 \pm 8.2	19.0 \pm 7.2
cLSTM	100.0\pm0.0	100.0\pm0.0	99.6\pm0.1	97.9\pm0.8	79.7 \pm 5.1	43.3 \pm 12.1
CUTS	96.8 \pm 1.3	80.8 \pm 8.9	90.1 \pm 7.1	64.6 \pm 14.9	65.6 \pm 4.1	25.5 \pm 6.4
CUTS+	100.0\pm0.0	100.0\pm0.0	99.4 \pm 0.3	96.0 \pm 2.9	82.0\pm4.7	45.9\pm10.0

Table 9: Nonlinear setting under measurement error with $\alpha = 1.2$ and $\alpha = 10.0$ ($T = 1000, F = 10$).

10 nodes	Vanilla		ME ($\alpha = 1.2$)		ME ($\alpha = 10.0$)	
	AUROC \uparrow	AUPRC \uparrow	AUROC \uparrow	AUPRC \uparrow	AUROC \uparrow	AUPRC \uparrow
VAR	83.3 \pm 3.6	66.6 \pm 5.6	73.8 \pm 3.4	50.3 \pm 3.8	55.3 \pm 4.7	36.5 \pm 2.8
LGC	83.8 \pm 2.6	72.4 \pm 4.5	73.5 \pm 3.9	50.3 \pm 4.4	55.1 \pm 4.7	36.4 \pm 2.8
VARLiNGAM	72.0 \pm 1.9	60.3 \pm 2.7	62.6 \pm 5.8	41.8 \pm 4.4	50.0 \pm 1.0	33.8 \pm 0.8
PCMCI	77.8 \pm 4.9	55.9 \pm 6.1	75.1 \pm 5.6	56.2 \pm 7.9	55.3 \pm 4.4	36.6 \pm 2.7
DYNOTEARS	86.1 \pm 2.1	71.2 \pm 3.4	61.1 \pm 1.9	39.5 \pm 1.3	51.6 \pm 2.4	34.1 \pm 1.2
TSCI	88.4 \pm 1.7	80.5 \pm 2.2	57.3 \pm 6.0	45.0 \pm 6.1	52.0 \pm 4.8	38.2 \pm 4.7
cMLP	99.9 \pm 0.0	99.9 \pm 0.0	57.7 \pm 1.5	42.4 \pm 1.5	51.9 \pm 5.0	38.8 \pm 4.3
cLSTM	100.0\pm0.0	99.9\pm0.0	77.5 \pm 2.3	69.2 \pm 2.7	52.2 \pm 8.3	38.2 \pm 7.4
CUTS	98.3 \pm 1.1	97.5 \pm 1.6	63.8 \pm 2.6	55.0 \pm 2.1	54.9 \pm 3.4	38.4 \pm 3.6
CUTS+	99.9 \pm 0.0	99.9 \pm 0.1	96.7\pm2.1	94.6\pm3.1	59.1\pm8.3	50.0\pm8.4

Table 10: Nonlinear setting under measurement error with $\alpha = 1.2$ and $\alpha = 10.0$ ($T = 1000, F = 40$).

10 nodes	Vanilla		ME ($\alpha = 1.2$)		ME ($\alpha = 10.0$)	
	AUROC↑	AUPRC↑	AUROC↑	AUPRC↑	AUROC↑	AUPRC↑
VAR	73.0±2.0	58.5±3.1	61.9±3.5	40.8±2.7	50.3±5.2	34.0±2.4
LGC	72.8±2.2	58.7±4.2	62.3±3.2	41.1±2.5	50.3±5.2	34.0±2.4
VARLiNGAM	65.5±2.7	45.0±3.0	53.9±3.5	36.6±3.2	50.0±1.3	33.8±0.8
PCMCI	75.5±1.5	59.8±4.0	62.1±5.9	42.7±6.0	48.3±5.1	33.7±2.0
DYNOTEARS	69.6±2.8	50.1±3.5	54.0±2.1	36.9±2.1	50.3±5.7	33.9±2.2
TSCI	71.3±4.6	56.1±4.6	52.3±7.1	35.1±4.3	48.7±5.0	35.8±4.7
cMLP	87.8±3.4	81.5±5.1	52.6±3.4	39.7±3.3	50.5±3.9	37.4±2.6
cLSTM	93.1±0.4	87.9±0.9	60.7±6.9	48.7±6.9	49.0±6.5	37.8±4.6
CUTS	90.2±2.1	76.0±6.1	56.7±5.0	44.1±5.2	54.7±4.8	38.8±4.0
CUTS+	99.8±0.1	99.7±0.2	78.8±4.8	67.9±6.6	51.9±6.9	38.1±6.7

Table 11: Linear setting under different levels of nonstationarity ($T = 500$).

10 nodes	Vanilla		Nonstationarity		Stronger nonstationarity	
	AUROC↑	AUPRC↑	AUROC↑	AUPRC↑	AUROC↑	AUPRC↑
VAR	95.2±1.0	57.3±5.0	78.8±8.2	25.4±8.7	56.7±8.7	22.0±14.3
LGC	97.6±1.1	73.6±9.1	90.4±9.9	59.3±31.2	80.0±10.0	27.4±9.7
VARLiNGAM	53.9±6.1	12.7±2.0	50.0±9.3	12.2±1.9	48.5±8.7	11.6±1.7
PCMCI	97.8±0.8	75.3±6.8	83.5±8.1	35.4±16.7	77.1±9.4	26.4±12.6
DYNOTEARS	100.0±0.0	100.0±0.0	92.2±4.8	66.3±22.2	78.9±7.9	29.9±11.5
TSCI	64.5±12.1	23.5±10.4	52.4±10.9	19.6±8.2	55.5±4.4	20.5±4.3
cMLP	99.9±0.0	99.6±0.4	93.7±4.0	72.8±14.1	89.3±5.6	55.4±14.5
cLSTM	100.0±0.0	100.0±0.0	93.9±6.3	80.7±22.3	82.9±7.8	52.2±23.8
CUTS	92.8±8.5	76.0±12.2	95.2±4.9	81.3±15.6	96.5±3.0	85.1±13.3
CUTS+	99.6±0.3	97.3±2.7	99.0±0.4	93.1±3.8	97.2±1.6	84.4±7.2

Table 12: Linear setting under different levels of nonstationarity ($T = 1000$).

10 nodes	Vanilla		Nonstationarity		Stronger nonstationarity	
	AUROC↑	AUPRC↑	AUROC↑	AUPRC↑	AUROC↑	AUPRC↑
VAR	99.7±0.3	96.3±4.4	92.7±2.6	48.4±10.9	88.7±5.4	40.2±14.5
LGC	100.0±0.0	100.0±0.0	97.7±2.2	78.6±19.1	94.3±3.0	56.5±15.1
VARLiNGAM	48.2±5.5	11.8±0.8	47.6±5.7	11.6±0.9	46.7±7.1	11.3±0.9
PCMCI	98.2±0.9	79.1±8.8	85.1±5.9	32.2±9.5	78.4±7.8	24.4±6.9
DYNOTEARS	100.0±0.0	100.0±0.0	94.8±5.8	80.4±16.9	92.0±6.4	52.0±19.6
TSCI	58.8±6.7	27.0±9.3	68.5±11.3	29.4±11.7	70.3±10.2	32.5±6.2
cMLP	99.9±0.0	99.8±0.3	81.8±22.1	67.2±38.9	73.6±15.3	38.3±29.6
cLSTM	100.0±0.0	100.0±0.0	99.4±0.5	95.8±5.0	77.1±12.8	48.5±29.9
CUTS	96.8±1.3	80.8±8.9	98.6±1.9	93.8±8.9	99.4±0.5	95.5±4.8
CUTS+	100.0±0.0	100.0±0.0	99.9±0.1	99.4±0.6	99.7±0.3	98.2±2.0

Table 13: Nonlinear setting under different levels of nonstationarity ($T = 500, F = 10$).

10 nodes	Vanilla		Nonstationarity		Stronger nonstationarity	
	AUROC↑	AUPRC↑	AUROC↑	AUPRC↑	AUROC↑	AUPRC↑
VAR	77.0±3.1	55.5±4.3	66.8±9.2	46.8±8.0	61.5±5.6	42.6±5.1
LGC	76.9±2.4	62.9±3.8	68.5±11.5	52.7±15.0	61.3±5.6	42.7±5.1
VARLiNGAM	72.1±6.4	61.1±9.4	60.5±11.5	44.9±13.1	54.1±4.6	36.4±3.2
PCMCI	71.3±5.2	50.4±7.0	65.0±8.1	46.1±7.3	66.3±6.8	46.3±6.4
DYNOTEARS	75.8±6.9	65.9±10.5	64.6±10.6	47.7±13.1	56.1±3.1	37.0±2.1
TSCI	86.3±2.7	77.3±3.3	71.0±11.2	56.6±13.2	56.7±7.4	41.5±8.1
cMLP	99.7±0.1	99.5±0.2	72.1±22.4	64.9±28.0	54.4±5.5	39.8±1.8
cLSTM	100.0±0.0	99.9±0.0	74.1±21.5	67.5±27.2	63.3±10.2	52.8±10.6
CUTS	93.6±1.7	91.6±2.3	66.8±20.6	58.8±24.2	57.0±9.5	44.4±7.5
CUTS+	99.7±0.2	99.4±0.5	80.1±19.1	74.1±22.3	75.0±14.5	65.3±17.0

Table 14: Nonlinear setting under different levels of nonstationarity ($T = 1000, F = 10$).

10 nodes	Vanilla		Nonstationarity		Stronger nonstationarity	
	AUROC↑	AUPRC↑	AUROC↑	AUPRC↑	AUROC↑	AUPRC↑
VAR	83.3±3.6	66.6±5.6	65.1±14.9	48.3±14.6	67.8±5.8	45.2±5.0
LGC	83.8±2.6	72.4±4.5	71.1±14.4	50.7±12.8	68.3±6.2	45.8±5.5
VARLiNGAM	72.0±1.9	60.3±2.7	63.0±12.6	45.1±10.8	57.9±5.3	39.0±3.8
PCMCI	77.8±4.9	55.9±6.1	70.3±13.2	52.6±14.0	69.3±9.2	50.0±10.2
DYNOTEARS	86.1±2.1	71.2±3.4	67.3±16.9	49.2±17.6	56.1±5.6	39.4±6.1
TSCI	88.4±1.7	80.5±2.2	74.7±11.5	60.2±15.6	60.9±7.2	45.9±8.4
cMLP	99.9±0.0	99.9±0.0	73.8±22.8	65.4±29.6	54.7±7.3	41.2±8.4
cLSTM	100.0±0.0	99.9±0.0	75.4±22.4	67.2±28.9	60.8±15.7	49.7±18.4
CUTS	98.3±1.1	97.5±1.6	70.7±22.9	62.8±27.7	62.5±10.6	50.7±6.8
CUTS+	99.9±0.0	99.9±0.1	83.4±19.3	78.0±24.9	86.3±9.6	83.8±10.0

Table 15: Nonlinear setting under different levels of nonstationarity ($T = 500, F = 40$).

10 nodes	Vanilla		Nonstationarity		Stronger nonstationarity	
	AUROC↑	AUPRC↑	AUROC↑	AUPRC↑	AUROC↑	AUPRC↑
VAR	68.8±4.1	48.3±4.2	60.6±9.1	42.3±7.8	56.1±4.6	37.6±3.4
LGC	68.5±3.7	48.0±3.8	60.6±9.1	42.3±7.8	55.8±4.3	37.3±3.2
VARLiNGAM	61.8±3.8	42.0±3.4	56.0±4.3	37.8±3.0	51.5±2.0	35.2±2.5
PCMCI	66.1±5.5	47.9±7.6	60.1±8.9	43.1±10.4	57.3±6.7	38.4±5.1
DYNOTEARS	66.0±2.5	43.6±2.0	58.6±7.6	39.1±4.6	55.1±4.0	36.5±2.5
TSCI	60.4±3.2	46.8±5.8	55.6±8.3	40.4±8.0	49.7±3.5	36.3±3.9
cMLP	83.0±3.6	72.5±4.6	69.1±21.8	61.5±26.9	57.9±11.9	46.7±14.8
cLSTM	94.2±0.4	89.3±0.3	70.9±20.1	63.3±21.7	57.2±8.1	45.5±10.6
CUTS	85.8±3.7	69.3±6.9	69.4±15.3	56.4±15.2	55.7±7.2	45.0±9.5
CUTS+	98.8±1.0	97.9±1.8	77.3±19.6	71.5±23.8	63.5±9.5	53.2±6.4

Table 16: Nonlinear setting under different levels of nonstationarity ($T = 1000, F = 40$).

10 nodes	Vanilla		Nonstationarity		Stronger nonstationarity	
	AUROC↑	AUPRC↑	AUROC↑	AUPRC↑	AUROC↑	AUPRC↑
VAR	73.0±2.0	58.5±3.1	60.5±9.7	44.7±11.1	59.5±7.8	39.1±5.2
LGC	72.8±2.2	58.7±4.2	60.5±9.7	44.7±11.1	59.8±7.9	39.3±5.5
VARLiNGAM	65.5±2.7	45.0±3.0	54.8±7.6	37.1±5.1	51.8±2.9	34.9±1.8
PCMCI	75.5±1.5	59.8±4.0	62.5±10.3	46.1±12.4	58.8±6.1	39.0±4.7
DYNOTEARS	69.6±2.8	50.1±3.5	59.0±9.7	41.2±7.8	53.6±1.9	36.4±1.5
TSCI	71.3±4.6	56.1±4.6	60.5±7.7	48.6±7.6	54.0±3.3	39.7±3.5
cMLP	87.8±3.4	81.5±5.1	74.5±20.8	66.3±27.7	60.4±11.5	44.7±11.8
cLSTM	93.1±0.4	87.9±0.9	72.0±20.9	63.9±24.6	60.7±9.0	48.5±11.1
CUTS	90.2±2.1	76.0±6.1	70.0±19.9	56.1±17.8	57.7±4.6	43.5±4.5
CUTS+	99.8±0.1	99.7±0.2	80.1±20.0	75.2±24.9	67.3±13.7	57.2±16.5

Table 17: Linear setting under nonstationary time-varying coefficients ($T = 1000$).

10 nodes	Vanilla		TV Coef ($\sigma_{TV} = 0.3$)		TV Coef ($\sigma_{TV} = 1.0$)	
	AUROC↑	AUPRC↑	AUROC↑	AUPRC↑	AUROC↑	AUPRC↑
VAR	99.7±0.3	96.3±4.4	89.5±5.2	47.5±17.2	82.5±8.0	29.7±11.0
LGC	100.0±0.0	100.0±0.0	88.8±5.8	58.3±15.2	79.5±12.0	31.8±15.6
VARLiNGAM	48.2±5.5	11.8±0.8	51.6±9.7	13.2±2.7	64.1±6.4	17.2±5.2
PCMCI	98.2±0.9	79.1±8.8	84.5±6.6	31.3±9.0	77.7±14.2	28.3±12.9
DYNOTEARS	100.0±0.0	100.0±0.0	88.5±5.3	46.2±13.6	73.2±12.1	33.8±24.6
TSCI	58.8±6.7	27.0±9.3	61.3±14.6	28.2±14.1	63.4±7.5	28.5±7.9
cMLP	99.9±0.0	99.8±0.3	83.8±2.8	53.7±6.4	84.6±3.2	54.2±9.0
cLSTM	100.0±0.0	100.0±0.0	74.0±9.4	38.6±20.8	63.9±15.3	33.8±22.2
CUTS	96.8±1.3	80.8±8.9	90.4±7.3	84.2±10.8	77.7±14.5	49.3±29.0
CUTS+	100.0±0.0	100.0±0.0	89.0±6.2	70.7±12.7	74.2±17.4	50.2±23.1

Table 18: Nonlinear setting under different levels of confounding ($T = 1000, F = 10$).

10 nodes	Vanilla		Confounders ($\rho = 0.5$)		Confounders ($\rho = 0.9$)	
	AUROC↑	AUPRC↑	AUROC↑	AUPRC↑	AUROC↑	AUPRC↑
VAR	83.3±3.6	66.6±5.6	59.8±9.5	39.7±5.9	54.0±3.4	38.4±4.2
LGC	83.8±2.6	72.4±4.5	60.0±9.6	39.9±6.0	54.0±3.4	38.4±4.2
VARLiNGAM	72.0±1.9	60.3±2.7	61.9±2.7	42.4±2.7	57.1±1.9	38.3±1.7
PCMCI	77.8±4.9	55.9±6.1	61.3±7.1	41.5±6.0	55.8±5.8	38.2±4.4
DYNOTEARS	86.1±2.1	71.2±3.4	61.8±2.9	42.7±3.8	57.3±3.3	38.7±3.1
TSCI	88.4±1.7	80.5±2.2	61.1±6.2	45.3±3.6	57.0±6.6	43.5±8.9
cMLP	99.9±0.0	99.9±0.0	66.5±7.6	52.0±10.3	59.3±3.8	45.8±5.3
cLSTM	100.0±0.0	99.9±0.0	91.7±1.9	86.8±1.4	85.4±6.1	77.7±8.5
CUTS	98.3±1.1	97.5±1.6	78.5±7.6	57.8±10.1	60.9±7.0	38.9±5.3
CUTS+	99.9±0.0	99.9±0.1	96.7±3.7	93.9±7.4	91.6±3.3	87.3±6.4

H Table Results for Non-Gaussian Noise

We consider the linear vanilla model with exponential noise. The results in Table 19 and Table 20 indicate that, overall, the methods achieving the best performance across diverse scenarios are almost invariably deep learning-based approaches. We also find that NTS-NOTEARS relies heavily on standardized preprocessing in practical applications: it performs poorly in the vanilla setting but exhibits strong performance once standardization is applied. Our results indicate that Gaussian noise does not affect the main conclusions of the paper.

I Table Results with Dataset-Specific Optimal Hyperparameters

We determine the hyperparameters of each method as dataset-specific optimal values. Additional experimental results under both linear and nonlinear settings, spanning different numbers of nodes, time series lengths, and external forcing intensities, are reported in the Appendix (Tables 21–40).

J Table Results with Hyperparameters Selected by Average Performance

We select, for each causal discovery method, a single hyperparameter configuration that maximizes average performance across all scenarios. Additional experimental results under both linear and nonlinear settings, spanning different numbers of nodes, time series lengths, and external forcing intensities, are reported in the Appendix (Tables 41–64).

K Table Results Aggregated over All Hyperparameters

For each scenario, we compute the mean and standard deviation of the evaluation metrics for each method across different hyperparameter settings. Additional experimental results under both linear and nonlinear settings, spanning different numbers of nodes, time series lengths, and external forcing intensities, are reported in the Appendix (Tables 65–88).

L Figure Results with Dataset-Specific Optimal Hyperparameters

We determine the hyperparameters of each method as dataset-specific optimal values. Additional figure results under both linear and nonlinear settings, spanning different numbers of nodes, time series lengths, and external forcing intensities, are reported in the Appendix (Figures 2–6).

M Figure Results with Hyperparameters Selected by Average Performance

We select, for each causal discovery method, a single hyperparameter configuration that maximizes average performance across all scenarios. Additional figure results under both linear and nonlinear settings, spanning different numbers of nodes, time series lengths, and external forcing intensities, are reported in the Appendix (Figures 7–12).

N Figure Results Aggregated over All Hyperparameters

For each scenario, we compute the mean and standard deviation of the evaluation metrics for each method across different hyperparameter settings. Additional figure results under both linear and nonlinear settings, spanning different numbers of nodes, time series lengths, and external forcing intensities, are reported in the Appendix (Figures 13–18).

Table 19: Linear Setting under exponential noise, 10-node case with $T = 1000$ (Part I).

10 nodes	Vanilla		Mixed data		Trend and seasonality		Min–max normalization	
	AUROC↑	AUPRC↑	AUROC↑	AUPRC↑	AUROC↑	AUPRC↑	AUROC↑	AUPRC↑
VAR	99.8±0.2	98.1±3.6	74.8±8.3	29.7±8.7	59.0±4.8	27.1±8.7	99.4±0.4	93.0±6.3
LGC	100.0±0.0	100.0±0.0	72.2±8.2	37.6±13.8	51.0±2.0	12.8±3.5	100.0±0.0	100.0±0.0
VARLiNGAM	48.2±5.5	11.8±0.8	48.1±7.5	11.7±0.8	51.5±2.6	13.6±3.5	48.2±5.5	11.8±0.8
PCMCI	98.5±0.3	80.7±3.1	88.1±0.8	61.3±7.7	58.6±1.0	13.1±0.2	98.5±0.3	80.7±3.1
DYNOTEARS	100.0±0.0	100.0±0.0	74.6±7.3	42.6±11.7	58.8±6.3	14.8±3.0	100.0±0.0	100.0±0.0
NTS-NOTEARS	55.9±12.0	21.7±21.3	56.0±3.7	21.7±6.6	57.4±6.5	13.1±1.8	53.8±7.7	16.6±11.0
TSCI	77.7±8.1	38.0±13.1	53.1±9.0	21.3±8.1	55.5±11.3	22.0±11.6	77.7±8.1	38.0±13.1
cMLP	100.0±0.0	100.0±0.0	76.4±11.8	54.8±16.1	50.7±3.5	18.2±3.4	100.0±0.0	100.0±0.0
cLSTM	100.0±0.0	100.0±0.0	93.8±4.5	76.5±16.2	64.0±11.5	24.4±9.8	100.0±0.0	100.0±0.0
CUTS	95.3±3.2	80.1±11.9	63.8±3.7	27.5±6.9	49.5±11.6	20.8±11.6	59.3±7.4	19.6±9.0
CUTS+	100.0±0.0	100.0±0.0	84.3±5.7	54.8±5.3	55.2±4.9	17.0±4.7	92.2±0.8	68.8±7.3

Table 20: Linear Setting under exponential noise, 10-node case with $T = 1000$ (Part II).

10 nodes	Latent confounders		Measurement error		Standardized		Missing		Nonstationary	
	AUROC↑	AUPRC↑	AUROC↑	AUPRC↑	AUROC↑	AUPRC↑	AUROC↑	AUPRC↑	AUROC↑	AUPRC↑
VAR	86.2±2.5	31.7±4.2	88.6±5.5	66.2±12.4	99.8±0.2	98.1±3.6	80.2±4.8	57.0±9.2	94.1±3.2	55.3±14.4
LGC	91.8±2.4	44.6±7.2	88.8±5.4	68.9±12.0	100.0±0.0	100.0±0.0	79.6±5.3	59.2±8.8	98.0±1.7	78.9±15.4
VARLiNGAM	48.0±6.5	12.0±1.9	58.7±9.8	15.7±6.7	48.2±5.5	11.8±0.8	50.6±7.0	13.1±2.5	51.3±7.5	12.9±1.8
PCMCI	75.3±3.5	20.5±2.3	92.0±4.3	66.8±8.3	98.5±0.3	80.7±3.1	94.8±2.9	72.3±10.0	87.7±4.9	36.5±10.7
DYNOTEARS	91.1±1.9	43.2±2.8	83.7±9.0	68.0±15.2	100.0±0.0	100.0±0.0	99.7±0.3	96.3±4.4	97.5±2.3	89.4±6.4
NTS-NOTEARS	82.1±11.8	39.8±15.3	54.8±9.7	14.5±6.9	99.8±0.2	98.1±3.6	59.8±14.9	27.1±23.4	81.8±18.2	56.4±35.1
TSCI	53.0±7.7	17.4±6.3	54.1±6.2	18.2±8.9	77.7±8.1	38.0±13.1	63.6±7.6	22.8±5.0	71.7±4.0	30.2±7.8
cMLP	100.0±0.0	100.0±0.0	85.2±6.4	55.6±15.0	100.0±0.0	100.0±0.0	94.6±3.2	78.8±10.7	96.5±4.4	84.2±16.4
cLSTM	99.9±0.0	99.8±0.3	99.9±0.1	99.4±0.6	100.0±0.0	100.0±0.0	99.9±0.1	99.4±0.6	98.3±2.4	92.8±10.3
CUTS	84.2±5.7	52.1±16.8	90.4±7.0	68.6±14.3	100.0±0.0	100.0±0.0	76.7±11.6	49.4±15.2	98.6±1.3	92.5±6.9
CUTS+	91.2±2.8	62.5±11.2	99.6±0.3	97.3±3.0	99.9±0.1	99.4±0.6	99.9±0.0	99.4±0.4	99.6±0.5	97.1±3.8

Table 21: Linear Setting, 10-node case with $T = 500$ (Part I).

10 nodes	Vanilla		Mixed data		Trend and seasonality		Min–max normalization	
	AUROC↑	AUPRC↑	AUROC↑	AUPRC↑	AUROC↑	AUPRC↑	AUROC↑	AUPRC↑
VAR	95.2±1.0	57.3±5.0	59.8±4.1	22.7±9.7	59.5±3.3	24.5±8.0	95.2±0.7	57.0±3.8
LGC	97.6±1.1	73.6±9.1	82.1±8.1	51.0±10.3	50.5±3.5	12.6±1.9	97.1±1.0	69.3±7.4
VARLiNGAM	53.9±6.1	12.7±2.0	51.3±4.1	12.9±3.0	50.5±2.9	12.3±1.5	51.2±8.5	12.9±1.9
PCMCI	97.8±0.8	75.3±6.8	91.1±4.0	67.3±12.0	63.2±2.3	14.6±0.8	97.8±0.8	75.3±6.8
DYNOTEARS	100.0±0.0	100.0±0.0	78.4±7.2	48.0±14.2	60.1±8.8	15.2±3.9	100.0±0.0	100.0±0.0
NTS-NOTEARS	59.0±12.0	27.1±21.3	73.5±2.1	47.6±7.0	52.8±7.9	15.5±8.9	85.0±12.6	73.3±22.4
TSCI	64.5±12.1	23.5±10.4	52.9±9.8	20.6±7.3	56.7±12.1	19.6±6.5	64.5±12.1	23.5±10.4
cMLP	99.9±0.0	99.6±0.4	89.5±4.2	60.1±13.1	50.7±3.5	18.2±3.4	99.7±0.4	98.8±1.8
cLSTM	100.0±0.0	100.0±0.0	89.3±3.0	82.3±5.8	64.6±9.5	24.5±10.0	100.0±0.0	100.0±0.0
CUTS	92.8±8.5	76.0±12.2	58.4±7.9	21.3±9.2	57.3±6.0	22.3±5.6	54.6±14.5	21.7±14.0
CUTS+	99.6±0.3	97.3±2.7	75.7±4.8	42.2±9.1	46.8±4.6	17.3±4.6	89.3±6.9	60.9±10.0

Table 22: Linear Setting, 10-node case with $T = 500$ (Part II).

10 nodes	Latent confounders		Measurement error		Standardized		Missing		Nonstationary	
	AUROC↑	AUPRC↑	AUROC↑	AUPRC↑	AUROC↑	AUPRC↑	AUROC↑	AUPRC↑	AUROC↑	AUPRC↑
VAR	55.0±3.1	20.0±5.6	90.7±2.3	46.3±3.5	94.6±1.1	54.3±5.5	86.0±6.2	42.9±12.8	78.8±8.2	25.4±8.7
LGC	91.8±4.4	59.2±18.2	85.8±5.5	47.5±9.9	99.8±0.2	98.1±3.6	85.7±6.5	55.1±14.3	90.4±9.9	59.3±31.2
VARLiNGAM	55.0±9.1	15.4±6.5	55.6±8.5	13.7±2.6	53.9±6.1	12.7±2.0	54.2±11.5	14.1±2.8	50.0±9.3	12.2±1.9
PCMCI	83.1±4.5	28.2±5.2	85.6±8.1	54.8±15.3	97.8±0.8	75.3±6.8	80.7±8.3	47.6±14.4	83.5±8.1	35.4±16.7
DYNOTEARNS	82.8±10.0	41.1±12.2	90.3±5.3	60.3±11.6	98.1±0.6	77.4±6.1	97.8±1.7	83.3±4.4	92.2±4.8	66.3±22.2
NTS-NOTEARNS	84.5±5.1	39.2±7.0	55.0±6.3	20.0±11.2	93.0±5.0	87.5±9.0	61.7±14.7	29.1±23.1	76.2±21.5	50.1±32.0
TSCI	53.8±10.3	21.4±9.3	47.2±9.4	14.0±4.0	64.5±12.1	23.5±10.4	63.6±4.5	21.0±6.7	52.4±10.9	19.6±8.2
cMLP	99.5±0.6	97.9±2.6	81.9±7.3	50.7±13.0	99.9±0.1	99.3±1.2	88.2±7.4	68.4±13.1	93.7±4.0	72.8±14.1
cLSTM	99.2±0.8	97.2±3.4	98.1±1.9	89.2±10.2	100.0±0.0	100.0±0.0	99.5±0.4	96.5±4.0	93.9±6.3	80.7±22.3
CUTS	83.6±5.6	49.4±9.7	91.9±2.5	66.4±8.2	99.9±0.1	99.4±1.0	84.5±5.3	57.4±13.3	95.2±4.9	81.3±15.6
CUTS+	91.1±6.3	64.3±21.2	97.3±1.1	84.9±6.3	99.1±0.4	93.6±3.7	98.6±0.7	89.8±6.7	99.0±0.4	93.1±3.8

Table 23: Linear Setting, 15-node case with $T = 500$ (Part I).

15 nodes	Vanilla		Mixed data		Trend and seasonality		Min-max normalization	
	AUROC↑	AUPRC↑	AUROC↑	AUPRC↑	AUROC↑	AUPRC↑	AUROC↑	AUPRC↑
VAR	90.7±3.2	59.6±8.1	62.5±1.9	29.0±4.6	72.3±4.3	23.9±2.7	89.6±4.6	57.6±9.6
LGC	91.8±2.5	72.0±4.9	71.4±5.2	42.1±7.2	50.8±1.0	15.0±1.0	87.1±5.9	59.3±8.7
VARLiNGAM	51.1±4.6	15.0±1.3	50.9±5.6	15.2±2.4	50.7±1.7	15.0±1.0	51.1±3.6	14.7±1.1
PCMCI	89.1±4.7	71.2±9.7	77.8±5.1	51.6±10.6	64.5±6.0	19.9±3.0	89.1±4.7	71.2±9.7
DYNOTEARNS	96.5±0.7	82.0±3.8	70.6±4.0	37.4±5.2	55.0±3.2	16.6±1.8	86.9±4.4	74.0±9.4
NTS-NOTEARNS	50.0±0.0	14.2±0.0	63.2±1.2	33.9±3.0	52.6±3.0	15.0±0.8	50.0±0.0	14.2±0.0
TSCI	58.4±4.5	20.4±3.5	51.1±3.9	16.9±2.6	52.9±2.1	17.9±2.6	58.4±4.5	20.4±3.5
cMLP	96.8±1.6	90.3±3.7	63.4±1.8	21.5±2.4	51.1±1.6	16.0±1.2	94.9±1.8	82.3±5.6
cLSTM	95.5±1.6	85.1±3.7	82.6±4.8	60.1±4.1	59.2±3.4	19.5±2.6	98.9±0.6	95.5±2.4
CUTS	87.1±3.2	61.0±3.9	55.5±3.5	20.3±1.5	51.4±8.3	17.1±4.3	50.3±1.6	18.4±3.6
CUTS+	97.6±1.3	90.6±3.6	68.7±1.7	35.9±4.9	53.8±9.8	21.4±5.7	77.9±3.4	42.8±6.1

Table 24: Linear Setting, 15-node case with $T = 500$ (Part II).

15 nodes	Latent confounders		Measurement error		Standardized		Missing		Nonstationary	
	AUROC↑	AUPRC↑	AUROC↑	AUPRC↑	AUROC↑	AUPRC↑	AUROC↑	AUPRC↑	AUROC↑	AUPRC↑
VAR	74.1±4.0	25.6±2.6	68.1±3.8	28.1±3.9	91.0±4.3	60.3±10.7	60.1±1.4	19.7±1.2	77.3±8.1	30.9±8.1
LGC	74.8±5.7	50.5±10.2	62.3±4.1	26.2±4.4	95.2±2.2	70.1±8.6	71.4±2.2	23.6±1.6	83.0±7.9	56.8±19.4
VARLiNGAM	53.0±1.9	15.7±1.3	51.3±3.3	15.9±2.6	51.6±3.7	15.0±1.2	50.6±1.0	14.7±0.4	49.5±4.3	14.4±0.6
PCMCI	83.4±3.5	42.7±4.6	64.1±3.0	28.0±3.8	89.1±4.7	71.2±9.7	72.8±1.7	29.8±1.8	82.8±5.5	41.1±9.8
DYNOTEARNS	76.5±4.2	33.5±5.3	75.0±4.0	30.3±4.2	90.0±3.8	68.0±6.5	70.0±6.0	41.3±7.2	76.9±9.3	50.5±19.8
NTS-NOTEARNS	77.7±1.3	30.0±0.8	50.0±0.0	14.2±0.0	88.9±1.9	58.9±6.3	50.0±0.0	14.2±0.0	73.4±12.1	45.2±21.0
TSCI	48.8±6.1	15.4±2.1	51.7±6.6	18.6±4.5	58.4±4.5	20.4±3.5	53.4±5.1	18.7±3.0	51.6±2.8	17.9±1.8
cMLP	96.3±2.4	87.0±7.3	66.5±3.2	29.8±3.4	89.9±2.3	58.2±8.6	73.8±2.2	48.3±4.0	81.3±7.9	45.0±14.1
cLSTM	96.0±2.8	86.0±9.3	82.9±3.2	52.1±5.0	99.8±0.1	98.9±0.7	88.1±2.8	65.3±7.4	89.4±15.6	79.0±27.1
CUTS	65.6±7.5	32.1±9.5	76.9±5.3	37.9±7.9	97.6±2.3	90.7±5.4	71.7±5.1	37.5±9.1	89.2±4.1	66.7±8.1
CUTS+	85.3±2.7	58.2±4.9	86.0±2.5	59.4±4.4	98.9±0.3	95.1±1.9	91.9±3.4	76.7±6.5	96.6±1.7	85.3±10.2

Table 25: Linear Setting, 15-node case with $T = 1000$ (Part I).

15 nodes	Vanilla		Mixed data		Trend and seasonality		Min-max normalization	
	AUROC↑	AUPRC↑	AUROC↑	AUPRC↑	AUROC↑	AUPRC↑	AUROC↑	AUPRC↑
VAR	93.2±2.6	84.2±6.4	61.1±2.0	31.9±4.1	81.7±2.2	35.6±2.9	92.9±2.1	81.3±5.8
LGC	90.9±2.7	83.9±5.0	74.7±5.3	52.4±12.2	50.0±0.0	14.2±0.0	92.0±2.3	83.1±4.9
VARLiNGAM	51.6±5.9	15.4±2.0	51.1±3.8	15.0±1.5	49.7±0.2	14.2±0.0	50.6±5.0	14.9±1.4
PCMCI	98.0±0.8	83.4±4.3	90.6±3.3	71.5±11.3	62.0±2.2	18.1±0.8	98.0±0.8	83.4±4.3
DYNOTEARS	99.0±0.8	95.1±3.1	72.8±3.9	49.3±8.2	58.1±4.6	17.4±1.8	97.8±0.3	79.8±2.9
NTS-NOTEARS	50.0±0.0	14.2±0.0	78.4±4.5	35.6±4.3	51.8±3.6	14.8±1.0	50.0±0.0	14.2±0.0
TSCI	57.5±1.8	22.3±1.5	54.1±4.2	19.6±2.4	52.2±3.8	18.0±2.9	57.5±1.8	22.3±1.5
cMLP	99.6±0.4	98.9±1.4	78.2±5.6	62.8±3.5	51.0±1.6	16.0±1.2	99.7±0.1	98.5±0.9
cLSTM	98.6±0.3	93.9±1.1	89.5±0.7	67.0±1.3	56.8±4.1	18.5±1.6	99.9±0.0	99.8±0.2
CUTS	92.0±3.7	75.4±5.4	53.9±4.3	20.0±4.2	50.7±2.7	16.7±3.6	51.9±6.0	18.0±3.0
CUTS+	99.9±0.0	99.5±0.4	67.6±2.7	41.9±4.1	55.4±3.9	18.3±1.9	83.8±4.2	61.0±6.5

Table 26: Linear Setting, 15-node case with $T = 1000$ (Part II).

15 nodes	Latent confounders		Measurement error		Standardized		Missing		Nonstationary	
	AUROC↑	AUPRC↑	AUROC↑	AUPRC↑	AUROC↑	AUPRC↑	AUROC↑	AUPRC↑	AUROC↑	AUPRC↑
VAR	79.2±7.2	36.9±9.1	82.0±2.0	32.6±2.5	92.6±1.9	83.6±3.8	77.9±3.4	29.0±3.6	90.2±5.0	60.2±13.6
LGC	91.1±2.9	60.0±6.8	81.4±2.0	34.0±2.8	98.3±0.8	84.5±8.2	85.1±2.1	44.7±5.0	85.8±1.9	70.0±5.3
VARLiNGAM	51.8±5.7	15.0±1.7	51.5±3.8	15.1±1.0	51.8±5.8	15.4±1.9	51.6±3.7	15.0±1.3	50.8±3.2	14.6±0.9
PCMCI	85.7±3.7	40.9±5.8	73.8±1.4	46.3±3.4	98.0±0.8	83.4±4.3	82.0±3.4	40.0±6.1	88.2±5.5	46.4±9.6
DYNOTEARS	82.1±3.9	33.5±4.0	86.6±2.7	60.2±2.8	93.2±2.1	84.8±4.2	92.3±1.1	58.2±7.4	89.3±6.0	65.4±19.6
NTS-NOTEARS	73.6±2.1	29.6±2.1	50.0±0.0	14.2±0.0	91.6±2.1	85.0±4.6	50.0±0.0	14.2±0.0	73.3±13.8	51.5±20.1
TSCI	48.3±3.2	15.8±2.0	55.3±4.9	18.3±2.6	57.5±1.8	22.3±1.5	53.7±3.1	18.6±2.6	56.2±5.8	21.5±4.1
cMLP	98.3±1.5	94.5±4.8	78.9±2.6	46.5±7.8	99.8±0.1	98.4±1.7	81.6±3.3	57.5±7.4	90.2±10.0	63.3±18.3
cLSTM	98.1±1.5	94.3±5.4	94.0±1.8	76.4±8.3	100.0±0.0	100.0±0.0	93.1±1.0	78.8±4.1	89.8±19.1	81.6±32.9
CUTS	74.9±3.1	36.8±2.2	82.9±4.0	51.7±10.2	99.7±0.1	98.6±0.8	76.0±4.3	45.5±8.3	93.7±5.4	81.9±12.5
CUTS+	90.0±4.7	64.8±11.5	96.4±1.2	85.3±4.8	99.8±0.1	99.2±0.6	98.4±0.8	93.2±3.5	97.9±2.6	93.8±8.4

Table 27: Nonlinear Setting, 10-node case with $T = 500$ and $F = 10$ (Part I).

10 nodes	Vanilla		Mixed data		Trend and seasonality		Min-max normalization	
	AUROC↑	AUPRC↑	AUROC↑	AUPRC↑	AUROC↑	AUPRC↑	AUROC↑	AUPRC↑
VAR	77.0±3.1	55.5±4.3	59.6±5.6	39.4±4.1	67.3±5.5	56.4±7.3	65.9±5.6	54.6±7.5
LGC	76.9±2.4	62.9±3.8	67.8±3.9	54.1±4.8	76.3±2.5	61.5±5.1	76.0±3.0	65.2±5.9
VARLiNGAM	72.1±6.4	61.1±9.4	66.1±2.7	46.3±2.7	71.5±3.9	60.2±6.2	74.3±6.4	65.0±9.3
PCMCI	71.3±5.2	50.4±7.0	73.8±0.8	52.7±1.4	72.8±5.9	52.2±7.8	71.3±5.2	50.4±7.0
DYNOTEARS	75.8±6.9	65.9±10.5	59.6±2.2	42.8±3.5	75.6±6.4	66.1±9.9	71.0±3.1	53.0±4.1
NTS-NOTEARS	68.8±3.2	44.6±2.6	69.8±0.6	52.7±3.1	51.3±0.4	33.9±0.1	50.0±0.0	33.3±0.0
TSCI	86.3±2.7	77.3±3.3	66.3±5.6	55.7±5.0	65.2±4.8	56.2±3.9	86.3±2.7	77.3±3.3
cMLP	99.7±0.1	99.5±0.2	60.8±4.4	44.2±4.1	51.1±1.0	45.8±1.0	56.0±3.8	40.1±3.5
cLSTM	100.0±0.0	99.9±0.0	59.8±3.5	50.5±4.0	89.0±4.8	81.4±8.1	50.0±3.4	37.6±1.4
CUTS	93.6±1.7	91.6±2.3	65.9±3.4	53.9±5.9	49.5±3.2	40.4±5.3	60.6±4.3	45.3±4.9
CUTS+	99.7±0.2	99.4±0.5	76.6±3.4	68.6±5.1	49.0±4.1	37.1±2.9	82.6±4.6	74.8±7.2

Table 28: Nonlinear Setting, 10-node case with $T = 500$ and $F = 10$ (Part II).

10 nodes	Latent confounders		Measurement error		Standardized		Missing		Nonstationary	
	AUROC↑	AUPRC↑	AUROC↑	AUPRC↑	AUROC↑	AUPRC↑	AUROC↑	AUPRC↑	AUROC↑	AUPRC↑
VAR	54.8±4.0	36.6±3.2	62.8±6.5	44.0±7.4	65.9±5.8	54.6±7.7	64.1±5.2	44.5±6.0	66.8±9.2	46.8±8.0
LGC	55.1±4.1	36.9±3.6	63.1±6.3	44.4±7.2	74.6±2.1	56.2±2.4	64.1±4.8	46.3±6.0	68.5±11.5	52.7±15.0
VARLiNGAM	57.0±5.0	38.4±4.6	55.8±3.9	37.3±3.1	73.6±7.9	63.5±11.4	62.6±4.8	42.7±4.4	60.5±11.5	44.9±13.1
PCMCI	57.0±5.3	38.5±4.7	65.6±5.1	45.6±5.7	71.3±5.2	50.4±7.0	63.5±3.2	47.7±4.6	65.0±8.1	46.1±7.3
DYNOTEARS	57.8±4.0	38.1±2.7	56.4±4.9	37.7±3.6	92.0±4.0	84.0±5.7	63.5±4.0	42.7±3.8	64.6±10.6	47.7±13.1
NTS-NOTEARS	50.0±0.0	33.3±0.0	50.0±0.0	33.3±0.0	98.6±1.6	98.2±2.1	50.0±0.0	33.3±0.0	53.8±7.6	35.6±4.5
TSCI	54.0±4.9	40.0±4.1	56.8±8.6	44.4±7.8	86.3±2.7	77.3±3.3	70.7±6.8	56.7±11.5	71.0±11.2	56.6±13.2
cMLP	62.2±4.8	47.1±4.8	51.7±5.2	38.0±3.5	99.3±0.6	99.0±0.9	76.2±5.8	66.9±6.8	72.1±22.4	64.9±28.0
cLSTM	88.3±1.9	81.8±2.4	72.9±6.2	60.1±7.9	98.9±1.4	98.6±1.5	93.7±2.3	91.5±2.9	74.1±21.5	67.5±27.2
CUTS	68.2±4.7	47.6±4.2	61.0±2.4	49.2±5.0	99.8±0.2	99.6±0.4	75.7±2.3	68.7±3.0	66.8±20.6	58.8±24.2
CUTS+	88.9±3.2	83.6±5.1	85.5±4.6	77.3±7.0	99.9±0.0	99.9±0.1	98.4±0.6	97.4±1.2	80.1±19.1	74.1±22.3

Table 29: Nonlinear Setting, 10-node case with $T = 500$ and $F = 40$ (Part I).

10 nodes	Vanilla		Mixed data		Trend and seasonality		Min-max normalization	
	AUROC↑	AUPRC↑	AUROC↑	AUPRC↑	AUROC↑	AUPRC↑	AUROC↑	AUPRC↑
VAR	68.8±4.1	48.3±4.2	54.8±2.6	38.3±2.8	63.6±5.5	42.2±4.4	68.3±2.9	47.8±2.9
LGC	68.5±3.7	48.0±3.8	61.9±2.7	41.6±2.9	63.8±5.8	42.5±5.0	63.0±4.6	44.6±5.0
VARLiNGAM	61.8±3.8	42.0±3.4	57.3±2.6	38.1±1.5	63.5±0.9	42.6±0.8	62.3±3.3	41.7±2.3
PCMCI	66.1±5.5	47.9±7.6	65.3±5.6	49.3±7.6	64.3±4.3	45.6±4.9	66.1±5.5	47.9±7.6
DYNOTEARS	66.0±2.5	43.6±2.0	56.3±2.3	38.2±2.4	64.4±3.5	42.5±2.9	64.0±4.1	45.0±3.9
NTS-NOTEARS	50.0±0.0	33.3±0.0	60.1±1.7	43.9±2.5	50.0±0.0	33.3±0.0	50.0±0.0	33.3±0.0
TSCI	60.4±3.2	46.8±5.8	52.8±2.1	41.4±4.2	60.4±5.7	48.8±4.7	60.4±3.2	46.8±5.8
cMLP	83.0±3.6	72.5±4.6	54.1±4.8	39.4±3.9	50.9±0.8	45.8±1.5	50.6±3.7	36.2±3.1
cLSTM	94.2±0.4	89.3±0.3	49.9±2.9	37.0±1.4	99.0±0.7	97.9±1.5	48.7±3.1	35.9±0.8
CUTS	85.8±3.7	69.3±6.9	60.9±3.5	45.2±5.1	49.6±3.2	38.9±4.5	58.3±5.8	42.2±5.8
CUTS+	98.8±1.0	97.9±1.8	65.4±1.5	55.0±2.0	50.8±2.6	39.3±2.5	71.1±4.6	63.0±6.1

Table 30: Nonlinear Setting, 10-node case with $T = 500$ and $F = 40$ (Part II).

10 nodes	Latent confounders		Measurement error		Standardized		Missing		Nonstationary	
	AUROC↑	AUPRC↑	AUROC↑	AUPRC↑	AUROC↑	AUPRC↑	AUROC↑	AUPRC↑	AUROC↑	AUPRC↑
VAR	51.8±2.1	34.4±1.2	57.6±2.6	39.3±2.5	69.0±3.6	48.3±3.3	59.0±5.2	38.2±3.1	60.6±9.1	42.3±7.8
LGC	51.8±2.1	34.4±1.2	57.8±2.8	39.5±2.7	68.5±4.0	49.0±5.2	58.8±4.8	38.1±2.9	60.6±9.1	42.3±7.8
VARLiNGAM	52.0±2.0	35.0±1.6	52.0±2.8	35.0±1.9	62.1±1.3	41.6±1.0	53.4±2.7	36.1±2.5	56.0±4.3	37.8±3.0
PCMCI	54.0±2.5	35.7±1.6	60.5±4.7	40.5±4.0	66.1±5.5	47.9±7.6	57.6±5.9	39.2±4.8	60.1±8.9	43.1±10.4
DYNOTEARS	57.6±4.7	38.7±3.3	54.5±2.2	35.9±1.4	72.3±4.2	55.8±6.1	56.1±4.8	37.6±3.2	58.6±7.6	39.1±4.6
NTS-NOTEARS	50.0±0.0	33.3±0.0	50.0±0.0	33.3±0.0	92.5±3.3	83.3±6.0	50.0±0.0	33.3±0.0	50.0±0.0	33.3±0.0
TSCI	52.2±4.5	36.8±4.1	56.1±7.7	42.5±6.3	60.4±3.2	46.8±5.8	61.7±1.8	46.8±4.5	55.6±8.3	40.4±8.0
cMLP	56.4±4.7	41.1±5.8	49.9±1.3	34.6±1.6	95.2±2.2	92.7±2.8	55.7±5.6	41.4±5.4	69.1±21.8	61.5±26.9
cLSTM	49.4±6.1	37.5±5.0	56.5±3.8	41.0±3.9	76.3±2.2	67.9±5.6	71.8±3.6	57.0±4.6	70.9±20.1	63.3±21.7
CUTS	51.0±3.2	37.5±3.6	56.3±9.4	43.3±9.2	98.6±0.7	97.4±1.4	48.7±9.1	39.6±6.9	69.4±15.3	56.4±15.2
CUTS+	58.5±8.5	42.1±9.1	70.2±2.5	60.4±5.9	99.4±0.4	98.9±0.6	86.5±5.4	80.6±3.5	77.3±19.6	71.5±23.8

Table 31: Nonlinear Setting, 10-node case with $T = 1000$ and $F = 40$ (Part I).

10 nodes	Vanilla		Mixed data		Trend and seasonality		Min-max normalization	
	AUROC↑	AUPRC↑	AUROC↑	AUPRC↑	AUROC↑	AUPRC↑	AUROC↑	AUPRC↑
VAR	73.0±2.0	58.5±3.1	62.1±1.3	42.0±1.3	68.5±3.2	49.7±4.3	73.6±2.3	60.0±5.0
LGC	72.8±2.2	58.7±4.2	66.3±3.2	47.2±3.3	68.5±2.4	49.9±3.6	70.5±4.2	57.1±6.1
VARLiNGAM	65.5±2.7	45.0±3.0	63.0±2.9	43.0±2.7	68.6±2.1	50.5±3.0	66.1±2.1	45.6±2.6
PCMCI	75.5±1.5	59.8±4.0	75.1±4.8	60.9±6.1	66.6±1.8	45.9±1.4	75.5±1.5	59.8±4.0
DYNOTEARS	69.6±2.8	50.1±3.5	56.5±2.4	39.1±2.8	70.6±2.4	50.7±3.6	70.0±4.6	58.0±7.4
NTS-NOTEARS	50.1±0.3	33.4±0.1	57.3±0.9	42.1±2.2	50.0±0.0	33.3±0.0	50.0±0.0	33.3±0.0
TSCI	71.3±4.6	56.1±4.6	59.8±1.7	43.7±2.1	60.6±5.5	47.1±4.2	71.3±4.6	56.1±4.6
cMLP	87.8±3.4	81.5±5.1	53.2±4.0	38.7±3.8	51.0±1.0	45.8±1.3	50.5±3.4	35.5±2.9
cLSTM	93.1±0.4	87.9±0.9	50.0±2.8	37.0±1.1	96.9±1.5	94.6±2.4	48.8±3.1	36.0±0.7
CUTS	90.2±2.1	76.0±6.1	57.9±3.8	45.6±6.2	52.3±3.5	41.9±2.5	57.8±7.6	41.1±6.4
CUTS+	99.8±0.1	99.7±0.2	70.0±2.5	61.7±2.5	52.2±2.2	38.7±2.3	81.9±4.1	76.7±5.3

Table 32: Nonlinear Setting, 10-node case with $T = 1000$ and $F = 40$ (Part II).

10 nodes	Latent confounders		Measurement error		Standardized		Missing		Nonstationary	
	AUROC↑	AUPRC↑	AUROC↑	AUPRC↑	AUROC↑	AUPRC↑	AUROC↑	AUPRC↑	AUROC↑	AUPRC↑
VAR	50.6±5.1	34.0±2.2	61.9±3.5	40.8±2.7	72.8±2.2	58.7±4.2	62.8±4.0	41.3±3.2	60.5±9.7	44.7±11.1
LGC	50.6±5.1	34.0±2.2	62.3±3.2	41.1±2.5	75.6±4.9	57.4±7.2	63.6±3.6	42.0±2.9	60.5±9.7	44.7±11.1
VARLiNGAM	53.3±1.5	36.5±2.1	53.9±3.5	36.6±3.2	66.6±3.4	46.4±4.1	52.6±2.5	35.3±1.6	54.8±7.6	37.1±5.1
PCMCI	51.8±2.7	34.4±1.5	62.1±5.9	42.7±6.0	75.5±1.5	59.8±4.0	63.5±5.4	43.9±5.7	62.5±10.3	46.1±12.4
DYNOTEARS	54.1±1.9	36.5±1.9	54.0±2.1	36.9±2.1	78.6±1.7	69.2±2.5	55.4±4.3	38.7±4.5	59.0±9.7	41.2±7.8
NTS-NOTEARS	50.0±0.0	33.3±0.0	50.0±0.0	33.3±0.0	87.5±5.7	77.8±7.2	50.0±0.0	33.3±0.0	50.0±0.0	33.3±0.0
TSCI	55.9±6.3	40.4±4.7	52.3±7.1	35.1±4.3	71.3±4.6	56.1±4.6	60.2±6.7	44.7±6.6	60.5±7.7	48.6±7.6
cMLP	53.2±3.2	38.9±3.4	52.6±3.4	39.7±3.3	98.6±1.3	97.7±2.1	57.6±4.9	43.1±6.9	74.5±20.8	66.3±27.7
cLSTM	53.8±2.0	39.7±3.7	60.7±6.9	48.7±6.9	78.1±5.1	72.3±6.8	76.5±4.3	69.2±5.0	72.0±20.9	63.9±24.6
CUTS	52.3±6.3	37.2±5.1	56.7±5.0	44.1±5.2	99.7±0.3	99.5±0.6	52.8±3.7	41.3±4.1	70.0±19.9	56.1±17.8
CUTS+	53.2±5.0	39.5±3.2	78.8±4.8	67.9±6.6	99.9±0.0	99.8±0.1	95.7±1.9	93.8±2.8	80.1±20.0	75.2±24.9

Table 33: Nonlinear Setting, 15-node case with $T = 500$ and $F = 10$ (Part I).

15 nodes	Vanilla		Mixed data		Trend and seasonality		Min-max normalization	
	AUROC↑	AUPRC↑	AUROC↑	AUPRC↑	AUROC↑	AUPRC↑	AUROC↑	AUPRC↑
VAR	80.8±3.6	46.8±4.8	62.2±2.9	27.7±1.8	80.6±1.8	46.3±2.5	81.0±3.7	47.0±4.8
LGC	78.8±4.5	58.4±5.2	69.9±2.7	50.3±5.2	78.4±4.2	58.3±4.6	78.7±4.8	63.5±7.0
VARLiNGAM	65.3±4.4	42.8±5.3	66.3±2.1	32.3±1.9	66.9±2.5	46.3±3.4	65.7±3.8	44.1±4.5
PCMCI	79.3±4.3	51.7±8.0	70.7±3.3	43.5±5.2	81.3±2.7	53.9±5.7	79.3±4.3	51.7±8.0
DYNOTEARS	89.5±3.0	64.7±5.6	60.8±2.0	31.9±3.1	89.1±4.0	64.5±6.8	74.1±4.1	48.2±6.6
NTS-NOTEARS	75.8±2.6	36.2±2.3	69.7±1.6	40.0±3.6	51.3±0.4	21.9±0.1	50.0±0.0	21.4±0.0
TSCI	89.8±2.8	74.2±4.7	69.7±4.9	47.0±5.7	65.1±5.5	44.2±5.7	89.8±2.8	74.2±4.7
cMLP	99.9±0.0	99.8±0.1	64.8±5.2	39.5±7.4	52.0±0.6	30.4±0.8	55.6±6.2	26.9±4.2
cLSTM	99.9±0.0	99.9±0.0	61.7±9.7	39.8±10.3	84.3±4.0	55.4±9.8	51.7±10.4	25.1±6.3
CUTS	90.0±2.0	82.5±2.7	62.5±1.3	39.2±1.4	55.2±3.1	26.5±1.8	60.2±1.0	34.9±5.4
CUTS+	99.7±0.1	99.2±0.5	79.3±1.4	60.9±4.4	48.8±1.6	23.4±2.0	86.7±2.6	73.0±8.3

Table 34: Nonlinear Setting, 15-node case with $T = 500$ and $F = 10$ (Part II).

15 nodes	Latent confounders		Measurement error		Standardized		Missing		Nonstationary	
	AUROC↑	AUPRC↑	AUROC↑	AUPRC↑	AUROC↑	AUPRC↑	AUROC↑	AUPRC↑	AUROC↑	AUPRC↑
VAR	55.7±3.7	24.3±2.1	62.9±2.4	30.9±2.6	81.1±3.2	46.9±4.2	69.7±1.9	37.3±2.7	59.6±13.8	28.7±11.7
LGC	54.9±3.3	24.2±2.6	63.2±2.9	31.8±3.8	81.4±3.1	47.0±5.1	68.4±2.1	40.5±3.3	58.9±12.7	30.3±15.1
VARLiNGAM	52.4±2.8	24.2±3.9	56.9±1.4	25.4±1.2	65.2±3.2	42.8±3.2	68.9±4.1	35.0±4.7	57.1±7.3	26.9±6.9
PCMCI	54.6±4.6	23.6±2.4	65.6±2.9	32.0±3.1	79.3±4.3	51.7±8.0	75.0±3.1	44.6±4.6	60.3±11.5	31.0±12.9
DYNOTEARS	60.7±2.5	27.4±1.9	60.1±2.8	27.4±2.5	92.9±2.9	79.9±5.5	63.2±4.6	35.1±6.9	59.7±14.6	30.5±16.5
NTS-NOTEARS	50.0±0.0	21.4±0.0	50.0±0.0	21.4±0.0	99.8±0.2	99.1±1.7	50.0±0.0	21.4±0.0	53.8±7.7	23.3±3.7
TSCI	50.8±8.1	24.9±6.4	61.1±6.8	32.8±4.9	89.8±2.8	74.2±4.7	74.3±1.9	47.6±4.5	64.8±17.8	42.0±23.7
cMLP	55.4±4.1	28.5±1.2	59.0±3.7	30.5±4.3	99.9±0.0	99.9±0.0	85.8±3.2	68.6±5.1	77.9±19.2	60.0±30.4
cLSTM	71.5±6.4	46.9±11.8	73.3±2.1	49.7±3.1	98.4±0.9	96.7±1.6	94.6±2.6	88.2±5.2	77.6±16.9	57.8±30.3
CUTS	50.3±5.2	23.5±4.1	67.1±3.9	43.6±5.9	99.7±0.3	99.3±0.6	73.2±2.1	55.6±4.9	63.0±17.7	42.5±23.9
CUTS+	63.8±4.3	35.2±5.8	91.4±2.1	79.6±4.1	99.8±0.2	99.2±0.8	97.4±0.7	92.5±1.7	86.7±9.2	71.4±18.7

Table 35: Nonlinear Setting, 15-node case with $T = 500$ and $F = 40$ (Part I).

15 nodes	Vanilla		Mixed data		Trend and seasonality		Min-max normalization	
	AUROC↑	AUPRC↑	AUROC↑	AUPRC↑	AUROC↑	AUPRC↑	AUROC↑	AUPRC↑
VAR	69.5±5.3	37.5±6.4	54.6±1.1	26.6±2.1	67.3±3.3	33.4±3.1	69.3±3.4	36.6±4.1
LGC	69.7±5.3	37.9±6.4	62.7±1.1	29.5±1.6	67.3±3.3	33.5±3.3	59.4±3.0	34.4±4.4
VARLiNGAM	62.8±1.8	31.0±1.6	59.7±4.8	28.7±4.8	64.4±3.3	36.8±5.2	63.6±2.2	31.8±2.3
PCMCI	65.9±3.2	38.2±5.3	64.8±3.0	38.0±4.7	63.7±3.5	33.1±4.6	65.9±3.2	38.2±5.3
DYNOTEARS	71.5±3.4	36.7±3.3	59.0±0.9	26.7±0.8	71.6±3.2	36.4±3.1	68.0±2.7	39.7±4.1
NTS-NOTEARS	50.0±0.0	21.4±0.0	58.2±1.8	28.1±1.6	50.0±0.0	21.4±0.0	50.0±0.0	21.4±0.0
TSCI	66.0±5.3	38.3±6.0	55.4±2.3	28.3±1.8	60.7±5.7	35.5±8.9	66.0±5.3	38.3±6.0
cMLP	80.6±2.0	59.5±6.8	53.7±5.7	27.7±3.6	51.8±0.5	30.3±0.7	52.0±4.3	22.9±1.5
cLSTM	99.1±0.2	96.9±0.7	51.9±9.8	25.2±5.9	98.9±0.5	96.8±1.6	50.6±10.1	24.3±5.7
CUTS	87.5±2.2	65.6±5.7	55.3±2.3	30.0±4.3	54.6±2.1	26.6±2.8	53.4±2.8	24.8±1.8
CUTS+	97.8±1.2	95.1±1.5	64.9±2.8	41.0±2.5	55.0±2.4	26.4±3.3	66.2±3.6	39.0±5.0

Table 36: Nonlinear Setting, 15-node case with $T = 500$ and $F = 40$ (Part II).

15 nodes	Latent confounders		Measurement error		Standardized		Missing		Nonstationary	
	AUROC↑	AUPRC↑	AUROC↑	AUPRC↑	AUROC↑	AUPRC↑	AUROC↑	AUPRC↑	AUROC↑	AUPRC↑
VAR	53.2±3.9	22.7±1.3	54.6±2.2	24.0±1.6	69.9±4.0	37.7±4.9	59.5±2.8	28.2±2.9	55.5±7.1	24.3±3.5
LGC	53.2±3.9	22.7±1.3	54.6±2.2	24.0±1.6	68.2±1.8	38.1±4.4	59.0±2.5	27.9±2.4	54.3±6.4	24.0±3.4
VARLiNGAM	50.2±1.3	21.8±0.7	52.4±2.7	23.3±2.3	63.5±2.4	31.9±2.6	51.7±1.7	23.1±2.5	55.3±5.5	25.1±4.0
PCMCI	52.9±2.4	22.9±1.5	57.5±4.2	26.3±3.8	65.9±3.2	38.2±5.3	55.7±3.4	27.2±4.3	55.0±5.3	25.5±4.4
DYNOTEARS	53.2±3.7	23.2±2.4	57.5±2.5	25.6±1.7	67.3±0.8	47.7±1.8	57.8±1.8	25.8±1.4	56.0±10.3	25.7±6.2
NTS-NOTEARS	50.0±0.0	21.4±0.0	50.0±0.0	21.4±0.0	92.3±3.0	76.5±5.0	50.0±0.0	21.4±0.0	50.0±0.0	21.4±0.0
TSCI	54.5±4.2	25.8±1.8	46.2±6.0	24.1±5.8	66.0±5.3	38.3±6.0	54.1±2.2	26.5±1.9	52.7±7.1	26.0±6.5
cMLP	56.6±5.3	28.4±4.6	51.4±3.3	24.2±1.2	97.3±1.1	93.2±2.8	57.1±3.1	27.6±2.1	68.6±21.6	48.7±30.9
cLSTM	50.7±4.2	23.2±3.2	63.5±6.3	35.1±7.0	74.6±5.3	55.4±7.4	73.4±2.2	48.2±2.0	72.5±20.5	54.6±32.0
CUTS	49.3±2.9	23.1±2.8	56.4±7.5	28.8±6.5	97.2±0.5	93.5±1.0	55.2±4.0	28.3±5.0	63.6±14.9	36.2±17.2
CUTS+	55.1±2.7	28.2±4.3	66.3±2.9	43.3±5.3	98.2±0.2	95.0±0.6	85.4±4.7	70.5±6.9	69.9±20.5	50.2±30.7

Table 37: Nonlinear Setting, 15-node case with $T = 1000$ and $F = 10$ (Part I).

15 nodes	Vanilla		Mixed data		Trend and seasonality		Min–max normalization	
	AUROC↑	AUPRC↑	AUROC↑	AUPRC↑	AUROC↑	AUPRC↑	AUROC↑	AUPRC↑
VAR	88.8±1.6	70.6±6.0	64.0±2.0	29.5±1.6	88.2±1.5	70.4±4.4	88.7±1.4	69.6±3.3
LGC	85.2±2.1	74.3±3.8	76.0±3.1	52.3±5.3	83.4±1.7	70.3±3.1	90.5±0.4	77.3±2.0
VARLiNGAM	73.2±1.7	54.4±4.0	74.4±2.5	40.1±3.1	72.8±0.3	53.8±2.5	72.9±1.1	54.5±3.5
PCMCI	83.0±2.3	53.2±3.7	79.8±2.7	55.3±3.5	88.5±1.3	62.0±2.4	83.0±2.3	53.2±3.7
DYNOTEARS	96.4±0.7	85.9±2.7	65.3±1.7	35.1±1.8	94.4±1.1	82.4±2.3	66.2±0.5	46.9±0.8
NTS-NOTEARS	86.6±0.5	50.5±1.0	70.9±1.7	47.0±5.2	53.6±1.9	22.7±0.7	50.0±0.0	21.4±0.0
TSCI	93.9±0.3	79.6±1.4	71.9±1.5	49.8±1.7	52.7±5.1	24.7±4.5	93.9±0.3	79.6±1.4
cMLP	100.0±0.0	100.0±0.0	64.6±5.5	39.3±6.0	52.1±0.5	30.3±0.5	54.4±6.1	26.1±4.0
cLSTM	100.0±0.0	100.0±0.0	61.8±8.8	38.6±9.2	61.4±4.9	33.6±2.5	51.5±10.2	24.8±6.0
CUTS	97.6±1.4	95.0±2.2	63.5±2.8	39.6±2.1	46.0±5.5	27.2±5.7	63.0±2.7	36.3±1.5
CUTS+	99.9±0.0	99.8±0.1	75.6±2.5	62.1±5.0	50.8±2.7	24.6±1.7	80.0±1.0	67.3±2.5

Table 38: Nonlinear Setting, 15-node case with $T = 1000$ and $F = 10$ (Part II).

15 nodes	Latent confounders		Measurement error		Standardized		Missing		Nonstationary	
	AUROC↑	AUPRC↑	AUROC↑	AUPRC↑	AUROC↑	AUPRC↑	AUROC↑	AUPRC↑	AUROC↑	AUPRC↑
VAR	57.7±4.2	24.9±2.1	74.6±4.0	36.6±3.6	88.4±2.3	69.4±6.1	65.4±3.9	39.7±6.2	61.5±6.8	29.0±5.3
LGC	57.8±4.0	24.9±2.1	75.5±4.5	38.0±4.4	85.5±2.1	69.4±3.9	84.5±3.7	53.1±5.9	61.4±7.0	30.6±8.2
VARLiNGAM	55.6±2.2	25.8±2.2	65.2±2.9	32.3±2.5	74.0±1.8	56.2±4.3	73.4±3.9	38.9±3.9	60.8±6.5	29.3±6.8
PCMCI	57.8±3.6	25.7±2.2	77.3±0.6	44.6±1.3	83.0±2.3	53.2±3.7	84.2±4.1	53.8±6.0	68.5±6.9	34.4±6.6
DYNOTEARS	59.0±2.3	28.9±2.6	59.5±2.5	31.5±3.5	98.3±1.0	97.1±1.3	78.9±5.2	46.9±8.0	60.6±9.2	30.9±13.4
NTS-NOTEARS	50.0±0.0	21.4±0.0	50.0±0.0	21.4±0.0	99.8±0.2	99.1±1.7	50.0±0.0	21.4±0.0	50.0±0.0	21.4±0.0
TSCI	56.5±4.1	27.5±2.8	60.7±6.8	32.3±5.7	93.9±0.3	79.6±1.4	82.1±1.7	59.8±3.3	73.1±16.3	49.9±25.6
cMLP	56.0±4.1	26.6±1.7	61.8±2.3	30.7±3.3	100.0±0.0	100.0±0.0	92.7±1.4	78.9±5.6	83.7±14.0	69.1±23.0
cLSTM	78.1±3.4	56.9±6.6	81.6±2.1	62.6±3.5	99.5±0.3	98.7±0.6	99.1±0.2	97.5±0.5	82.1±11.3	64.2±20.3
CUTS	51.7±3.2	26.2±2.2	71.2±3.6	48.0±4.6	100.0±0.0	100.0±0.0	87.1±2.6	73.9±5.7	69.1±15.5	47.0±26.0
CUTS+	79.4±4.1	56.8±7.0	96.7±1.9	92.3±2.8	100.0±0.0	100.0±0.0	99.8±0.1	99.4±0.5	93.4±3.7	84.0±7.7

Table 39: Nonlinear Setting, 15-node case with $T = 1000$ and $F = 40$ (Part I).

15 nodes	Vanilla		Mixed data		Trend and seasonality		Min–max normalization	
	AUROC↑	AUPRC↑	AUROC↑	AUPRC↑	AUROC↑	AUPRC↑	AUROC↑	AUPRC↑
VAR	74.6±3.7	52.7±6.2	62.9±3.9	29.6±3.5	72.0±2.4	45.8±3.6	72.7±1.5	50.5±2.7
LGC	74.3±3.5	52.6±6.0	67.4±2.5	37.1±3.0	72.1±2.5	46.3±4.1	69.6±2.1	48.0±4.6
VARLiNGAM	67.9±1.8	35.5±2.3	65.0±4.7	33.4±5.8	68.3±1.8	40.4±2.4	67.8±1.6	35.0±1.8
PCMCI	76.8±3.2	51.1±5.6	74.1±3.3	49.4±6.4	72.3±2.0	41.4±2.8	76.8±3.2	51.1±5.6
DYNOTEARS	76.0±1.4	48.5±3.5	61.6±2.5	28.6±2.3	76.3±2.6	48.9±4.5	70.1±0.8	49.8±3.6
NTS-NOTEARS	50.0±0.0	21.4±0.0	57.6±0.8	30.7±1.0	50.0±0.0	21.4±0.0	50.0±0.0	21.4±0.0
TSCI	75.7±3.1	51.1±2.6	59.8±1.8	34.5±2.5	57.5±4.1	30.5±3.4	75.7±3.1	51.1±2.6
cMLP	91.8±1.0	79.4±2.2	54.2±5.2	28.4±4.8	51.9±0.5	30.4±0.8	51.7±4.2	22.8±1.4
cLSTM	97.9±0.2	92.8±1.0	52.1±10.1	25.2±5.6	91.7±1.5	72.4±7.3	50.5±10.1	24.2±5.6
CUTS	94.8±0.6	79.1±4.3	58.0±3.7	34.2±5.0	46.2±3.8	30.0±6.4	52.0±4.0	24.6±1.9
CUTS+	99.8±0.1	99.5±0.3	71.6±1.3	53.2±3.9	54.7±2.0	27.6±3.6	79.1±2.9	64.2±5.3

Table 40: Nonlinear Setting, 15-node case with $T = 1000$ and $F = 40$ (Part II).

15 nodes	Latent confounders		Measurement error		Standardized		Missing		Nonstationary	
	AUROC↑	AUPRC↑	AUROC↑	AUPRC↑	AUROC↑	AUPRC↑	AUROC↑	AUPRC↑	AUROC↑	AUPRC↑
VAR	54.1±4.2	23.2±1.6	60.7±3.4	26.8±2.0	74.1±2.9	52.3±5.4	65.3±3.1	29.8±2.5	57.5±8.7	30.0±13.7
LGC	54.3±4.3	23.2±1.6	61.0±3.5	27.0±2.1	73.3±2.2	50.8±4.7	65.6±3.1	30.0±2.5	57.6±8.7	30.2±13.6
VARLiNGAM	52.8±1.9	23.8±1.8	53.7±3.0	24.5±2.5	66.5±1.8	36.4±1.9	53.6±0.6	24.1±0.9	57.3±6.7	26.8±6.9
PCMCI	55.2±2.8	23.6±1.3	63.8±3.1	29.3±2.3	76.8±3.2	51.1±5.6	62.1±2.5	29.4±2.3	60.7±11.4	31.0±14.2
DYNOTEARS	56.4±2.2	28.4±3.4	60.3±2.0	26.0±1.1	76.2±1.8	59.3±3.9	61.4±4.2	26.8±2.6	59.9±8.1	29.7±9.7
NTS-NOTEARS	50.0±0.0	21.4±0.0	50.0±0.0	21.4±0.0	90.4±4.9	79.0±7.9	50.0±0.0	21.4±0.0	50.0±0.0	21.4±0.0
TSCI	52.1±6.4	25.0±4.7	53.0±5.1	26.9±3.0	75.7±3.1	51.1±2.6	56.0±4.0	28.8±4.0	61.8±9.7	36.4±11.0
cMLP	55.6±5.3	26.3±4.2	56.5±3.7	27.8±2.9	99.3±0.2	97.7±0.9	61.4±4.2	31.8±2.8	64.8±18.3	44.2±26.8
cLSTM	50.3±4.0	23.1±2.5	65.6±3.1	37.9±6.0	80.1±6.4	66.1±8.4	78.7±2.7	62.1±3.4	77.8±11.4	58.0±20.1
CUTS	49.5±4.4	24.0±2.9	60.6±3.3	30.6±4.0	99.7±0.1	99.2±0.5	65.0±3.9	33.4±4.0	63.2±16.2	36.6±22.3
CUTS+	53.8±4.8	27.3±4.4	79.4±2.8	61.8±6.2	99.8±0.0	99.4±0.3	95.8±1.8	89.2±5.0	86.0±7.7	70.7±15.2

Table 41: Linear Setting, 10-node case with $T = 500$ (Part I). Hyperparameters are selected to maximize average performance across all scenarios.

10 nodes	Vanilla		Mixed data		Trend and seasonality		Min–max normalization	
	AUROC↑	AUPRC↑	AUROC↑	AUPRC↑	AUROC↑	AUPRC↑	AUROC↑	AUPRC↑
VAR	95.2±1.0	57.3±5.0	70.8±7.5	20.4±4.8	57.8±2.0	12.9±0.5	95.2±0.7	57.0±3.8
LGC	97.6±1.1	73.6±9.1	82.1±8.1	51.0±10.3	51.2±4.2	12.4±2.2	97.1±1.0	69.3±7.4
VARLiNGAM	53.9±6.1	12.7±2.0	52.1±8.5	12.7±1.3	49.6±2.2	11.0±0.4	53.8±6.1	12.6±1.9
PCMCI	97.8±0.8	75.3±6.8	89.4±2.4	66.1±8.9	54.3±4.2	12.1±0.9	97.8±0.8	75.3±6.8
DYNOTEARS	100.0±0.0	100.0±0.0	75.2±7.5	25.7±7.0	56.4±8.1	13.2±2.7	99.8±0.2	98.1±3.6
NTS-NOTEARS	59.0±12.0	27.1±21.3	73.5±5.8	32.1±7.6	50.0±0.6	11.1±0.1	85.0±12.6	73.3±22.4
TSCI	64.5±12.1	23.5±10.4	52.0±12.0	19.9±7.3	56.7±12.1	19.6±6.5	64.5±12.1	23.5±10.4
cMLP	92.2±6.7	75.5±14.6	77.6±5.7	46.0±6.8	50.7±3.5	18.2±3.4	97.9±2.9	91.1±11.3
cLSTM	100.0±0.0	100.0±0.0	93.3±3.5	74.8±9.5	57.9±9.5	17.6±5.6	100.0±0.0	100.0±0.0
CUTS	92.3±3.8	74.1±11.4	57.4±9.4	20.9±8.9	49.2±11.4	14.3±5.1	53.5±14.3	21.0±13.8
CUTS+	99.6±0.3	97.3±2.7	77.6±3.6	41.7±6.6	55.1±7.8	16.7±3.9	88.2±5.8	59.1±10.5

Table 42: Linear Setting, 10-node case with $T = 500$ (Part II). Hyperparameters are selected to maximize average performance across all scenarios.

10 nodes	Latent confounders		Measurement error		Standardized		Missing		Nonstationary	
	AUROC↑	AUPRC↑	AUROC↑	AUPRC↑	AUROC↑	AUPRC↑	AUROC↑	AUPRC↑	AUROC↑	AUPRC↑
VAR	74.1±2.5	19.9±2.0	90.7±2.3	46.3±3.5	94.6±1.1	54.3±5.5	86.0±6.2	42.9±12.8	78.8±8.2	25.4±8.7
LGC	86.0±5.0	41.9±15.2	85.8±5.5	47.5±9.9	99.3±0.5	91.5±7.4	85.7±6.5	55.1±14.3	90.4±9.9	59.3±31.2
VARLiNGAM	45.3±8.1	10.6±1.2	53.0±7.7	12.5±1.8	53.9±6.1	12.7±2.0	54.2±11.5	14.1±2.8	50.1±5.1	11.3±1.1
PCMCI	81.7±5.9	27.6±8.2	85.6±8.1	54.8±15.3	97.8±0.8	75.3±6.8	80.7±8.3	47.6±14.4	83.5±8.1	35.4±16.7
DYNOTEARS	87.5±3.8	35.8±5.1	90.3±5.3	60.3±11.6	94.8±0.9	55.3±4.9	78.8±13.2	61.0±24.1	85.2±8.2	34.2±11.9
NTS-NOTEARS	67.8±10.7	22.3±9.9	55.0±6.3	20.0±11.2	50.2±0.3	11.1±0.0	50.0±0.0	11.1±0.0	68.6±17.5	36.9±30.2
TSCI	52.2±10.2	17.5±5.6	48.9±7.1	13.4±2.4	64.5±12.1	23.5±10.4	63.6±4.5	21.0±6.7	54.1±6.4	17.6±4.3
cMLP	95.4±3.1	84.6±9.0	81.9±7.3	50.7±13.0	55.3±3.6	17.7±4.4	82.4±9.1	51.8±17.5	80.0±15.4	48.5±27.3
cLSTM	98.5±2.4	95.6±5.8	98.1±1.9	89.2±10.2	63.2±7.3	24.3±4.9	99.5±0.4	96.5±4.0	83.9±14.2	59.3±30.7
CUTS	64.4±6.8	32.7±7.8	91.9±2.5	66.4±8.2	98.8±0.6	93.0±3.3	84.5±5.3	57.4±13.3	96.2±2.2	78.5±13.9
CUTS+	90.9±5.2	58.8±18.0	96.9±1.3	84.2±6.8	99.1±0.4	93.6±3.7	98.6±0.7	89.8±6.7	99.0±0.4	93.1±3.8

Table 43: Linear Setting, 10-node case with $T = 1000$ (Part I). Hyperparameters are selected to maximize average performance across all scenarios.

10 nodes	Vanilla		Mixed data		Trend and seasonality		Min–max normalization	
	AUROC↑	AUPRC↑	AUROC↑	AUPRC↑	AUROC↑	AUPRC↑	AUROC↑	AUPRC↑
VAR	99.7±0.3	96.3±4.4	74.5±5.9	24.3±5.1	58.7±2.2	13.1±0.6	99.6±0.5	94.8±6.7
LGC	100.0±0.0	100.0±0.0	82.5±7.0	57.9±15.1	50.0±0.0	11.1±0.0	99.8±0.2	98.1±3.6
VARLiNGAM	48.3±4.8	11.5±0.5	52.7±6.5	12.5±2.0	50.1±3.8	11.1±0.6	47.8±4.4	11.3±0.4
PCMCI	98.2±0.9	79.1±8.8	96.7±1.9	72.2±5.8	55.0±3.4	12.2±0.7	98.2±0.9	79.1±8.8
DYNOTEARS	100.0±0.0	100.0±0.0	79.1±5.7	34.1±7.9	57.3±5.5	13.5±2.1	100.0±0.0	100.0±0.0
NTS-NOTEARS	50.0±0.0	11.1±0.0	60.8±2.0	29.3±4.9	50.0±0.0	11.1±0.0	50.0±0.0	11.1±0.0
TSCI	58.8±6.7	27.0±9.3	55.0±6.7	19.0±5.8	55.3±9.5	20.0±6.7	58.8±6.7	27.0±9.3
cMLP	94.0±4.7	76.0±7.7	84.8±5.7	61.2±11.2	50.7±3.5	18.2±3.4	98.4±1.2	92.5±4.0
cLSTM	100.0±0.0	100.0±0.0	98.5±0.8	90.8±3.2	52.3±7.4	15.1±4.2	100.0±0.0	100.0±0.0
CUTS	96.8±1.3	80.8±8.9	57.4±11.0	20.0±8.1	46.1±6.1	14.4±3.8	54.1±7.3	16.6±4.6
CUTS+	100.0±0.0	100.0±0.0	75.0±6.6	45.4±7.4	49.7±3.0	14.5±1.7	91.3±4.4	54.4±21.4

Table 44: Linear Setting, 10-node case with $T = 1000$ (Part II). Hyperparameters are selected to maximize average performance across all scenarios.

10 nodes	Latent confounders		Measurement error		Standardized		Missing		Nonstationary	
	AUROC↑	AUPRC↑	AUROC↑	AUPRC↑	AUROC↑	AUPRC↑	AUROC↑	AUPRC↑	AUROC↑	AUPRC↑
VAR	83.3±6.5	29.3±6.7	85.2±8.9	65.6±18.8	99.7±0.3	96.3±4.4	77.3±5.4	53.9±12.8	92.7±2.6	48.4±10.9
LGC	87.6±7.4	38.7±13.7	84.5±7.4	66.9±17.4	100.0±0.0	100.0±0.0	76.0±5.8	57.3±10.3	97.7±2.2	78.6±19.1
VARLiNGAM	48.6±3.8	10.9±0.6	58.2±5.1	13.7±1.8	48.3±4.8	11.5±0.5	51.6±5.7	12.0±2.0	48.0±5.3	11.0±1.0
PCMCI	73.5±5.4	19.5±3.1	91.3±6.0	68.5±11.9	98.2±0.9	79.1±8.8	93.3±4.5	66.0±14.7	85.1±5.9	32.2±9.5
DYNOTEARS	89.1±7.4	42.3±10.3	76.8±9.3	57.4±17.1	99.8±0.2	98.1±3.6	63.9±2.0	36.0±3.5	95.8±3.2	66.2±20.0
NTS-NOTEARS	67.0±6.1	24.5±7.6	50.0±0.0	11.1±0.0	99.8±0.2	98.1±3.6	50.0±0.0	11.1±0.0	80.6±18.8	53.9±33.2
TSCI	57.3±8.8	18.9±2.3	44.9±8.7	11.2±2.1	58.8±6.7	27.0±9.3	54.0±9.8	17.1±8.8	69.0±10.0	27.0±9.5
cMLP	97.3±3.5	91.5±8.7	84.3±6.2	54.3±11.6	51.6±10.4	16.9±5.0	79.0±6.8	44.7±12.3	76.5±18.0	49.6±32.3
cLSTM	99.4±0.6	97.1±3.2	99.6±0.1	97.9±0.8	74.6±5.8	33.1±8.9	99.8±0.2	98.6±1.9	85.9±16.9	62.6±33.0
CUTS	70.3±12.2	44.5±11.8	90.4±2.7	60.4±14.4	99.9±0.2	99.3±1.3	76.7±11.6	49.4±15.2	98.3±1.5	92.6±6.8
CUTS+	92.7±5.4	65.6±20.3	99.4±0.2	96.0±2.0	99.9±0.0	99.8±0.3	99.9±0.0	99.4±0.4	99.9±0.1	99.4±0.6

Table 45: Linear Setting, 15-node case with $T = 500$ (Part I). Hyperparameters are selected to maximize average performance across all scenarios.

15 nodes	Vanilla		Mixed data		Trend and seasonality		Min–max normalization	
	AUROC↑	AUPRC↑	AUROC↑	AUPRC↑	AUROC↑	AUPRC↑	AUROC↑	AUPRC↑
VAR	90.7±3.2	59.6±8.1	66.5±6.0	22.3±3.9	66.6±3.2	20.4±1.7	89.6±4.6	57.6±9.6
LGC	91.8±2.5	72.0±4.9	71.4±5.2	42.1±7.2	50.0±0.0	14.2±0.0	87.1±5.9	59.3±8.7
VARLiNGAM	51.1±4.6	15.0±1.3	50.9±5.6	15.2±2.4	47.3±4.9	13.8±0.7	50.5±2.8	14.6±0.7
PCMCI	89.1±4.7	71.2±9.7	77.8±5.1	51.6±10.6	56.5±3.3	16.2±1.1	89.1±4.7	71.2±9.7
DYNOTEARS	77.8±6.0	61.0±11.3	69.6±4.8	25.8±3.8	55.0±3.2	16.6±1.8	86.6±4.4	73.4±9.5
NTS-NOTEARS	50.0±0.0	14.2±0.0	50.0±0.0	14.2±0.0	49.7±0.5	14.2±0.1	50.0±0.0	14.2±0.0
TSCI	58.7±4.8	20.1±3.3	51.5±3.6	16.5±0.9	52.9±2.1	17.9±2.6	58.7±4.8	20.1±3.3
cMLP	96.8±1.6	90.3±3.7	53.7±1.8	16.2±0.8	51.1±1.6	16.0±1.2	94.9±1.8	82.3±5.6
cLSTM	95.5±1.6	85.1±3.7	78.5±2.0	49.0±2.4	46.9±4.8	15.2±2.2	98.9±0.6	95.5±2.4
CUTS	85.9±5.1	52.5±10.7	55.5±3.5	20.3±1.5	46.6±6.4	14.7±4.0	50.5±3.4	16.7±3.5
CUTS+	97.6±1.3	90.6±3.6	68.3±2.6	33.5±6.4	52.9±5.4	16.9±3.0	77.9±3.4	42.8±6.1

Table 46: Linear Setting, 15-node case with $T = 500$ (Part II). Hyperparameters are selected to maximize average performance across all scenarios.

15 nodes	Latent confounders		Measurement error		Standardized		Missing		Nonstationary	
	AUROC↑	AUPRC↑	AUROC↑	AUPRC↑	AUROC↑	AUPRC↑	AUROC↑	AUPRC↑	AUROC↑	AUPRC↑
VAR	74.1±4.0	25.6±2.6	68.1±3.8	28.1±3.9	91.0±4.3	60.3±10.7	60.1±1.4	19.7±1.2	77.3±8.1	30.9±8.1
LGC	72.5±5.6	46.6±9.5	54.7±2.6	18.8±2.7	81.7±6.0	66.8±12.2	58.6±1.6	21.4±1.9	83.0±7.9	56.8±19.4
VARLiNGAM	51.4±1.1	14.6±0.3	50.8±4.2	15.2±1.3	51.6±3.7	15.0±1.2	50.0±2.1	14.5±0.6	47.5±3.7	13.8±0.7
PCMCI	83.4±3.5	42.7±4.6	64.1±3.0	28.0±3.8	89.1±4.7	71.2±9.7	60.8±3.5	25.0±4.3	82.8±5.5	41.1±9.8
DYNOTEARS	76.0±1.7	33.2±2.2	60.0±2.7	25.9±4.4	90.6±2.9	58.5±6.4	52.6±0.7	18.4±1.3	78.7±9.8	35.8±12.9
NTS-NOTEARS	64.5±2.9	22.7±2.4	50.0±0.0	14.2±0.0	88.9±1.9	58.9±6.3	50.0±0.0	14.2±0.0	53.9±7.7	18.4±8.2
TSCI	48.9±6.7	15.0±2.1	51.4±7.2	17.4±3.3	58.7±4.8	20.1±3.3	53.4±5.1	18.7±3.0	51.6±2.8	17.9±1.8
cMLP	54.2±1.2	16.4±1.5	58.0±5.1	20.3±3.5	61.5±4.1	24.2±4.4	73.8±2.2	48.3±4.0	58.2±5.4	20.1±4.5
cLSTM	93.9±2.6	82.6±5.3	82.9±3.2	52.1±5.0	57.4±5.0	21.7±3.1	88.1±2.8	65.3±7.4	80.9±17.2	57.8±30.1
CUTS	54.4±4.1	21.0±1.7	73.1±4.6	34.8±6.4	95.6±3.2	83.4±6.8	72.9±4.7	34.7±6.6	89.2±4.1	66.7±8.1
CUTS+	84.7±1.3	54.5±3.0	85.9±3.0	59.0±3.2	97.1±0.9	86.3±3.7	91.9±3.4	76.7±6.5	96.8±2.4	84.7±11.9

Table 47: Linear Setting, 15-node case with $T = 1000$ (Part I). Hyperparameters are selected to maximize average performance across all scenarios.

15 nodes	Vanilla		Mixed data		Trend and seasonality		Min-max normalization	
	AUROC↑	AUPRC↑	AUROC↑	AUPRC↑	AUROC↑	AUPRC↑	AUROC↑	AUPRC↑
VAR	93.2±2.6	84.2±6.4	68.5±6.4	25.6±5.5	68.3±3.1	21.5±1.7	92.9±2.1	81.3±5.8
LGC	90.9±2.7	83.9±5.0	74.7±5.3	52.4±12.2	50.0±0.0	14.2±0.0	92.0±2.3	83.1±4.9
VARLiNGAM	51.6±5.9	15.4±2.0	52.1±2.8	15.0±0.8	49.7±2.5	14.2±0.5	50.6±5.0	14.9±1.4
PCMCI	98.0±0.8	83.4±4.3	90.6±3.3	71.5±11.3	55.3±4.8	15.8±1.4	98.0±0.8	83.4±4.3
DYNOTEARS	98.6±0.8	94.5±3.4	71.7±5.6	25.5±4.2	53.2±6.3	15.5±1.8	97.4±0.5	76.7±4.0
NTS-NOTEARS	50.0±0.0	14.2±0.0	50.0±0.0	14.2±0.0	50.0±0.0	14.2±0.0	50.0±0.0	14.2±0.0
TSCI	57.5±1.8	22.3±1.5	54.1±4.2	19.6±2.4	52.2±3.8	18.0±2.9	57.5±1.8	22.3±1.5
cMLP	99.6±0.4	98.9±1.4	54.1±1.2	17.6±2.0	51.0±1.6	16.0±1.2	99.7±0.1	98.5±0.9
cLSTM	98.6±0.3	93.9±1.1	89.5±0.7	67.0±1.3	45.6±5.0	14.9±2.1	99.9±0.0	99.8±0.2
CUTS	85.7±4.6	62.8±9.1	49.0±4.5	16.1±3.9	50.2±7.8	15.6±2.8	49.4±4.8	15.3±2.6
CUTS+	99.9±0.0	99.5±0.4	67.6±2.7	41.9±4.1	48.8±4.8	15.4±1.9	84.4±3.0	57.7±5.2

Table 48: Linear Setting, 15-node case with $T = 1000$ (Part II). Hyperparameters are selected to maximize average performance across all scenarios.

15 nodes	Latent confounders		Measurement error		Standardized		Missing		Nonstationary	
	AUROC↑	AUPRC↑	AUROC↑	AUPRC↑	AUROC↑	AUPRC↑	AUROC↑	AUPRC↑	AUROC↑	AUPRC↑
VAR	79.2±7.2	36.9±9.1	59.5±2.7	29.7±4.2	92.6±1.9	83.6±3.8	55.1±2.0	21.4±4.5	90.2±5.0	60.2±13.6
LGC	72.8±5.1	45.3±6.2	57.5±2.2	26.3±3.6	82.3±3.5	69.7±6.1	53.9±1.4	20.8±2.8	85.8±1.9	70.0±5.3
VARLiNGAM	49.4±3.0	14.2±0.8	51.1±4.0	14.8±1.1	51.8±5.8	15.4±1.9	51.6±3.7	15.0±1.3	47.6±4.1	13.9±0.9
PCMCI	85.7±3.7	40.9±5.8	73.8±1.4	46.3±3.4	98.0±0.8	83.4±4.3	70.3±4.1	37.6±5.4	88.2±5.5	46.4±9.6
DYNOTEARS	82.1±3.9	33.5±4.0	86.6±2.7	60.2±2.8	83.2±1.1	33.2±1.4	69.1±7.1	45.1±11.3	75.9±8.3	27.0±5.3
NTS-NOTEARS	63.3±4.0	22.4±3.4	50.0±0.0	14.2±0.0	91.6±2.1	85.0±4.6	50.0±0.0	14.2±0.0	56.6±13.3	25.7±22.8
TSCI	50.0±4.1	15.4±1.1	53.8±4.9	16.8±1.7	57.5±1.8	22.3±1.5	56.6±4.0	18.3±2.0	55.4±8.7	21.5±5.5
cMLP	56.2±4.2	18.0±1.5	78.9±2.6	46.5±7.8	51.6±4.1	16.7±3.0	81.6±3.3	57.5±7.4	58.0±3.2	20.6±3.2
cLSTM	97.4±1.9	92.4±4.9	94.0±1.8	76.4±8.3	58.8±6.2	21.8±4.8	93.1±1.0	78.8±4.1	83.0±18.9	63.5±33.1
CUTS	42.7±6.4	13.0±1.8	83.2±4.7	50.9±9.2	99.7±0.1	98.6±0.8	76.0±4.3	45.5±8.3	93.7±4.9	80.9±14.1
CUTS+	89.2±4.4	62.5±10.6	96.6±0.9	85.1±3.4	99.6±0.1	97.7±1.0	98.4±0.8	93.2±3.5	98.2±2.7	92.3±11.6

Table 49: Nonlinear Setting, 10-node case with $T = 500$ and $F = 10$ (Part I). Hyperparameters are selected to maximize average performance across all scenarios.

10 nodes	Vanilla		Mixed data		Trend and seasonality		Min-max normalization	
	AUROC↑	AUPRC↑	AUROC↑	AUPRC↑	AUROC↑	AUPRC↑	AUROC↑	AUPRC↑
VAR	77.0±3.1	55.5±4.3	59.6±5.6	39.4±4.1	74.6±3.9	53.1±5.4	76.0±3.7	54.4±4.5
LGC	76.9±2.4	62.9±3.8	67.8±3.9	54.1±4.8	76.3±2.5	61.5±5.1	76.0±3.0	65.2±5.9
VARLiNGAM	72.1±6.4	61.1±9.4	61.1±1.1	42.5±1.2	71.1±4.9	58.6±7.6	74.3±6.4	65.0±9.3
PCMCI	71.3±5.2	50.4±7.0	69.1±3.0	51.3±4.0	72.8±5.9	52.2±7.8	71.3±5.2	50.4±7.0
DYNOTEARS	76.1±7.3	65.8±11.3	54.6±3.3	35.9±2.0	75.5±6.5	65.6±10.2	52.5±6.1	35.8±4.4
NTS-NOTEARS	68.8±3.2	44.6±2.6	50.0±0.0	33.3±0.0	51.3±0.4	33.9±0.1	50.0±0.0	33.3±0.0
TSCI	86.5±1.9	77.3±2.6	65.0±4.1	54.5±4.3	65.2±4.8	56.2±3.9	86.5±1.9	77.3±2.6
cMLP	99.7±0.1	99.5±0.2	60.8±4.4	44.2±4.1	51.1±1.0	45.8±1.0	56.0±3.8	40.1±3.5
cLSTM	100.0±0.0	99.9±0.0	58.8±3.6	48.3±3.3	89.0±4.8	81.4±8.1	50.0±3.4	37.3±1.1
CUTS	93.7±1.6	91.5±2.2	62.7±3.3	48.4±3.3	46.2±3.1	36.0±3.0	61.3±5.9	44.4±6.8
CUTS+	97.5±0.9	94.8±2.1	76.6±3.4	68.6±5.1	49.0±4.1	37.1±2.9	82.6±4.6	74.8±7.2

Table 50: Nonlinear Setting, 10-node case with $T = 500$ and $F = 10$ (Part II). Hyperparameters are selected to maximize average performance across all scenarios.

10 nodes	Latent confounders		Measurement error		Standardized		Missing		Nonstationary	
	AUROC↑	AUPRC↑	AUROC↑	AUPRC↑	AUROC↑	AUPRC↑	AUROC↑	AUPRC↑	AUROC↑	AUPRC↑
VAR	54.8±4.0	36.6±3.2	62.8±6.5	44.0±7.4	75.1±1.9	53.1±2.2	64.1±5.2	44.5±6.0	66.8±9.2	46.8±8.0
LGC	55.1±4.1	36.9±3.6	63.1±6.3	44.4±7.2	74.6±2.1	56.2±2.4	64.1±4.8	46.3±6.0	68.5±11.5	52.7±15.0
VARLiNGAM	50.5±2.0	34.1±1.2	52.3±2.7	35.4±1.8	73.6±7.9	63.5±11.4	56.8±2.4	39.8±2.4	60.5±11.5	44.9±13.1
PCMCI	54.1±2.1	36.7±1.8	60.3±4.1	42.7±4.2	71.3±5.2	50.4±7.0	63.5±3.2	47.7±4.6	65.0±8.1	46.1±7.3
DYNOTEARS	56.8±4.4	37.5±2.8	56.4±4.9	37.7±3.6	79.8±4.0	72.7±5.9	60.6±3.0	42.4±3.6	64.6±10.6	47.7±13.1
NTS-NOTEARS	50.0±0.0	33.3±0.0	50.0±0.0	33.3±0.0	98.6±1.6	98.2±2.1	50.0±0.0	33.3±0.0	53.8±7.6	35.6±4.5
TSCI	54.0±4.9	40.0±4.1	56.5±9.3	42.5±4.9	86.5±1.9	77.3±2.6	70.7±6.8	56.7±11.5	71.0±11.2	56.6±13.2
cMLP	59.7±3.4	41.3±2.9	50.7±5.4	36.4±3.8	99.3±0.6	99.0±0.9	76.2±5.8	66.9±6.8	72.1±22.4	64.9±28.0
cLSTM	87.5±2.3	80.5±2.7	72.0±6.3	58.7±7.4	98.1±1.4	97.3±1.5	91.4±2.4	88.3±2.9	73.4±21.9	66.0±28.0
CUTS	68.2±4.8	47.6±4.2	59.9±6.6	47.2±7.2	99.8±0.2	99.6±0.4	75.7±2.4	68.6±3.2	66.8±20.5	58.8±24.1
CUTS+	81.1±2.3	71.0±4.7	87.3±3.9	76.1±6.7	98.1±0.8	96.1±1.8	95.3±1.5	91.3±2.7	81.4±18.1	71.9±24.7

Table 51: Nonlinear Setting, 10-node case with $T = 500$ and $F = 40$ (Part I). Hyperparameters are selected to maximize average performance across all scenarios.

10 nodes	Vanilla		Mixed data		Trend and seasonality		Min-max normalization	
	AUROC↑	AUPRC↑	AUROC↑	AUPRC↑	AUROC↑	AUPRC↑	AUROC↑	AUPRC↑
VAR	68.8±4.1	48.3±4.2	57.9±2.7	38.1±2.0	63.0±3.5	42.0±2.9	68.3±2.9	47.8±2.9
LGC	68.5±3.7	48.0±3.8	55.9±2.6	38.9±2.5	63.0±3.5	42.0±2.9	63.0±4.6	44.6±5.0
VARLiNGAM	62.0±3.5	41.5±2.6	57.3±2.6	38.1±1.5	63.0±4.4	41.8±3.4	62.3±3.3	41.7±2.3
PCMCI	68.6±3.5	47.9±3.8	68.3±4.8	47.9±5.4	64.3±3.0	42.9±3.0	68.6±3.5	47.9±3.8
DYNOTEARS	63.6±4.3	42.1±3.5	57.1±3.0	37.5±1.9	62.6±3.0	41.1±2.2	58.6±2.3	39.4±2.1
NTS-NOTEARS	50.0±0.0	33.3±0.0	50.0±0.0	33.3±0.0	50.0±0.0	33.3±0.0	50.0±0.0	33.3±0.0
TSCI	61.0±1.8	46.7±4.5	52.3±1.8	40.7±6.1	60.4±5.7	48.8±4.7	61.0±1.8	46.7±4.5
cMLP	83.0±3.6	72.5±4.6	54.1±4.8	39.4±3.9	50.9±0.8	45.8±1.5	50.6±3.7	36.2±3.1
cLSTM	93.7±0.4	88.5±0.2	49.9±2.9	37.0±1.4	98.8±0.7	97.4±1.4	48.7±3.1	35.9±0.8
CUTS	85.8±3.7	69.3±6.9	60.9±3.5	45.2±5.1	43.0±2.6	34.9±2.4	57.9±4.7	40.6±5.3
CUTS+	98.8±1.0	97.8±1.9	65.4±1.5	55.0±2.0	51.3±3.6	38.2±3.5	71.1±4.6	63.0±6.1

Table 52: Nonlinear Setting, 10-node case with $T = 500$ and $F = 40$ (Part II). Hyperparameters are selected to maximize average performance across all scenarios.

10 nodes	Latent confounders		Measurement error		Standardized		Missing		Nonstationary	
	AUROC↑	AUPRC↑	AUROC↑	AUPRC↑	AUROC↑	AUPRC↑	AUROC↑	AUPRC↑	AUROC↑	AUPRC↑
VAR	51.8±2.1	34.4±1.2	57.6±2.6	39.3±2.5	69.0±3.6	48.3±3.3	54.5±4.1	36.5±2.4	60.6±9.1	42.3±7.8
LGC	51.8±2.1	34.4±1.2	57.8±2.8	39.5±2.7	59.0±5.3	44.0±6.5	55.0±4.2	37.0±2.9	60.6±9.1	42.3±7.8
VARLiNGAM	51.4±0.9	34.4±0.8	51.1±2.2	34.3±1.5	62.1±1.3	41.6±1.0	53.4±2.7	36.1±2.5	56.1±5.2	37.6±3.6
PCMCI	54.0±2.5	35.7±1.6	59.1±3.6	40.0±3.3	68.6±3.5	47.9±3.8	57.6±5.9	39.2±4.8	61.1±8.5	41.8±6.6
DYNOTEARS	57.6±4.7	38.7±3.3	53.3±2.7	35.3±1.9	73.0±3.7	52.1±3.9	56.0±4.8	37.4±3.2	57.1±5.4	37.8±3.3
NTS-NOTEARS	50.0±0.0	33.3±0.0	50.0±0.0	33.3±0.0	92.5±3.3	83.3±6.0	50.0±0.0	33.3±0.0	50.0±0.0	33.3±0.0
TSCI	52.2±4.5	36.8±4.1	56.9±7.8	42.4±6.5	61.0±1.8	46.7±4.5	57.5±2.2	40.6±2.3	55.6±8.3	40.4±8.0
cMLP	56.4±4.7	41.1±5.8	49.1±1.0	34.2±1.3	95.2±2.2	92.7±2.8	55.7±5.6	41.4±5.4	69.1±21.8	61.5±26.9
cLSTM	49.4±6.1	37.5±5.0	56.5±3.0	40.8±1.9	74.9±3.3	66.6±5.3	69.5±3.4	52.9±4.8	70.6±20.3	62.1±22.7
CUTS	45.3±5.1	31.4±3.1	56.3±9.4	43.3±9.2	98.6±0.7	97.4±1.4	50.0±2.7	37.8±4.1	69.4±15.3	56.4±15.2
CUTS+	51.7±5.4	38.0±6.5	70.3±2.6	60.2±5.9	99.4±0.4	98.9±0.6	86.5±5.4	80.6±3.5	77.3±19.6	71.5±23.8

Table 53: Nonlinear Setting, 10-node case with $T = 1000$ and $F = 10$ (Part I). Hyperparameters are selected to maximize average performance across all scenarios.

10 nodes	Vanilla		Mixed data		Trend and seasonality		Min–max normalization	
	AUROC↑	AUPRC↑	AUROC↑	AUPRC↑	AUROC↑	AUPRC↑	AUROC↑	AUPRC↑
VAR	83.3±3.6	66.6±5.6	60.8±4.2	40.2±3.4	82.5±2.4	65.7±3.8	82.6±2.8	65.8±4.8
LGC	83.8±2.6	72.4±4.5	64.5±4.3	47.0±6.6	81.8±2.3	69.3±3.8	77.5±2.4	69.5±2.8
VARLiNGAM	72.0±1.9	60.3±2.7	65.8±4.2	47.6±4.7	71.6±2.6	58.7±5.2	72.3±1.8	60.7±2.6
PCMCI	77.8±4.9	55.9±6.1	73.3±3.6	54.0±4.4	79.5±3.5	58.2±5.4	77.8±4.9	55.9±6.1
DYNOTEARS	86.1±2.1	71.2±3.4	53.9±1.6	35.4±0.9	86.3±1.9	71.5±3.3	53.5±4.5	35.7±2.9
NTS-NOTEARS	82.9±1.4	59.5±2.0	50.0±0.0	33.3±0.0	60.6±4.0	39.0±2.6	50.0±0.0	33.3±0.0
TSCI	88.7±1.3	80.1±1.6	66.7±3.0	55.1±3.6	55.2±7.7	45.3±10.0	88.7±1.3	80.1±1.6
cMLP	99.9±0.0	99.9±0.0	59.6±5.5	43.5±4.2	51.2±1.0	46.1±1.5	54.8±3.7	39.0±3.2
cLSTM	100.0±0.0	99.9±0.0	59.6±3.9	49.3±3.3	72.2±2.8	54.1±4.0	49.6±3.0	36.8±1.0
CUTS	98.3±1.1	97.5±1.6	57.7±6.1	47.2±3.6	46.4±2.2	41.8±5.5	60.2±6.3	42.7±5.4
CUTS+	99.0±0.3	98.1±0.5	72.9±1.6	63.0±4.7	49.3±3.1	34.6±3.6	69.9±2.1	62.6±4.0

Table 54: Nonlinear Setting, 10-node case with $T = 1000$ and $F = 10$ (Part II). Hyperparameters are selected to maximize average performance across all scenarios.

10 nodes	Latent confounders		Measurement error		Standardized		Missing		Nonstationary	
	AUROC↑	AUPRC↑	AUROC↑	AUPRC↑	AUROC↑	AUPRC↑	AUROC↑	AUPRC↑	AUROC↑	AUPRC↑
VAR	55.1±2.6	38.3±2.8	56.1±2.8	40.7±3.9	83.6±4.1	67.1±6.5	64.8±3.6	49.2±4.8	65.1±14.9	48.3±14.6
LGC	55.1±2.6	38.3±2.8	56.1±2.8	40.7±3.9	83.5±3.2	67.3±5.0	61.4±3.4	46.6±5.4	63.3±13.2	48.0±15.0
VARLiNGAM	50.8±1.4	34.0±1.0	50.5±1.8	34.1±0.9	74.0±2.9	63.7±4.0	51.8±1.6	34.8±1.0	59.1±11.5	44.9±14.3
PCMCI	56.6±3.7	38.4±2.9	68.1±2.3	53.1±4.8	77.8±4.9	55.9±6.1	72.5±4.3	58.8±4.3	70.3±13.2	52.6±14.0
DYNOTEARS	58.5±4.7	37.9±2.9	61.1±1.9	39.5±1.3	90.3±3.1	84.7±4.8	68.3±2.6	46.2±2.4	66.1±14.5	46.9±14.1
NTS-NOTEARS	50.0±0.0	33.3±0.0	50.0±0.0	33.3±0.0	99.3±1.3	99.1±1.7	50.0±0.0	33.3±0.0	57.3±13.0	38.9±10.5
TSCI	61.1±6.2	45.3±3.6	57.3±6.0	45.0±6.1	88.7±1.3	80.1±1.6	70.7±4.1	56.4±4.6	73.8±13.0	60.1±14.1
cMLP	63.0±6.4	45.4±7.8	57.7±1.5	42.4±1.5	99.8±0.2	99.7±0.3	82.2±2.4	70.7±5.3	73.8±22.8	65.4±29.6
cLSTM	90.7±2.4	85.3±1.6	75.0±2.4	65.2±3.4	99.8±0.1	99.6±0.2	94.1±1.2	92.0±1.5	75.0±21.6	67.2±27.7
CUTS	78.5±7.6	57.8±10.1	62.9±3.6	51.4±5.5	100.0±0.0	99.9±0.0	89.7±3.2	86.2±5.3	70.5±23.1	62.6±27.7
CUTS+	91.1±5.7	86.8±8.7	96.4±1.5	93.8±2.5	98.9±0.5	97.7±1.2	99.2±0.5	98.4±1.0	83.4±19.3	78.0±24.9

Table 55: Nonlinear Setting, 10-node case with $T = 1000$ and $F = 40$ (Part I). Hyperparameters are selected to maximize average performance across all scenarios.

10 nodes	Vanilla		Mixed data		Trend and seasonality		Min-max normalization	
	AUROC↑	AUPRC↑	AUROC↑	AUPRC↑	AUROC↑	AUPRC↑	AUROC↑	AUPRC↑
VAR	72.6±2.1	58.3±4.3	62.1±1.3	42.0±1.3	66.6±3.2	47.5±4.0	73.6±2.3	60.0±5.0
LGC	72.8±2.2	58.7±4.2	58.1±2.6	42.7±2.5	66.3±3.8	47.2±4.4	70.3±4.1	56.7±6.1
VARLiNGAM	65.5±2.7	45.0±3.0	62.8±2.2	42.6±1.7	57.3±3.3	37.2±2.1	66.1±2.1	45.6±2.6
PCMCI	75.5±1.5	59.8±4.0	75.1±4.8	60.9±6.1	65.9±2.3	45.2±3.1	75.5±1.5	59.8±4.0
DYNOTEARS	67.5±1.6	47.0±1.7	57.4±0.9	37.7±0.6	69.3±2.5	49.1±3.2	70.0±4.6	58.0±7.4
NTS-NOTEARS	50.1±0.3	33.4±0.1	50.0±0.0	33.3±0.0	50.0±0.0	33.3±0.0	50.0±0.0	33.3±0.0
TSCI	71.3±4.6	56.1±4.6	59.8±1.7	43.7±2.1	60.7±2.9	45.2±5.0	71.3±4.6	56.1±4.6
cMLP	88.4±2.1	79.6±3.3	53.2±4.0	38.7±3.8	51.0±1.0	45.8±1.3	50.5±3.4	35.5±2.9
cLSTM	92.5±0.3	86.5±0.9	50.0±2.6	37.0±1.2	96.9±1.5	94.6±2.4	48.8±3.1	36.0±0.7
CUTS	90.2±2.1	76.0±6.1	60.6±3.1	45.0±1.6	41.9±2.5	38.6±4.6	58.4±7.5	40.2±5.4
CUTS+	99.8±0.1	99.6±0.2	70.0±2.5	61.7±2.5	53.5±3.0	37.6±2.9	81.9±4.1	76.7±5.3

Table 56: Nonlinear Setting, 10-node case with $T = 1000$ and $F = 40$ (Part II). Hyperparameters are selected to maximize average performance across all scenarios.

10 nodes	Latent confounders		Measurement error		Standardized		Missing		Nonstationary	
	AUROC↑	AUPRC↑	AUROC↑	AUPRC↑	AUROC↑	AUPRC↑	AUROC↑	AUPRC↑	AUROC↑	AUPRC↑
VAR	48.1±0.6	33.3±0.0	53.1±1.8	37.3±2.5	72.8±2.2	58.7±4.2	53.8±3.2	37.8±4.5	60.5±9.7	44.7±11.1
LGC	48.1±0.6	33.3±0.0	53.1±1.8	37.3±2.5	64.6±2.2	52.2±3.1	53.8±3.2	37.8±4.5	60.5±9.7	44.7±11.1
VARLiNGAM	52.3±2.3	35.4±2.3	53.8±1.8	36.0±1.4	66.6±3.4	46.4±4.1	51.1±3.5	34.7±2.2	54.8±7.6	37.1±5.1
PCMCI	49.8±3.7	34.3±1.4	57.1±3.3	40.7±4.9	75.5±1.5	59.8±4.0	58.5±5.4	42.6±7.5	62.5±10.3	46.1±12.4
DYNOTEARS	50.1±3.5	34.1±2.1	53.3±3.2	36.4±2.3	74.1±2.2	57.5±4.3	55.4±4.3	38.7±4.5	57.4±10.6	40.3±7.4
NTS-NOTEARS	50.0±0.0	33.3±0.0	50.0±0.0	33.3±0.0	87.5±5.7	77.8±7.2	50.0±0.0	33.3±0.0	50.0±0.0	33.3±0.0
TSCI	55.7±8.1	39.7±5.5	52.3±7.1	35.1±4.3	71.3±4.6	56.1±4.6	58.1±6.5	44.1±4.6	60.5±7.7	48.6±7.6
cMLP	53.2±3.2	38.9±3.4	52.5±3.9	38.3±3.4	98.6±1.3	97.7±2.1	57.9±4.7	41.6±6.2	74.5±20.8	66.3±27.7
cLSTM	52.4±1.8	36.9±2.2	59.7±7.7	48.1±7.7	78.1±5.1	72.3±6.8	75.1±3.9	66.6±4.3	71.4±20.6	63.0±23.9
CUTS	35.0±4.9	28.3±3.2	55.9±5.8	39.6±2.9	99.7±0.3	99.5±0.6	61.2±3.8	39.4±2.4	70.0±19.9	56.1±17.8
CUTS+	53.9±5.4	37.3±4.9	78.8±4.8	67.9±6.6	99.8±0.1	99.7±0.2	95.7±2.0	93.6±3.0	80.1±20.0	75.2±24.9

Table 57: Nonlinear Setting, 15-node case with $T = 500$ and $F = 10$ (Part I). Hyperparameters are selected to maximize average performance across all scenarios.

15 nodes	Vanilla		Mixed data		Trend and seasonality		Min-max normalization	
	AUROC↑	AUPRC↑	AUROC↑	AUPRC↑	AUROC↑	AUPRC↑	AUROC↑	AUPRC↑
VAR	80.8±3.6	46.8±4.8	62.2±2.9	27.7±1.8	80.6±1.8	46.3±2.5	81.0±3.7	47.0±4.8
LGC	78.8±4.5	58.4±5.2	69.9±2.7	50.3±5.2	78.4±4.2	58.3±4.6	78.7±4.8	63.5±7.0
VARLiNGAM	71.2±2.1	42.7±2.4	61.9±1.6	30.4±1.6	71.5±2.8	43.2±3.5	71.1±2.3	42.3±2.2
PCMCI	79.3±4.3	51.7±8.0	70.7±3.3	43.5±5.2	81.3±2.7	53.9±5.7	79.3±4.3	51.7±8.0
DYNOTEARS	88.7±4.3	63.6±7.5	54.8±0.6	23.5±0.3	88.3±4.1	63.5±7.2	52.6±2.7	22.6±1.2
NTS-NOTEARS	51.2±0.7	21.8±0.2	61.1±0.9	38.8±1.5	50.0±0.1	21.4±0.0	50.0±0.0	21.4±0.0
TSCI	89.8±2.8	74.2±4.7	69.7±4.9	47.0±5.7	65.1±5.5	44.2±5.7	89.8±2.8	74.2±4.7
cMLP	99.9±0.0	99.8±0.1	64.8±5.2	39.5±7.4	52.0±0.5	30.4±0.8	55.6±6.2	26.9±4.2
cLSTM	99.9±0.0	99.9±0.0	61.7±9.7	39.8±10.3	77.9±6.0	45.2±5.8	51.7±10.4	25.1±6.3
CUTS	90.0±2.0	82.5±2.7	56.9±5.9	33.9±4.6	48.7±4.7	24.0±3.6	54.5±5.7	25.0±2.3
CUTS+	98.2±0.4	93.2±2.1	79.3±1.4	60.9±4.4	49.1±1.2	23.1±1.9	86.7±2.6	73.0±8.3

Table 58: Nonlinear Setting, 15-node case with $T = 500$ and $F = 10$ (Part II). Hyperparameters are selected to maximize average performance across all scenarios.

15 nodes	Latent confounders		Measurement error		Standardized		Missing		Nonstationary	
	AUROC↑	AUPRC↑	AUROC↑	AUPRC↑	AUROC↑	AUPRC↑	AUROC↑	AUPRC↑	AUROC↑	AUPRC↑
VAR	54.9±3.3	24.2±2.6	62.9±2.4	30.9±2.6	81.1±3.2	46.9±4.2	69.7±1.9	37.3±2.7	59.6±13.8	28.7±11.7
LGC	54.9±3.3	24.2±2.6	63.2±2.9	31.8±3.8	72.7±5.4	46.0±4.8	68.4±2.1	40.5±3.3	58.9±12.7	30.3±15.1
VARLiNGAM	52.4±2.8	24.2±3.9	54.4±1.6	23.8±1.0	71.4±2.5	42.6±2.6	63.8±3.2	33.0±3.5	57.1±7.3	26.9±6.9
PCMCI	52.4±1.9	23.0±1.5	58.5±2.1	29.3±3.2	79.3±4.3	51.7±8.0	66.3±3.9	44.1±7.5	60.3±11.5	31.0±12.9
DYNOTEARS	52.8±1.5	22.4±0.5	58.2±1.9	24.7±0.8	86.6±3.4	69.1±6.3	69.5±2.1	32.1±1.5	60.1±14.5	30.2±15.2
NTS-NOTEARS	50.0±0.0	21.4±0.0	50.0±0.0	21.4±0.0	99.8±0.2	99.1±1.7	50.0±0.0	21.4±0.0	50.1±0.3	21.4±0.1
TSCI	50.8±8.1	24.9±6.4	59.9±8.7	30.6±5.7	89.8±2.8	74.2±4.7	72.8±2.9	46.2±5.4	64.6±17.5	39.6±20.5
cMLP	51.1±2.9	24.0±1.6	59.0±3.7	30.5±4.3	99.9±0.0	99.9±0.0	85.8±3.2	68.6±5.1	77.9±19.2	60.0±30.4
cLSTM	70.7±6.4	45.8±11.3	72.3±2.3	47.8±2.9	98.4±0.9	96.7±1.6	92.9±3.2	84.7±6.1	77.8±16.3	57.0±30.2
CUTS	53.7±4.6	23.4±2.1	60.0±6.5	37.7±7.0	99.7±0.3	99.3±0.6	73.2±2.1	55.6±4.9	63.1±17.8	42.5±24.1
CUTS+	53.3±1.6	27.3±2.4	91.4±2.1	79.6±4.1	98.9±0.2	96.2±1.1	95.7±0.5	86.0±1.2	85.3±10.2	70.3±19.2

Table 59: Nonlinear Setting, 15-node case with $T = 500$ and $F = 40$ (Part I). Hyperparameters are selected to maximize average performance across all scenarios.

15 nodes	Vanilla		Mixed data		Trend and seasonality		Min–max normalization	
	AUROC↑	AUPRC↑	AUROC↑	AUPRC↑	AUROC↑	AUPRC↑	AUROC↑	AUPRC↑
VAR	69.5±5.3	37.5±6.4	58.4±3.1	25.6±2.0	67.3±3.3	33.4±3.1	69.3±3.4	36.6±4.1
LGC	69.7±5.3	37.9±6.4	51.8±0.9	23.1±1.0	67.3±3.3	33.5±3.3	53.2±1.5	24.3±1.6
VARLiNGAM	62.8±2.5	30.6±2.4	59.7±4.8	28.7±4.8	66.2±1.1	31.3±1.0	63.5±2.4	31.5±2.7
PCMCI	65.9±3.2	38.2±5.3	64.8±3.0	38.0±4.7	62.9±1.8	32.9±1.9	65.9±3.2	38.2±5.3
DYNOTEARS	71.0±3.2	36.0±3.1	59.8±2.8	26.4±1.7	70.8±3.4	35.5±3.1	68.0±2.7	39.7±4.1
NTS-NOTEARS	50.0±0.0	21.4±0.0	50.4±0.5	22.1±0.8	50.0±0.0	21.4±0.0	50.0±0.0	21.4±0.0
TSCI	66.6±4.1	37.3±4.0	54.8±1.9	28.0±1.7	61.1±6.0	34.5±7.4	66.6±4.1	37.3±4.0
cMLP	80.6±2.4	57.9±5.3	53.7±5.7	27.7±3.6	51.8±0.5	30.3±0.7	49.2±6.4	22.0±3.2
cLSTM	98.9±0.3	96.2±1.0	51.8±9.8	25.1±5.9	98.1±0.9	95.2±1.8	50.6±10.2	24.3±5.7
CUTS	87.5±2.1	65.6±5.8	53.7±6.0	26.5±1.9	49.6±4.2	25.4±4.3	49.3±5.3	21.8±1.2
CUTS+	97.8±1.2	95.1±1.5	64.9±2.8	41.0±2.5	55.1±2.4	26.0±3.4	66.2±3.6	39.0±5.0

Table 60: Nonlinear Setting, 15-node case with $T = 500$ and $F = 40$ (Part II). Hyperparameters are selected to maximize average performance across all scenarios.

15 nodes	Latent confounders		Measurement error		Standardized		Missing		Nonstationary	
	AUROC↑	AUPRC↑	AUROC↑	AUPRC↑	AUROC↑	AUPRC↑	AUROC↑	AUPRC↑	AUROC↑	AUPRC↑
VAR	51.2±3.2	22.3±1.2	54.6±2.2	24.0±1.6	69.9±4.0	37.7±4.9	59.5±2.8	28.2±2.9	54.5±6.7	24.2±3.7
LGC	51.2±3.2	22.3±1.2	54.6±2.2	24.0±1.6	57.9±2.8	32.7±4.9	59.0±2.5	27.9±2.4	54.3±6.4	24.0±3.4
VARLiNGAM	50.2±1.3	21.8±0.7	52.2±1.3	23.0±1.1	62.9±1.4	30.6±1.5	51.3±1.7	22.5±1.7	55.2±5.5	25.1±4.1
PCMCI	50.1±2.3	22.0±1.2	53.4±1.9	24.4±1.8	65.9±3.2	38.2±5.3	55.7±3.4	27.2±4.3	55.0±5.3	25.5±4.4
DYNOTEARS	53.1±3.8	23.2±2.4	57.3±2.5	25.4±1.7	69.6±4.5	35.9±5.7	57.5±1.8	25.6±1.5	56.1±9.5	25.6±5.9
NTS-NOTEARS	50.0±0.0	21.4±0.0	50.0±0.0	21.4±0.0	92.3±3.0	76.5±5.0	50.0±0.0	21.4±0.0	50.0±0.0	21.4±0.0
TSCI	54.5±4.2	25.8±1.8	46.2±6.0	24.1±5.8	66.6±4.1	37.3±4.0	54.1±2.2	26.5±1.9	52.7±7.1	26.0±6.5
cMLP	56.6±5.3	28.4±4.6	51.0±4.2	23.9±1.7	97.3±1.1	93.2±2.8	55.7±5.4	26.5±3.7	68.6±21.6	48.7±30.9
cLSTM	50.7±4.2	23.2±3.2	62.7±6.3	33.9±7.0	74.2±6.0	53.6±9.0	73.1±2.5	46.8±2.0	72.5±20.5	54.3±32.0
CUTS	50.4±6.0	22.2±2.8	56.4±7.7	28.8±6.6	97.2±0.5	93.5±1.0	55.2±4.0	28.3±5.0	63.6±14.9	36.1±17.3
CUTS+	46.3±5.3	22.4±4.2	66.0±3.1	42.6±4.9	98.2±0.2	95.0±0.6	85.4±4.7	70.5±6.9	69.9±20.5	50.2±30.7

Table 61: Nonlinear Setting, 15-node case with $T = 1000$ and $F = 10$ (Part I). Hyperparameters are selected to maximize average performance across all scenarios.

15 nodes	Vanilla		Mixed data		Trend and seasonality		Min–max normalization	
	AUROC↑	AUPRC↑	AUROC↑	AUPRC↑	AUROC↑	AUPRC↑	AUROC↑	AUPRC↑
VAR	88.8±1.6	70.6±6.0	64.0±2.0	29.5±1.6	88.2±1.5	70.4±4.4	88.7±1.4	69.6±3.3
LGC	91.6±1.5	69.1±4.2	76.9±1.6	49.8±2.3	89.5±2.2	63.7±5.3	90.5±0.4	77.3±2.0
VARLiNGAM	77.3±1.9	49.4±2.2	68.2±1.0	37.7±1.8	76.8±1.2	50.1±3.3	77.5±2.5	50.0±3.4
PCMCI	83.0±2.3	53.2±3.7	79.8±2.7	55.3±3.5	88.5±1.3	62.0±2.4	83.0±2.3	53.2±3.7
DYNOTEARS	96.4±0.7	85.9±2.7	55.4±3.1	24.1±1.8	93.8±1.1	81.5±3.8	53.5±4.2	23.4±2.3
NTS-NOTEARS	86.6±0.5	50.5±1.0	50.0±0.0	21.4±0.0	53.6±1.9	22.7±0.7	50.0±0.0	21.4±0.0
TSCI	93.9±0.3	79.6±1.4	71.9±1.5	49.8±1.7	52.7±5.1	24.7±4.5	93.9±0.3	79.6±1.4
cMLP	100.0±0.0	100.0±0.0	64.6±5.5	39.3±6.0	52.1±0.5	30.3±0.5	54.4±6.1	26.1±4.0
cLSTM	100.0±0.0	100.0±0.0	61.8±8.8	38.6±9.2	53.9±1.8	29.8±1.6	51.3±10.2	24.5±6.1
CUTS	97.7±1.4	94.9±2.2	56.2±5.2	36.0±5.1	46.0±5.5	27.2±5.7	56.8±3.8	27.4±2.5
CUTS+	99.8±0.1	99.6±0.3	76.8±0.8	59.6±3.4	52.6±2.9	22.4±1.0	80.0±1.0	67.3±2.5

Table 62: Nonlinear Setting, 15-node case with $T = 1000$ and $F = 10$ (Part II). Hyperparameters are selected to maximize average performance across all scenarios.

15 nodes	Latent confounders		Measurement error		Standardized		Missing		Nonstationary	
	AUROC↑	AUPRC↑	AUROC↑	AUPRC↑	AUROC↑	AUPRC↑	AUROC↑	AUPRC↑	AUROC↑	AUPRC↑
VAR	52.9±2.1	24.2±2.5	59.8±1.2	33.5±1.6	88.4±2.3	69.4±6.1	65.4±3.9	39.7±6.2	61.5±6.8	29.0±5.3
LGC	57.8±4.0	24.9±2.1	75.5±4.5	38.0±4.4	81.6±1.7	45.1±3.4	84.5±3.7	53.1±5.9	65.3±8.9	29.7±6.9
VARLiNGAM	55.6±2.2	25.8±2.2	59.7±2.4	29.0±3.0	77.3±2.3	49.9±2.7	63.8±3.9	32.8±3.8	60.8±6.5	29.3±6.8
PCMCI	54.6±2.0	24.7±1.8	69.2±1.7	44.5±1.5	83.0±2.3	53.2±3.7	75.8±5.2	53.4±7.0	68.5±6.9	34.4±6.6
DYNOTEARS	60.3±1.0	25.8±0.6	66.4±2.3	29.7±1.4	89.5±2.6	82.2±4.3	78.6±4.8	46.5±7.5	62.4±11.5	29.2±10.1
NTS-NOTEARS	50.0±0.0	21.4±0.0	50.0±0.0	21.4±0.0	99.3±0.8	98.9±1.3	50.0±0.0	21.4±0.0	50.0±0.0	21.4±0.0
TSCI	56.5±4.1	27.5±2.8	60.7±6.8	32.3±5.7	93.9±0.3	79.6±1.4	82.6±2.3	57.3±4.6	73.1±16.3	49.9±25.6
cMLP	53.1±1.8	25.5±1.0	61.8±2.3	30.7±3.3	100.0±0.0	100.0±0.0	92.7±1.4	78.9±5.6	83.7±14.0	69.1±23.0
cLSTM	75.9±4.0	54.6±5.9	80.0±2.0	60.6±3.4	99.5±0.3	98.7±0.6	98.1±0.6	95.0±1.0	81.2±11.8	62.5±20.9
CUTS	57.6±6.6	26.1±4.4	66.0±2.3	43.1±1.8	100.0±0.0	100.0±0.0	87.2±2.6	73.7±5.8	69.0±15.6	46.8±26.1
CUTS+	79.4±4.1	56.8±7.0	92.2±1.1	80.9±2.8	99.9±0.0	99.9±0.0	99.7±0.2	99.0±0.9	89.7±5.9	75.4±13.2

Table 63: Nonlinear Setting, 15-node case with $T = 1000$ and $F = 40$ (Part I). Hyperparameters are selected to maximize average performance across all scenarios.

15 nodes	Vanilla		Mixed data		Trend and seasonality		Min–max normalization	
	AUROC↑	AUPRC↑	AUROC↑	AUPRC↑	AUROC↑	AUPRC↑	AUROC↑	AUPRC↑
VAR	74.6±3.7	52.7±6.2	62.9±3.9	29.6±3.5	72.0±2.4	45.8±3.6	72.7±1.5	50.5±2.7
LGC	74.3±3.5	52.6±6.0	58.2±2.2	32.2±3.7	72.1±2.5	46.3±4.1	69.6±2.1	48.0±4.6
VARLiNGAM	67.9±1.8	35.5±2.3	65.0±4.7	33.4±5.8	67.4±1.4	30.7±1.0	67.5±2.3	34.8±2.5
PCMCI	76.8±3.2	51.1±5.6	74.1±3.3	49.4±6.4	71.7±2.5	40.3±3.2	76.8±3.2	51.1±5.6
DYNOTEARS	73.3±1.5	44.5±3.3	61.6±2.5	28.6±2.3	75.4±2.4	47.0±4.1	70.1±0.8	49.8±3.6
NTS-NOTEARS	50.0±0.0	21.4±0.0	50.0±0.0	21.4±0.0	50.0±0.0	21.4±0.0	50.0±0.0	21.4±0.0
TSCI	75.7±3.1	51.1±2.6	59.8±1.8	34.5±2.5	56.7±3.7	30.1±4.3	75.7±3.1	51.1±2.6
cMLP	91.8±1.0	79.4±2.2	54.2±5.2	28.4±4.8	52.0±0.5	30.4±0.7	48.8±6.8	21.8±3.5
cLSTM	97.5±0.2	91.6±0.7	52.1±10.1	25.2±5.6	91.7±1.5	72.4±7.3	50.5±10.1	24.2±5.6
CUTS	94.8±0.6	79.1±4.3	54.6±3.6	29.2±1.7	46.1±3.8	29.9±6.5	48.9±3.2	22.5±0.9
CUTS+	99.8±0.1	99.5±0.3	71.6±1.3	53.2±3.9	55.0±2.5	24.6±1.8	79.1±2.9	64.2±5.3

Table 64: Nonlinear Setting, 15-node case with $T = 1000$ and $F = 40$ (Part II). Hyperparameters are selected to maximize average performance across all scenarios.

15 nodes	Latent confounders		Measurement error		Standardized		Missing		Nonstationary	
	AUROC↑	AUPRC↑	AUROC↑	AUPRC↑	AUROC↑	AUPRC↑	AUROC↑	AUPRC↑	AUROC↑	AUPRC↑
VAR	50.2±0.7	21.7±0.4	52.5±1.1	24.9±1.8	74.1±2.9	52.3±5.4	55.4±2.9	28.0±4.9	57.5±8.7	30.0±13.7
LGC	50.2±0.7	21.7±0.4	52.5±1.1	24.9±1.8	58.5±2.7	34.3±4.8	55.0±2.4	27.3±4.1	57.6±8.7	30.2±13.6
VARLiNGAM	52.8±1.9	23.8±1.8	54.2±1.4	24.3±1.5	67.7±2.2	35.7±2.3	53.6±0.6	24.1±0.9	57.3±6.7	26.8±6.9
PCMCI	51.9±1.1	22.6±0.8	57.7±2.8	28.6±3.5	76.8±3.2	51.1±5.6	57.8±1.9	28.8±2.6	59.2±10.3	30.3±13.2
DYNOTEARS	55.9±2.6	27.7±3.8	53.8±2.8	25.3±2.7	75.3±2.8	49.8±4.9	54.7±2.3	25.5±2.6	59.7±8.3	29.5±9.8
NTS-NOTEARS	50.0±0.0	21.4±0.0	50.0±0.0	21.4±0.0	90.4±4.9	79.0±7.9	50.0±0.0	21.4±0.0	50.0±0.0	21.4±0.0
TSCI	52.3±5.2	24.7±3.9	53.0±5.1	26.9±3.0	75.7±3.1	51.1±2.6	56.0±4.0	28.8±4.0	60.7±7.3	33.2±9.0
cMLP	55.6±5.3	26.3±4.2	51.9±2.9	25.2±3.8	99.3±0.2	97.7±0.9	58.8±3.0	29.4±1.8	64.8±18.3	44.2±26.8
cLSTM	51.7±3.7	22.6±2.1	63.9±2.6	35.2±5.4	80.1±6.4	66.1±8.4	77.0±3.0	58.8±4.1	76.4±12.3	55.8±21.7
CUTS	45.3±3.3	20.9±2.1	60.6±3.3	30.6±3.9	99.7±0.1	99.2±0.5	65.0±3.8	33.3±4.0	63.2±16.1	36.5±22.3
CUTS+	52.9±5.1	26.9±4.5	79.4±2.8	61.8±6.2	99.8±0.0	99.4±0.3	95.7±1.7	89.0±4.9	85.9±7.6	70.5±15.6

Table 65: Linear Setting, 10-node case with $T = 500$ (Part I). Results aggregated over all hyperparameters.

10 nodes	Vanilla		Mixed data		Trend and seasonality		Min–max normalization	
	AUROC↑	AUPRC↑	AUROC↑	AUPRC↑	AUROC↑	AUPRC↑	AUROC↑	AUPRC↑
VAR	61.3±17.0	19.7±15.8	58.8±9.1	15.4±5.7	53.6±5.1	13.4±4.9	61.7±17.0	19.9±15.5
LGC	64.1±18.8	24.3±22.8	70.7±11.2	27.9±15.1	49.7±3.9	11.4±1.3	65.7±17.7	23.7±20.6
VARLiNGAM	51.4±5.8	12.1±1.4	50.9±5.3	12.0±1.8	51.5±4.5	11.7±1.1	51.5±5.9	12.3±1.8
PCMCI	89.6±7.2	45.8±19.9	87.1±4.6	44.3±18.0	55.6±4.1	12.4±1.1	89.6±7.2	45.8±19.9
DYNOTEARS	69.0±19.0	33.2±28.6	64.8±11.4	19.7±9.2	53.7±6.2	12.3±2.1	70.6±17.1	30.4±25.9
NTS-NOTEARS	50.7±4.3	12.0±5.4	55.7±9.4	15.1±7.9	51.9±5.3	11.9±2.2	53.2±9.8	14.8±13.3
TSCI	57.4±13.9	19.2±10.0	51.3±10.5	18.5±6.9	55.9±11.6	19.4±6.7	57.4±13.9	19.2±10.0
cMLP	72.1±20.9	45.7±35.5	67.4±12.9	33.7±16.4	50.7±3.5	18.2±3.4	79.0±21.6	58.7±37.9
cLSTM	70.6±20.1	40.6±33.5	81.0±17.5	61.4±27.6	55.8±9.6	19.0±8.0	77.5±21.8	55.2±36.1
CUTS	75.5±18.8	44.3±20.7	48.7±11.0	15.1±5.9	51.3±9.1	16.4±5.5	48.3±9.6	15.2±6.5
CUTS+	84.0±17.1	65.6±23.0	74.6±4.7	39.2±7.0	49.9±4.8	13.9±3.2	72.6±11.7	41.7±13.5

Table 66: Linear Setting, 10-node case with $T = 500$ (Part II). Results aggregated over all hyperparameters.

10 nodes	Latent confounders		Measurement error		Standardized		Missing		Nonstationary	
	AUROC↑	AUPRC↑	AUROC↑	AUPRC↑	AUROC↑	AUPRC↑	AUROC↑	AUPRC↑	AUROC↑	AUPRC↑
VAR	56.5±8.8	14.6±4.7	59.9±14.9	17.3±11.6	61.3±16.8	19.2±14.8	59.4±13.6	17.0±11.6	56.5±10.2	14.8±6.3
LGC	73.4±13.9	26.3±16.5	68.4±13.2	21.7±11.5	80.3±18.0	43.2±32.3	62.6±15.2	20.8±15.9	69.1±15.5	26.0±22.5
VARLiNGAM	50.2±7.7	11.8±2.8	52.6±6.3	12.2±1.9	51.3±5.8	12.1±1.4	51.8±7.9	12.5±2.2	49.3±6.1	11.5±1.5
PCMCI	72.7±8.9	20.5±7.0	82.7±5.5	33.8±12.8	89.6±7.2	45.8±19.9	82.7±6.9	36.0±12.6	71.3±11.6	21.8±12.0
DYNOTEARS	70.8±11.8	23.5±9.8	59.9±13.1	19.2±14.0	70.8±19.0	28.1±20.6	66.5±16.5	28.9±21.9	67.3±15.7	23.2±15.4
NTS-NOTEARS	63.2±13.6	18.7±8.8	50.5±2.7	11.5±2.4	59.3±15.3	19.7±18.7	50.7±4.1	11.8±4.8	58.4±13.5	18.9±16.4
TSCI	53.4±10.0	19.7±7.7	48.0±8.4	13.7±3.3	57.4±13.9	19.2±10.0	54.9±8.7	16.9±5.5	50.2±11.2	16.7±6.4
cMLP	88.7±14.3	73.9±29.6	62.0±12.8	24.4±17.0	71.2±20.5	44.3±36.2	67.6±17.3	35.5±26.7	75.4±16.3	41.6±28.3
cLSTM	97.6±3.2	92.1±7.7	68.9±19.3	37.8±30.4	87.3±17.2	71.7±34.3	70.1±20.1	39.3±33.0	85.9±17.1	67.7±33.6
CUTS	58.4±18.8	25.7±16.0	75.1±13.6	37.9±15.4	94.9±13.0	86.9±18.6	68.6±15.4	35.6±14.3	87.1±13.4	63.5±24.0
CUTS+	88.1±5.2	53.4±17.6	78.8±16.2	51.8±19.5	97.0±1.8	80.4±11.0	72.7±23.1	48.5±24.3	94.3±6.1	77.4±12.9

Table 67: Linear Setting, 10-node case with $T = 1000$ (Part I). Results aggregated over all hyperparameters.

10 nodes	Vanilla		Mixed data		Trend and seasonality		Min–max normalization	
	AUROC↑	AUPRC↑	AUROC↑	AUPRC↑	AUROC↑	AUPRC↑	AUROC↑	AUPRC↑
VAR	66.3±20.8	30.9±32.6	60.5±9.1	18.4±8.1	54.9±7.0	14.8±6.2	66.1±20.6	30.6±32.4
LGC	68.8±22.0	35.5±34.8	71.4±10.2	31.7±17.3	50.1±0.7	11.3±1.2	67.9±21.7	33.6±33.9
VARLiNGAM	48.4±4.8	11.5±0.7	51.1±6.2	12.3±2.1	50.2±5.4	11.8±2.7	48.4±4.7	11.5±0.7
PCMCI	90.4±6.5	47.7±21.2	87.7±7.0	41.8±18.6	52.9±3.4	11.7±0.7	90.4±6.5	47.7±21.2
DYNOTEARS	67.2±19.8	33.4±32.3	65.5±10.4	21.1±10.3	53.6±5.6	12.3±2.0	69.8±18.2	32.3±31.1
NTS-NOTEARS	50.1±1.2	11.3±1.8	56.2±10.3	16.4±10.5	50.4±3.0	11.2±0.7	51.9±7.3	14.0±11.3
TSCI	57.0±9.5	22.9±9.8	54.4±7.5	17.6±6.3	54.9±10.0	20.5±7.9	57.0±9.5	22.9±9.8
cMLP	71.7±21.2	43.8±34.9	72.8±15.3	46.1±25.9	50.7±3.5	18.2±3.4	79.3±21.7	59.2±37.9
cLSTM	68.8±19.5	37.6±32.7	82.7±17.3	66.5±28.3	54.3±9.0	17.5±7.7	74.5±21.7	51.0±36.6
CUTS	66.5±23.8	40.1±22.2	44.1±11.7	13.8±6.4	51.5±9.2	16.6±6.7	46.3±9.5	14.2±4.3
CUTS+	78.2±25.6	63.1±32.1	73.6±6.1	42.3±8.4	49.3±6.0	13.7±3.5	78.4±11.4	44.4±15.8

Table 68: Linear Setting, 10-node case with $T = 1000$ (Part II). Results aggregated over all hyperparameters.

10 nodes	Latent confounders		Measurement error		Standardized		Missing		Nonstationary	
	AUROC↑	AUPRC↑	AUROC↑	AUPRC↑	AUROC↑	AUPRC↑	AUROC↑	AUPRC↑	AUROC↑	AUPRC↑
VAR	59.1±13.4	16.2±7.9	62.2±15.5	23.3±21.0	66.3±20.7	30.8±32.3	61.5±14.7	22.4±19.3	60.5±16.0	18.5±14.1
LGC	65.7±14.4	20.0±11.9	63.0±15.5	24.2±21.2	79.1±19.0	47.1±37.7	64.2±16.5	26.6±20.2	73.0±18.2	32.2±27.3
VARLiNGAM	49.1±4.6	11.1±0.9	53.0±5.7	12.3±1.8	48.4±4.7	11.5±0.6	50.8±5.7	11.9±2.2	46.7±5.5	10.9±0.8
PCMCI	66.0±7.4	16.1±3.4	88.4±6.0	45.3±18.2	90.4±6.5	47.7±21.2	87.7±6.6	42.6±18.6	72.1±10.7	20.7±8.5
DYNOTEARS	70.3±12.1	23.2±10.1	59.8±14.1	20.7±16.2	74.3±20.4	37.5±31.2	63.8±16.6	26.8±22.7	70.6±18.1	29.7±24.0
NTS-NOTEARS	63.3±13.3	18.9±8.8	50.1±1.0	11.1±0.6	62.6±18.0	25.7±26.1	50.2±2.0	11.3±2.7	60.1±15.8	21.4±20.8
TSCI	57.2±9.0	18.0±3.3	46.1±7.6	11.5±2.1	57.0±9.5	22.9±9.8	55.5±8.2	17.3±5.2	64.5±11.8	24.5±10.5
cMLP	92.4±10.5	78.7±25.9	65.4±16.2	30.8±22.6	69.7±22.6	44.3±39.4	65.6±16.6	32.2±25.8	75.2±19.0	51.1±33.7
cLSTM	97.9±4.9	92.7±12.2	68.3±19.4	36.6±32.3	91.6±12.2	77.5±32.0	67.7±18.7	35.1±31.9	89.7±18.3	77.0±33.7
CUTS	52.3±21.7	25.1±19.8	73.5±17.0	41.2±18.4	93.6±15.8	89.4±23.8	62.7±17.4	33.0±14.4	86.7±18.4	73.2±28.7
CUTS+	90.1±5.8	58.7±17.7	77.0±25.4	57.9±29.7	98.2±1.5	88.8±9.1	68.4±30.6	51.9±35.4	97.2±5.9	90.0±11.7

Table 69: Linear Setting, 15-node case with $T = 500$ (Part I). Results aggregated over all hyperparameters.

15 nodes	Vanilla		Mixed data		Trend and seasonality		Min–max normalization	
	AUROC↑	AUPRC↑	AUROC↑	AUPRC↑	AUROC↑	AUPRC↑	AUROC↑	AUPRC↑
VAR	60.4±15.3	22.6±15.4	57.1±6.8	18.6±5.6	54.5±7.8	16.1±3.3	60.5±15.3	22.6±15.1
LGC	62.7±16.4	26.3±20.0	66.2±8.5	25.7±7.9	50.1±0.9	14.4±0.6	66.5±14.2	26.8±14.4
VARLiNGAM	50.2±3.0	14.5±0.8	49.6±4.4	14.6±1.5	48.7±4.7	14.2±1.1	50.2±2.8	14.5±0.8
PCMCI	87.2±4.2	49.4±14.9	80.6±5.1	40.1±10.2	56.4±5.6	16.3±2.3	87.2±4.2	49.4±14.9
DYNOTEARS	60.6±15.9	26.3±20.6	59.5±7.6	19.5±5.5	52.2±3.7	15.1±1.3	63.4±15.0	26.4±18.5
NTS-NOTEARS	50.0±0.0	14.2±0.0	53.2±6.0	16.4±4.6	50.2±1.7	14.3±0.5	50.0±0.0	14.2±0.0
TSCI	57.9±4.3	20.0±3.4	51.3±3.7	16.7±1.9	52.7±1.9	17.7±2.7	57.9±4.3	20.0±3.4
cMLP	64.2±17.2	33.5±27.2	57.2±4.9	19.6±3.6	51.1±1.6	16.0±1.2	69.1±19.3	41.8±28.8
cLSTM	59.1±16.6	27.4±25.9	68.8±14.0	41.9±20.0	52.3±4.9	17.2±2.4	64.0±17.7	32.7±28.9
CUTS	67.7±13.1	33.2±15.0	51.5±6.4	17.5±3.6	48.4±5.9	15.4±2.9	49.2±4.4	15.9±2.7
CUTS+	69.8±20.4	46.0±25.5	66.3±2.8	32.6±5.0	51.9±4.8	16.6±2.7	62.9±8.0	28.3±7.6

Table 70: Linear Setting, 15-node case with $T = 500$ (Part II). Results aggregated over all hyperparameters.

15 nodes	Latent confounders		Measurement error		Standardized		Missing		Nonstationary	
	AUROC↑	AUPRC↑	AUROC↑	AUPRC↑	AUROC↑	AUPRC↑	AUROC↑	AUPRC↑	AUROC↑	AUPRC↑
VAR	55.1±8.4	16.3±3.7	55.0±7.0	16.9±4.5	60.5±15.4	22.7±15.7	53.9±5.5	15.9±2.4	56.1±10.0	17.3±5.9
LGC	72.8±13.1	33.1±14.8	54.8±4.7	18.1±4.7	75.2±15.1	39.7±23.1	55.8±7.3	17.2±3.7	67.2±14.0	28.1±17.3
VARLiNGAM	49.8±3.3	14.4±0.9	51.1±3.1	15.0±1.4	50.4±2.8	14.5±0.8	49.6±1.9	14.4±0.5	48.3±3.3	14.0±0.6
PCMCI	78.1±5.5	31.6±8.3	67.6±4.9	24.9±3.7	87.2±4.2	49.4±14.9	68.6±5.4	26.0±3.3	74.7±9.0	28.7±10.0
DYNOTEARNS	59.7±8.6	19.0±5.0	54.2±7.2	17.0±4.8	65.6±15.1	26.5±15.5	55.8±9.8	19.1±8.6	60.9±12.7	22.0±12.8
NTS-NOTEARNS	59.0±10.1	18.7±5.2	50.0±0.0	14.2±0.0	55.3±10.8	18.0±9.0	50.0±0.0	14.2±0.0	54.2±8.1	17.2±7.7
TSCI	48.2±4.8	14.9±1.7	51.5±6.9	18.0±4.0	57.9±4.3	20.0±3.4	51.5±4.5	17.1±2.4	51.7±4.8	17.2±2.8
cMLP	82.3±15.6	60.1±27.0	55.9±7.1	19.6±6.8	67.4±11.9	30.8±14.3	57.9±9.5	23.8±12.7	65.5±10.6	27.0±11.4
cLSTM	91.3±5.8	75.7±13.6	56.6±12.3	21.9±13.9	75.3±18.1	48.1±34.1	57.4±14.1	23.7±18.9	78.8±19.9	59.0±34.7
CUTS	54.6±9.4	20.4±7.7	61.0±9.7	24.7±8.2	93.5±3.7	77.9±10.1	61.6±9.2	26.5±7.0	77.0±12.2	46.3±16.0
CUTS+	82.4±3.7	50.3±7.0	63.8±15.9	32.0±14.9	96.4±2.5	83.4±9.1	61.0±19.2	32.7±21.0	92.1±6.3	73.7±16.9

Table 71: Linear Setting, 15-node case with $T = 1000$ (Part I). Results aggregated over all hyperparameters.

15 nodes	Vanilla		Mixed data		Trend and seasonality		Min-max normalization	
	AUROC↑	AUPRC↑	AUROC↑	AUPRC↑	AUROC↑	AUPRC↑	AUROC↑	AUPRC↑
VAR	64.4±18.2	30.7±26.3	59.1±7.6	20.8±6.9	56.0±10.2	17.4±6.5	64.5±18.3	30.5±25.8
LGC	66.7±19.0	34.1±26.9	67.6±10.8	30.3±16.4	50.0±0.0	14.2±0.0	65.6±18.7	32.2±26.4
VARLiNGAM	49.7±4.0	14.6±1.2	50.0±3.1	14.6±0.9	48.5±2.6	14.0±0.5	49.7±3.8	14.5±1.1
PCMCI	89.9±6.6	52.7±20.7	87.8±4.6	50.9±16.2	54.9±4.5	15.7±1.4	89.9±6.6	52.7±20.7
DYNOTEARNS	60.5±16.9	27.8±24.4	61.9±9.1	21.8±7.9	52.4±4.1	15.2±1.5	63.9±16.3	28.9±22.2
NTS-NOTEARNS	50.0±0.0	14.2±0.0	53.8±7.1	17.1±5.7	50.0±0.8	14.3±0.2	50.0±0.0	14.2±0.0
TSCI	57.9±3.5	21.9±1.5	53.9±4.3	19.1±2.5	52.4±3.5	18.0±2.7	57.9±3.5	21.9±1.5
cMLP	65.2±18.4	35.4±30.4	62.4±11.2	31.4±18.3	50.7±1.8	15.8±1.3	69.9±21.1	44.0±33.7
cLSTM	59.8±17.8	29.0±29.1	69.3±16.6	44.2±24.8	50.7±4.5	16.3±1.8	63.6±18.1	33.1±30.5
CUTS	67.9±15.3	38.5±17.9	47.6±6.7	15.8±3.7	48.9±6.1	15.5±2.7	47.8±5.5	15.4±2.7
CUTS+	68.9±27.5	51.0±36.2	67.9±4.0	38.4±5.1	50.5±5.8	16.0±2.8	68.3±9.4	33.7±14.0

Table 72: Linear Setting, 15-node case with $T = 1000$ (Part II). Results aggregated over all hyperparameters.

15 nodes	Latent confounders		Measurement error		Standardized		Missing		Nonstationary	
	AUROC↑	AUPRC↑	AUROC↑	AUPRC↑	AUROC↑	AUPRC↑	AUROC↑	AUPRC↑	AUROC↑	AUPRC↑
VAR	58.0±11.8	19.1±8.8	57.4±11.0	19.9±7.5	64.4±18.1	30.7±26.3	55.8±9.4	17.6±5.1	61.2±15.7	23.9±17.2
LGC	73.8±13.6	34.4±15.6	56.4±10.1	19.0±6.9	76.2±15.8	42.7±25.6	58.6±12.8	21.2±10.6	71.6±16.2	36.4±24.1
VARLiNGAM	49.8±3.9	14.4±1.0	50.5±3.1	14.6±0.8	49.8±4.0	14.6±1.2	50.7±2.1	14.6±0.8	49.1±3.6	14.2±0.8
PCMCI	77.0±7.5	29.3±8.9	78.9±5.4	37.3±7.2	89.9±6.6	52.7±20.7	76.7±5.7	34.2±5.9	76.9±9.7	30.2±10.8
DYNOTEARNS	60.4±8.9	19.6±5.4	55.4±10.4	18.9±11.1	68.9±17.4	33.6±24.0	56.7±12.0	21.2±13.2	64.4±15.3	27.5±19.7
NTS-NOTEARNS	59.2±10.5	18.9±5.5	50.0±0.0	14.2±0.0	58.1±15.0	22.2±18.2	50.0±0.0	14.2±0.0	54.9±10.2	18.5±11.0
TSCI	49.4±3.0	15.5±1.5	54.6±5.0	17.5±2.3	57.9±3.5	21.9±1.5	54.2±4.0	17.9±3.1	55.3±7.2	21.3±5.0
cMLP	87.1±15.5	71.5±28.8	60.3±11.8	24.9±13.3	67.5±23.2	43.5±38.9	60.0±12.3	25.8±16.1	67.3±14.8	31.6±18.7
cLSTM	93.8±5.1	83.1±12.2	58.8±16.2	26.3±22.9	84.0±18.6	65.0±33.1	58.5±15.8	26.4±23.7	79.5±22.8	63.3±37.6
CUTS	50.9±11.1	18.5±7.2	65.5±12.7	30.9±12.4	96.0±10.2	89.8±17.0	64.3±11.3	32.1±9.9	78.0±16.9	55.3±24.2
CUTS+	87.1±4.0	58.0±8.5	66.2±23.9	41.1±27.4	99.2±0.6	96.0±3.1	59.9±28.2	39.6±32.6	96.3±4.7	88.4±13.5

Table 73: Nonlinear Setting, 10-node case with $T = 500$ and $F = 10$ (Part I). Results aggregated over all hyperparameters.

10 nodes	Vanilla		Mixed data		Trend and seasonality		Min–max normalization	
	AUROC↑	AUPRC↑	AUROC↑	AUPRC↑	AUROC↑	AUPRC↑	AUROC↑	AUPRC↑
VAR	58.6±9.2	40.7±9.1	54.0±4.4	35.8±3.0	58.6±8.9	40.7±9.0	58.6±9.2	40.7±8.9
LGC	62.2±11.1	44.4±10.6	61.8±7.6	43.0±8.0	61.7±10.4	44.0±10.1	63.4±13.1	46.9±13.9
VARLiNGAM	63.7±7.9	45.6±9.8	60.4±4.6	41.2±3.4	63.6±7.4	45.9±9.4	63.9±7.9	46.0±10.3
PCMCI	66.8±6.2	44.7±6.3	70.3±3.5	49.0±3.9	67.9±6.4	45.6±6.6	66.8±6.2	44.7±6.3
DYNOTEARS	61.7±10.7	43.7±11.3	54.5±4.1	36.6±3.1	61.7±10.3	43.6±10.9	56.3±6.6	39.2±6.7
NTS-NOTEARS	56.5±8.9	37.2±5.4	59.9±8.1	44.2±8.4	50.4±0.6	33.5±0.3	50.0±0.0	33.3±0.0
TSCI	79.2±8.7	66.8±11.4	64.5±4.8	52.4±5.7	61.0±5.7	49.5±6.2	79.2±8.7	66.8±11.4
cMLP	95.3±3.3	92.9±4.8	52.4±4.8	37.0±4.0	51.0±1.0	45.8±0.9	50.4±3.7	35.6±3.1
cLSTM	100.0±0.0	99.9±0.0	55.6±4.9	44.3±5.6	86.5±6.7	77.3±12.2	49.3±3.3	36.9±1.3
CUTS	69.2±11.9	62.3±13.9	57.1±6.3	43.3±6.8	47.1±6.1	37.2±4.5	54.5±6.7	39.4±5.9
CUTS+	93.3±6.2	90.7±7.2	63.7±9.1	56.3±8.5	48.5±2.8	35.5±2.7	58.2±12.1	48.2±12.5

Table 74: Nonlinear Setting, 10-node case with $T = 500$ and $F = 10$ (Part II). Results aggregated over all hyperparameters.

10 nodes	Latent confounders		Measurement error		Standardized		Missing		Nonstationary	
	AUROC↑	AUPRC↑	AUROC↑	AUPRC↑	AUROC↑	AUPRC↑	AUROC↑	AUPRC↑	AUROC↑	AUPRC↑
VAR	51.5±3.2	34.2±1.9	53.6±5.7	35.7±4.5	58.5±8.9	40.5±8.6	54.2±6.2	36.1±4.5	54.6±7.2	36.9±6.2
LGC	51.6±3.3	34.3±2.1	53.7±5.7	35.8±4.5	60.8±9.4	42.2±8.4	55.4±7.0	37.2±5.4	55.9±9.6	38.5±9.3
VARLiNGAM	53.6±4.2	36.0±3.4	53.4±3.3	35.6±2.1	64.2±8.2	46.3±10.6	58.9±6.2	39.6±4.4	56.5±7.5	38.5±7.4
PCMCI	56.1±4.1	37.4±3.1	62.1±5.8	42.1±5.2	66.8±6.2	44.7±6.3	65.1±4.1	45.0±4.2	62.8±7.8	42.3±6.2
DYNOTEARS	52.1±4.2	34.5±2.4	51.9±3.8	34.4±2.4	69.4±14.6	54.1±17.6	54.9±5.7	36.5±4.1	54.8±8.9	37.3±7.8
NTS-NOTEARS	50.0±0.0	33.3±0.0	50.0±0.0	33.3±0.0	90.9±11.1	81.4±22.0	50.0±0.0	33.3±0.0	51.4±4.7	34.1±2.8
TSCI	54.2±4.8	39.5±4.5	56.5±9.4	43.2±6.0	79.2±8.7	66.8±11.4	64.0±7.7	47.6±10.2	68.1±9.6	52.6±11.4
cMLP	60.5±4.2	44.0±5.4	50.6±5.7	36.8±3.6	84.3±8.7	77.3±12.5	72.0±4.8	61.6±7.5	69.0±21.3	60.6±25.1
cLSTM	87.8±2.2	81.0±2.7	72.4±6.2	59.3±7.9	94.9±4.5	92.9±6.1	92.6±2.5	89.8±3.1	73.7±21.8	66.5±27.9
CUTS	50.7±8.6	37.0±6.1	58.4±6.5	44.7±6.6	93.2±6.0	87.7±10.4	56.1±8.9	47.8±9.6	59.1±12.4	49.3±14.6
CUTS+	68.3±14.9	59.4±16.7	77.9±9.4	70.0±9.9	97.2±1.9	94.3±4.2	88.1±8.8	83.5±10.2	74.9±18.6	68.2±22.3

Table 75: Nonlinear Setting, 10-node case with $T = 500$ and $F = 40$ (Part I). Results aggregated over all hyperparameters.

10 nodes	Vanilla		Mixed data		Trend and seasonality		Min–max normalization	
	AUROC↑	AUPRC↑	AUROC↑	AUPRC↑	AUROC↑	AUPRC↑	AUROC↑	AUPRC↑
VAR	54.6±7.1	36.5±5.4	53.8±3.8	35.8±2.6	53.4±5.6	35.5±3.8	54.5±6.7	36.3±4.9
LGC	54.6±7.0	36.4±5.3	56.3±4.7	37.7±3.4	53.5±5.6	35.5±3.9	55.2±4.7	37.0±4.0
VARLiNGAM	57.6±5.4	38.6±3.9	53.4±3.4	35.6±2.2	59.2±5.7	39.6±4.2	57.7±5.3	38.7±3.9
PCMCI	66.8±5.0	46.2±5.4	66.0±4.9	46.0±5.7	62.5±4.5	42.0±4.3	66.8±5.0	46.2±5.4
DYNOTEARS	54.7±6.4	36.3±4.2	52.8±3.7	35.2±2.4	54.1±5.8	35.9±3.7	51.6±5.2	34.8±3.3
NTS-NOTEARS	50.0±0.0	33.3±0.0	54.0±4.6	37.7±4.9	50.0±0.0	33.3±0.0	50.0±0.0	33.3±0.0
TSCI	60.5±2.4	45.6±4.9	52.5±2.1	40.8±4.8	58.1±6.1	46.0±5.2	60.5±2.4	45.6±4.9
cMLP	80.1±3.6	67.9±5.1	49.3±3.5	35.0±2.9	50.9±0.8	45.8±1.4	48.1±2.7	33.9±2.0
cLSTM	93.8±0.5	88.7±0.6	49.3±3.0	36.5±1.3	98.2±1.0	96.6±1.8	48.7±3.0	35.8±0.9
CUTS	64.8±10.9	52.9±10.5	53.6±5.5	38.8±4.6	47.0±5.1	35.7±4.1	52.7±6.0	37.9±5.1
CUTS+	80.0±17.6	76.5±19.0	52.4±6.9	40.2±7.9	50.0±2.3	36.9±2.9	52.4±9.6	39.8±10.1

Table 76: Nonlinear Setting, 10-node case with $T = 500$ and $F = 40$ (Part II). Results aggregated over all hyperparameters.

10 nodes	Latent confounders		Measurement error		Standardized		Missing		Nonstationary	
	AUROC↑	AUPRC↑	AUROC↑	AUPRC↑	AUROC↑	AUPRC↑	AUROC↑	AUPRC↑	AUROC↑	AUPRC↑
VAR	49.8±2.3	33.3±1.0	52.5±3.6	34.9±2.4	54.8±7.1	36.6±5.3	52.4±4.2	34.7±2.4	53.0±6.2	35.4±4.7
LGC	49.8±2.3	33.3±1.0	52.5±3.6	34.9±2.5	59.8±7.3	40.8±6.4	52.5±4.2	34.8±2.5	53.0±6.1	35.4±4.6
VARLiNGAM	51.1±1.4	34.2±1.1	50.7±2.0	34.1±1.5	57.6±5.1	38.7±3.8	51.4±2.2	34.5±1.8	53.7±4.4	36.1±3.2
PCMCI	51.2±3.9	34.3±2.0	58.4±3.8	39.5±2.9	66.8±5.0	46.2±5.4	56.9±5.6	38.5±4.2	60.5±7.8	41.5±7.1
DYNOTEARNS	51.0±3.8	34.0±2.2	51.4±2.5	34.1±1.4	59.7±9.7	41.6±9.3	52.3±4.2	34.7±2.4	52.8±5.1	35.2±3.1
NTS-NOTEARNS	50.0±0.0	33.3±0.0	50.0±0.0	33.3±0.0	80.1±13.7	63.1±18.6	50.0±0.0	33.3±0.0	50.0±0.0	33.3±0.0
TSCI	51.2±4.1	36.3±3.7	56.5±7.8	42.5±6.4	60.5±2.4	45.6±4.9	53.8±7.2	40.0±6.1	55.4±8.5	39.6±7.8
cMLP	51.8±3.5	36.6±3.7	48.8±3.2	33.9±2.1	72.4±11.8	60.9±16.5	55.1±5.5	40.6±5.0	57.7±14.0	44.3±16.2
cLSTM	48.2±5.3	36.6±5.1	56.3±3.7	40.4±3.2	69.4±6.6	60.0±8.7	70.5±3.7	54.7±5.5	70.6±20.2	62.3±22.5
CUTS	45.9±5.1	32.7±3.4	51.8±6.2	39.3±5.3	83.2±10.8	75.4±15.1	46.6±6.2	36.2±4.8	56.7±11.4	45.4±12.0
CUTS+	51.1±7.9	36.6±6.7	57.7±9.8	46.0±9.8	93.2±5.5	87.2±10.3	67.8±16.7	60.0±15.5	63.1±18.9	55.8±21.4

Table 77: Nonlinear Setting, 10-node case with $T = 1000$ and $F = 10$ (Part I). Results aggregated over all hyperparameters.

10 nodes	Vanilla		Mixed data		Trend and seasonality		Min-max normalization	
	AUROC↑	AUPRC↑	AUROC↑	AUPRC↑	AUROC↑	AUPRC↑	AUROC↑	AUPRC↑
VAR	60.9±11.6	42.9±10.9	55.8±4.6	36.8±3.3	61.0±11.4	43.1±10.8	61.0±11.5	43.0±10.9
LGC	63.0±13.1	45.1±12.9	61.6±7.4	42.4±7.1	62.4±12.6	44.5±12.3	64.1±14.4	48.9±17.4
VARLiNGAM	64.8±7.7	46.4±8.8	61.5±5.3	41.7±4.4	63.7±7.8	45.3±8.6	64.7±7.5	46.2±8.6
PCMCI	68.4±7.3	45.7±7.0	70.0±4.9	47.9±5.5	70.5±7.0	47.5±7.3	68.4±7.3	45.7±7.0
DYNOTEARNS	62.8±11.0	44.9±11.3	54.5±4.0	36.4±2.9	63.5±11.3	45.7±11.8	54.8±6.2	38.0±6.5
NTS-NOTEARNS	65.6±13.6	44.6±11.1	59.4±8.0	43.6±8.2	53.6±5.5	35.2±3.0	50.0±0.0	33.3±0.0
TSCI	82.4±6.8	69.5±11.7	65.5±2.9	52.8±4.1	51.0±6.8	39.6±8.0	82.4±6.8	69.5±11.7
cMLP	98.6±1.1	97.5±2.1	51.8±4.8	36.6±3.9	51.2±1.0	46.0±1.3	49.8±3.6	35.2±2.9
cLSTM	99.9±0.0	99.9±0.0	55.5±4.9	43.0±5.6	73.6±3.4	56.8±5.6	49.2±3.1	36.5±1.0
CUTS	75.2±15.5	70.4±16.2	57.2±5.8	44.3±6.1	44.6±7.0	36.3±4.7	55.0±7.2	40.0±6.6
CUTS+	98.1±1.7	96.1±3.6	67.4±4.5	58.6±6.4	47.9±3.4	33.8±3.5	60.0±10.2	47.4±10.3

Table 78: Nonlinear Setting, 10-node case with $T = 1000$ and $F = 10$ (Part II). Results aggregated over all hyperparameters.

10 nodes	Latent confounders		Measurement error		Standardized		Missing		Nonstationary	
	AUROC↑	AUPRC↑	AUROC↑	AUPRC↑	AUROC↑	AUPRC↑	AUROC↑	AUPRC↑	AUROC↑	AUPRC↑
VAR	52.8±5.2	35.3±3.5	55.1±8.1	37.3±5.9	61.1±11.8	43.1±11.2	56.6±8.8	38.7±7.3	55.8±9.8	37.9±8.3
LGC	52.7±5.3	35.3±3.5	55.2±8.3	37.4±6.1	61.3±11.6	43.1±11.0	58.4±10.9	40.7±9.7	57.2±11.6	39.8±11.2
VARLiNGAM	55.5±4.9	37.5±3.8	55.2±6.0	36.8±4.0	64.4±7.6	46.1±9.0	58.4±7.2	38.7±4.7	57.7±9.5	39.7±8.5
PCMCI	58.7±5.5	39.1±4.1	70.5±5.8	50.6±6.7	68.4±7.3	45.7±7.0	73.2±5.4	53.4±7.2	65.2±11.6	44.8±10.4
DYNOTEARNS	54.5±5.4	36.4±4.3	53.1±3.9	35.4±2.5	70.5±15.7	55.6±18.7	56.0±6.6	37.9±5.2	55.5±9.7	38.1±8.9
NTS-NOTEARNS	50.0±0.0	33.3±0.0	50.0±0.0	33.3±0.0	93.0±9.3	84.6±20.7	50.0±0.0	33.3±0.0	53.4±8.8	35.7±6.8
TSCI	61.5±5.1	45.0±3.6	56.4±5.2	43.9±5.5	82.4±6.8	69.5±11.7	67.4±5.3	50.3±6.4	70.9±10.9	55.2±12.7
cMLP	64.5±7.2	48.5±9.5	56.6±2.4	41.8±2.7	86.4±8.0	80.1±11.6	76.4±5.0	63.5±6.8	72.9±23.4	64.0±29.4
cLSTM	91.2±2.1	86.1±1.7	76.4±2.7	67.3±3.4	96.1±3.3	94.0±5.0	94.9±1.6	92.9±2.1	74.3±22.8	66.2±29.2
CUTS	59.8±11.5	43.4±10.1	60.2±6.5	45.6±7.9	94.1±8.8	90.7±12.2	61.6±13.2	56.0±14.4	61.7±14.1	51.5±17.9
CUTS+	86.3±10.7	80.7±13.8	93.5±4.6	89.7±6.5	98.1±1.7	96.2±3.6	98.0±1.4	96.1±3.0	82.1±19.2	76.1±24.1

Table 79: Nonlinear Setting, 10-node case with $T = 1000$ and $F = 40$ (Part I). Results aggregated over all hyperparameters.

10 nodes	Vanilla		Mixed data		Trend and seasonality		Min-max normalization	
	AUROC↑	AUPRC↑	AUROC↑	AUPRC↑	AUROC↑	AUPRC↑	AUROC↑	AUPRC↑
VAR	57.2±9.5	39.8±9.9	55.6±5.2	37.3±3.7	55.1±7.2	37.2±6.2	57.3±9.7	40.1±10.5
LGC	57.3±9.5	39.9±9.9	58.1±5.5	39.7±4.9	55.1±7.1	37.2±6.2	57.2±9.0	39.9±9.6
VARLiNGAM	60.2±6.6	41.1±5.3	57.0±5.4	38.6±4.1	59.4±6.5	39.9±5.8	60.6±6.4	41.5±5.2
PCMCI	70.8±4.8	50.4±7.6	73.3±4.5	53.5±7.2	64.1±3.5	42.4±3.3	70.8±4.8	50.4±7.6
DYNOTEARS	55.8±7.6	37.6±6.2	52.8±3.5	35.2±2.2	56.9±8.3	38.4±6.9	52.1±7.1	36.2±6.4
NTS-NOTEARS	50.0±0.2	33.3±0.0	52.8±3.2	36.8±4.0	50.0±0.0	33.3±0.0	50.0±0.0	33.3±0.0
TSCI	71.1±4.1	55.2±3.8	59.2±1.8	43.5±3.1	57.9±6.2	43.9±5.5	71.1±4.1	55.2±3.8
cMLP	87.6±3.0	79.8±4.9	49.1±3.2	34.8±2.8	51.0±1.0	45.7±1.4	48.2±2.6	33.8±1.8
cLSTM	92.8±0.4	87.3±1.1	49.5±2.9	36.6±1.0	95.7±2.2	92.6±3.3	48.8±3.0	36.0±0.9
CUTS	76.3±10.9	66.4±10.1	54.2±5.9	39.3±5.1	45.7±4.2	37.3±4.6	52.4±6.6	37.8±5.1
CUTS+	98.3±1.8	97.2±2.8	55.8±7.6	44.8±8.3	49.7±2.9	36.5±2.6	55.1±11.4	43.2±13.3

Table 80: Nonlinear Setting, 10-node case with $T = 1000$ and $F = 40$ (Part II). Results aggregated over all hyperparameters.

10 nodes	Latent confounders		Measurement error		Standardized		Missing		Nonstationary	
	AUROC↑	AUPRC↑	AUROC↑	AUPRC↑	AUROC↑	AUPRC↑	AUROC↑	AUPRC↑	AUROC↑	AUPRC↑
VAR	49.7±2.4	33.4±1.0	52.5±4.1	35.2±2.9	57.1±9.3	39.7±9.6	53.2±4.9	35.6±3.6	53.7±7.4	36.5±6.9
LGC	49.7±2.4	33.4±1.0	52.6±4.2	35.3±3.0	62.4±8.7	44.2±9.3	53.2±5.2	35.7±3.8	53.7±7.4	36.6±7.0
VARLiNGAM	51.6±1.8	34.8±1.9	52.3±2.7	35.3±2.3	60.9±6.9	41.9±5.8	50.9±2.4	34.2±1.6	52.9±6.0	35.6±4.1
PCMCI	49.6±3.7	33.6±1.4	59.0±5.0	40.1±4.8	70.8±4.8	50.4±7.6	61.6±5.3	42.5±5.5	61.3±9.7	42.5±9.2
DYNOTEARS	51.4±3.0	34.2±1.8	52.1±2.9	34.7±1.8	63.6±12.2	47.5±14.0	52.5±3.7	35.1±3.0	52.9±6.6	35.6±4.9
NTS-NOTEARS	50.0±0.0	33.3±0.0	50.0±0.0	33.3±0.0	80.7±10.7	64.3±16.0	50.0±0.0	33.3±0.0	50.0±0.0	33.3±0.0
TSCI	55.8±7.2	40.1±5.1	50.5±7.4	34.5±4.1	71.1±4.1	55.2±3.8	55.6±7.1	39.4±6.3	58.5±8.5	46.4±8.0
cMLP	49.3±2.7	34.3±2.7	52.3±3.7	38.7±4.9	78.0±11.9	68.5±17.3	56.1±4.9	41.4±5.5	62.1±15.9	50.3±18.4
cLSTM	52.3±2.2	37.5±3.1	60.0±7.3	48.2±7.2	70.4±7.7	61.6±9.6	76.2±4.0	68.2±4.6	71.5±21.1	63.3±24.6
CUTS	44.9±8.5	33.3±5.6	53.3±7.4	40.1±5.3	90.7±8.1	87.1±10.4	49.7±8.2	37.6±6.3	62.7±14.3	50.0±15.1
CUTS+	52.1±6.4	37.2±5.1	69.9±7.6	60.3±9.6	99.0±1.2	98.1±2.3	89.2±7.0	84.1±9.5	75.9±20.4	68.3±26.1

Table 81: Nonlinear Setting, 15-node case with $T = 500$ and $F = 10$ (Part I). Results aggregated over all hyperparameters.

15 nodes	Vanilla		Mixed data		Trend and seasonality		Min-max normalization	
	AUROC↑	AUPRC↑	AUROC↑	AUPRC↑	AUROC↑	AUPRC↑	AUROC↑	AUPRC↑
VAR	59.6±10.3	29.0±9.1	54.5±4.0	23.4±2.0	59.6±10.3	29.2±9.1	59.8±10.4	29.2±9.1
LGC	63.9±13.6	34.8±13.9	63.6±7.8	33.3±9.9	63.4±13.2	34.2±13.5	64.4±14.9	37.2±17.7
VARLiNGAM	64.8±7.8	34.7±7.9	60.1±5.2	28.2±3.4	65.0±7.5	34.8±8.6	65.0±8.0	34.7±7.7
PCMCI	75.8±5.1	41.4±8.9	71.9±4.3	38.2±5.5	78.0±4.8	43.3±8.7	75.8±5.1	41.4±8.9
DYNOTEARS	64.1±12.0	34.1±13.4	56.4±4.0	25.3±3.0	64.2±11.8	34.2±13.1	56.9±7.8	27.9±8.1
NTS-NOTEARS	59.0±12.0	26.5±7.0	60.2±8.1	33.4±8.8	50.4±0.6	21.5±0.2	50.0±0.0	21.4±0.0
TSCI	84.8±5.6	64.3±11.4	67.8±5.2	43.2±6.4	60.5±6.5	38.0±6.3	84.8±5.6	64.3±11.4
cMLP	96.1±2.8	90.5±6.8	57.5±6.3	28.4±6.4	52.0±0.6	30.4±0.8	53.8±5.5	24.7±2.8
cLSTM	99.9±0.0	99.9±0.0	57.5±10.7	32.9±10.5	80.2±5.7	48.7±8.4	51.2±10.3	24.6±6.1
CUTS	69.3±11.0	50.6±15.9	55.5±5.5	29.5±5.9	49.9±4.7	24.2±3.4	51.7±5.4	24.6±4.3
CUTS+	92.2±6.9	84.0±10.8	63.2±10.8	45.0±10.2	49.1±2.0	22.3±2.1	56.9±15.0	37.8±16.8

Table 82: Nonlinear Setting, 15-node case with $T = 500$ and $F = 10$ (Part II). Results aggregated over all hyperparameters.

15 nodes	Latent confounders		Measurement error		Standardized		Missing		Nonstationary	
	AUROC↑	AUPRC↑	AUROC↑	AUPRC↑	AUROC↑	AUPRC↑	AUROC↑	AUPRC↑	AUROC↑	AUPRC↑
VAR	51.4±2.9	22.1±1.6	53.8±5.7	23.6±3.5	59.7±10.5	29.2±9.1	55.4±7.6	24.7±5.2	52.8±6.7	23.3±5.0
LGC	51.4±2.9	22.1±1.6	54.0±5.8	23.8±3.9	62.9±10.7	31.8±9.5	57.1±8.9	26.5±7.1	53.7±8.7	24.4±8.2
VARLiNGAM	51.4±1.9	22.6±2.0	53.3±3.6	23.6±2.3	64.9±8.0	34.4±7.6	59.4±7.8	28.2±5.9	54.6±7.0	24.8±5.3
PCMCI	53.1±3.7	23.0±1.8	62.9±4.6	29.8±3.4	75.8±5.1	41.4±8.9	71.1±4.8	39.7±6.1	61.0±10.8	29.1±10.4
DYNOTEARNS	53.2±4.7	23.0±2.6	53.5±4.2	23.1±2.3	69.7±14.6	42.8±18.4	56.2±7.1	25.2±5.0	53.5±7.6	24.1±7.0
NTS-NOTEARS	50.0±0.0	21.4±0.0	50.0±0.0	21.4±0.0	92.9±8.9	79.2±27.0	50.0±0.0	21.4±0.0	51.3±4.8	22.0±2.3
TSCI	50.6±8.0	24.6±6.5	60.0±7.1	31.2±5.3	84.8±5.6	64.3±11.4	68.3±5.8	40.0±8.1	64.2±17.2	39.8±21.7
cMLP	53.5±4.1	26.0±2.7	58.2±3.0	29.1±3.4	90.3±6.5	79.0±13.3	78.8±5.5	54.2±9.5	72.3±17.4	49.6±26.6
cLSTM	71.1±6.5	45.9±11.9	73.0±2.2	48.6±2.9	94.5±4.1	89.3±7.8	93.4±3.3	86.1±6.1	77.6±16.7	57.4±30.3
CUTS	49.0±5.6	22.2±3.1	61.3±6.7	34.4±7.1	93.1±5.7	81.4±14.1	57.7±7.9	35.7±9.6	57.9±10.6	33.6±13.7
CUTS+	52.1±6.8	27.0±5.5	79.4±10.7	63.8±12.2	97.6±1.9	90.9±6.7	88.2±8.3	76.1±11.6	76.5±15.3	58.6±22.1

Table 83: Nonlinear Setting, 15-node case with $T = 500$ and $F = 40$ (Part I). Results aggregated over all hyperparameters.

15 nodes	Vanilla		Mixed data		Trend and seasonality		Min-max normalization	
	AUROC↑	AUPRC↑	AUROC↑	AUPRC↑	AUROC↑	AUPRC↑	AUROC↑	AUPRC↑
VAR	55.1±7.6	24.6±5.7	53.8±3.9	23.5±2.3	54.5±6.5	23.9±4.1	55.1±7.4	24.6±5.2
LGC	55.2±7.7	24.7±5.8	55.9±4.6	25.5±3.1	54.5±6.5	23.9±4.1	54.3±4.0	25.8±5.0
VARLiNGAM	58.3±5.6	27.7±4.4	54.7±4.7	25.0±3.8	61.7±6.4	29.8±5.3	58.7±5.9	28.1±4.8
PCMCI	65.5±3.6	32.8±5.2	66.1±3.7	33.8±5.1	63.4±2.5	30.0±3.3	65.5±3.6	32.8±5.2
DYNOTEARNS	56.4±8.2	25.1±5.5	53.9±3.3	23.5±1.9	56.3±8.3	25.1±5.4	54.3±5.3	24.2±4.0
NTS-NOTEARS	50.0±0.0	21.4±0.0	53.5±3.5	24.8±2.7	50.0±0.0	21.4±0.0	50.0±0.0	21.4±0.0
TSCI	64.8±4.9	36.3±5.1	55.1±2.1	28.1±1.7	57.0±6.3	30.3±6.8	64.8±4.9	36.3±5.1
cMLP	77.5±3.4	53.5±7.4	52.2±5.0	24.2±2.5	51.6±0.8	30.2±0.7	50.9±5.3	22.5±2.1
cLSTM	99.0±0.3	96.4±1.0	51.3±9.9	24.8±5.8	98.5±0.9	96.0±2.0	50.6±10.1	24.2±5.7
CUTS	61.9±11.3	39.4±11.8	50.8±4.4	24.1±3.5	50.8±3.2	24.7±3.3	49.7±4.0	22.8±2.6
CUTS+	77.8±17.2	66.4±23.3	53.1±5.8	28.2±6.3	51.3±2.4	24.2±2.8	52.7±5.3	25.8±4.7

Table 84: Nonlinear Setting, 15-node case with $T = 500$ and $F = 40$ (Part II). Results aggregated over all hyperparameters.

15 nodes	Latent confounders		Measurement error		Standardized		Missing		Nonstationary	
	AUROC↑	AUPRC↑	AUROC↑	AUPRC↑	AUROC↑	AUPRC↑	AUROC↑	AUPRC↑	AUROC↑	AUPRC↑
VAR	50.7±2.1	21.7±0.8	51.7±2.6	22.2±1.3	55.2±7.7	24.7±5.7	52.6±4.1	22.8±2.5	51.5±4.2	22.2±2.1
LGC	50.7±2.1	21.7±0.8	51.7±2.6	22.2±1.3	60.4±6.9	29.2±6.1	52.6±4.1	22.8±2.4	51.5±4.0	22.1±1.9
VARLiNGAM	49.9±1.0	21.6±0.5	51.3±1.9	22.4±1.5	58.2±5.7	27.5±4.5	50.6±1.4	22.0±1.3	52.7±3.9	23.2±2.8
PCMCI	51.4±2.4	22.1±1.1	55.9±4.7	25.0±3.1	65.5±3.6	32.8±5.2	57.5±4.7	26.3±3.7	54.8±7.5	24.5±4.2
DYNOTEARNS	51.0±2.2	21.9±1.1	52.1±3.2	22.4±1.6	60.5±9.8	30.3±10.0	52.6±3.6	22.7±1.9	51.7±5.0	22.4±2.8
NTS-NOTEARS	50.0±0.0	21.4±0.0	50.0±0.0	21.4±0.0	81.0±13.2	53.0±20.6	50.0±0.0	21.4±0.0	50.0±0.0	21.4±0.0
TSCI	54.3±3.5	25.7±1.4	46.4±5.5	23.7±5.3	64.8±4.9	36.3±5.1	49.3±5.0	22.9±3.5	51.9±6.5	25.6±5.9
cMLP	54.5±4.5	25.2±3.5	50.4±5.2	23.7±3.3	76.8±10.6	53.9±19.6	55.4±3.6	26.1±2.8	59.7±13.9	32.7±17.8
cLSTM	50.7±4.7	22.4±3.1	63.0±6.2	34.3±7.2	69.2±8.9	46.8±11.8	73.2±2.4	47.4±2.3	72.2±20.7	54.2±31.9
CUTS	48.3±4.9	21.9±3.2	51.3±6.5	25.5±4.8	78.2±11.1	60.3±17.5	50.1±6.3	25.6±5.0	54.6±9.0	28.9±8.8
CUTS+	50.4±4.5	24.4±3.5	56.5±7.9	32.9±8.6	90.4±5.9	77.8±11.8	70.0±12.7	49.1±15.7	61.4±16.5	39.5±23.2

Table 85: Nonlinear Setting, 15-node case with $T = 1000$ and $F = 10$ (Part I). Results aggregated over all hyperparameters.

15 nodes	Vanilla		Mixed data		Trend and seasonality		Min–max normalization	
	AUROC↑	AUPRC↑	AUROC↑	AUPRC↑	AUROC↑	AUPRC↑	AUROC↑	AUPRC↑
VAR	63.1±13.4	33.8±14.9	57.2±4.6	25.0±2.6	63.0±13.1	33.9±14.7	63.1±13.3	33.7±14.6
LGC	67.1±16.0	40.2±19.9	66.6±9.8	36.2±11.1	65.7±15.4	38.2±18.5	67.1±15.4	42.6±22.9
VARLiNGAM	68.7±8.8	39.3±10.7	65.3±7.1	33.5±4.8	67.5±8.1	37.8±10.8	68.7±8.7	39.4±10.7
PCMCI	77.9±4.7	42.1±7.9	78.9±3.6	45.4±7.8	80.6±5.5	45.3±10.0	77.9±4.7	42.1±7.9
DYNOTEARS	67.8±14.4	39.9±18.4	58.2±5.1	27.1±3.9	67.9±13.7	39.8±17.4	56.6±8.4	28.5±8.3
NTS-NOTEARS	66.6±15.1	33.0±12.6	59.3±8.8	33.7±11.0	51.2±2.0	21.8±0.7	50.0±0.0	21.4±0.0
TSCI	88.5±6.2	68.3±13.0	70.2±2.5	46.2±4.6	50.5±5.9	22.9±3.9	88.5±6.2	68.3±13.0
cMLP	99.4±0.5	98.2±1.5	57.5±6.1	28.2±6.0	52.0±0.5	30.3±0.5	53.4±5.2	24.2±2.5
cLSTM	99.9±0.0	99.9±0.0	57.4±10.1	32.1±9.4	56.8±4.5	31.7±2.1	51.0±10.2	24.3±5.9
CUTS	72.7±14.9	60.1±17.8	57.1±5.1	31.6±5.2	46.8±5.8	23.6±3.8	53.4±5.8	25.3±4.7
CUTS+	98.4±1.8	94.9±4.9	71.7±5.1	55.6±5.7	49.7±3.5	22.3±2.0	62.3±12.6	39.8±14.0

Table 86: Nonlinear Setting, 15-node case with $T = 1000$ and $F = 10$ (Part II). Results aggregated over all hyperparameters.

15 nodes	Latent confounders		Measurement error		Standardized		Missing		Nonstationary	
	AUROC↑	AUPRC↑	AUROC↑	AUPRC↑	AUROC↑	AUPRC↑	AUROC↑	AUPRC↑	AUROC↑	AUPRC↑
VAR	52.1±3.4	22.6±2.0	55.8±8.2	25.7±5.8	63.1±13.4	33.8±14.6	57.5±9.8	27.2±8.0	53.9±6.0	23.4±3.4
LGC	52.1±3.4	22.6±2.0	55.9±8.5	25.7±5.9	64.4±12.9	34.9±14.5	59.4±12.5	30.3±11.8	54.6±7.5	24.2±5.4
VARLiNGAM	53.8±3.1	24.2±2.4	57.0±6.5	26.2±4.7	68.9±8.8	39.6±10.8	61.7±9.5	30.0±6.8	56.9±6.8	25.9±5.5
PCMCI	56.1±3.3	24.7±1.9	72.0±4.3	39.0±5.4	77.9±4.7	42.1±7.9	78.9±5.5	47.4±8.2	63.4±6.6	28.7±5.2
DYNOTEARS	53.9±4.4	23.7±3.1	55.4±6.0	25.1±4.5	72.4±16.1	48.8±22.6	58.9±9.7	28.6±8.5	54.3±6.4	23.9±5.3
NTS-NOTEARS	50.0±0.0	21.4±0.0	50.0±0.0	21.4±0.0	95.6±5.6	83.5±21.9	50.0±0.0	21.4±0.0	50.0±0.0	21.4±0.0
TSCI	55.3±4.6	27.4±3.3	58.1±5.8	29.5±5.1	88.5±6.2	68.3±13.0	77.2±7.2	50.1±9.7	72.5±15.8	48.0±24.3
cMLP	53.9±3.7	25.7±1.7	61.0±2.8	29.9±3.7	94.3±4.6	86.2±10.5	87.4±3.9	66.6±9.4	79.7±13.6	59.8±23.8
cLSTM	76.9±3.8	55.5±7.0	80.9±2.6	61.1±3.7	95.9±3.2	91.0±7.4	98.4±0.8	95.8±1.6	81.3±11.6	62.8±21.1
CUTS	51.4±5.7	24.1±3.5	62.9±5.5	38.5±7.3	97.5±3.4	93.3±7.5	60.7±12.0	45.6±12.8	61.2±10.3	37.4±14.7
CUTS+	63.5±10.1	38.8±10.7	94.9±3.3	87.0±5.8	98.7±1.2	95.0±5.2	97.5±2.5	93.9±5.1	91.6±4.7	80.9±9.7

Table 87: Nonlinear Setting, 15-node case with $T = 1000$ and $F = 40$ (Part I). Results aggregated over all hyperparameters.

15 nodes	Vanilla		Mixed data		Trend and seasonality		Min–max normalization	
	AUROC↑	AUPRC↑	AUROC↑	AUPRC↑	AUROC↑	AUPRC↑	AUROC↑	AUPRC↑
VAR	58.4±10.6	29.0±11.6	56.3±6.0	25.4±3.8	57.1±9.2	27.4±9.2	58.0±10.1	28.6±10.7
LGC	58.4±10.6	29.1±11.5	58.7±5.9	27.9±5.0	57.2±9.3	27.5±9.4	56.2±8.1	27.3±9.0
VARLiNGAM	61.4±7.3	30.6±6.1	57.0±7.0	26.7±6.3	64.5±7.6	31.5±6.1	61.3±7.3	30.4±6.0
PCMCI	73.9±4.5	41.0±8.3	73.6±3.6	40.9±7.5	69.1±4.0	34.5±5.7	73.9±4.5	41.0±8.3
DYNOTEARS	59.2±10.3	29.0±10.4	54.6±3.9	24.1±2.4	59.6±10.7	29.3±10.7	54.6±6.4	25.3±6.2
NTS-NOTEARS	50.0±0.0	21.4±0.0	53.0±3.4	25.3±4.1	50.0±0.0	21.4±0.0	50.0±0.0	21.4±0.0
TSCI	76.1±3.2	50.8±3.3	59.3±2.1	33.9±3.1	52.8±5.1	26.4±4.7	76.1±3.2	50.8±3.3
cMLP	90.3±1.5	76.3±2.9	52.6±5.1	24.4±3.3	51.9±0.5	30.4±0.8	50.7±5.3	22.5±2.1
cLSTM	97.7±0.2	92.3±1.0	51.5±10.1	24.8±5.6	90.6±2.4	69.9±7.9	50.6±10.1	24.1±5.6
CUTS	77.4±10.2	60.6±11.1	52.0±4.3	25.1±3.6	47.9±3.7	24.5±4.8	50.0±4.0	22.9±2.2
CUTS+	98.2±1.6	95.8±3.3	56.7±7.6	34.9±8.6	51.5±2.6	23.7±2.5	56.7±9.6	31.6±12.2

Table 88: Nonlinear Setting, 15-node case with $T = 1000$ and $F = 40$ (Part II). Results aggregated over all hyperparameters.

15 nodes	Latent confounders		Measurement error		Standardized		Missing		Nonstationary	
	AUROC↑	AUPRC↑	AUROC↑	AUPRC↑	AUROC↑	AUPRC↑	AUROC↑	AUPRC↑	AUROC↑	AUPRC↑
VAR	50.7±2.2	21.8±0.9	52.5±4.0	23.0±2.3	58.4±10.6	29.1±11.5	53.4±5.2	23.7±3.7	52.8±6.1	23.6±6.7
LGC	50.7±2.2	21.8±0.9	52.6±4.1	23.0±2.3	64.4±9.6	34.0±9.9	53.4±5.2	23.6±3.6	52.8±6.1	23.6±6.6
VARLiNGAM	51.0±1.6	22.3±1.4	52.0±2.4	23.0±1.9	61.5±7.4	30.9±6.3	51.4±1.6	22.5±1.4	54.1±5.2	24.4±4.6
PCMCI	53.2±3.2	23.0±1.4	60.6±3.9	28.4±3.2	73.9±4.5	41.0±8.3	60.1±3.1	27.8±2.4	59.4±9.4	28.0±9.7
DYNOTEARS	53.5±4.4	23.8±3.3	53.2±4.4	23.3±2.4	63.5±11.4	35.0±13.2	53.1±4.4	23.2±2.6	53.9±6.4	24.0±6.1
NTS-NOTEARS	50.0±0.0	21.4±0.0	50.0±0.0	21.4±0.0	84.8±9.5	61.3±20.6	50.0±0.0	21.4±0.0	50.0±0.0	21.4±0.0
TSCI	52.2±5.9	24.8±4.3	52.5±4.6	26.5±2.5	76.1±3.2	50.8±3.3	52.8±5.7	25.1±4.0	61.2±8.6	34.8±10.1
cMLP	53.4±4.4	24.5±2.4	54.3±4.2	26.5±3.5	81.5±10.6	62.1±19.4	59.9±4.1	30.4±2.6	58.2±13.9	32.6±18.1
cLSTM	50.9±3.2	22.5±2.0	65.0±2.8	36.7±5.9	72.6±10.2	52.6±14.0	78.0±2.9	60.4±4.2	77.2±11.6	56.7±20.7
CUTS	46.5±4.1	21.2±2.7	56.2±4.1	29.5±3.8	88.8±9.5	79.7±14.9	54.0±5.1	29.4±4.2	57.7±11.6	31.3±15.3
CUTS+	52.4±4.5	24.9±3.4	69.1±7.5	44.9±10.2	98.5±1.2	95.0±3.7	88.8±6.4	77.3±8.8	73.7±14.0	55.4±21.9

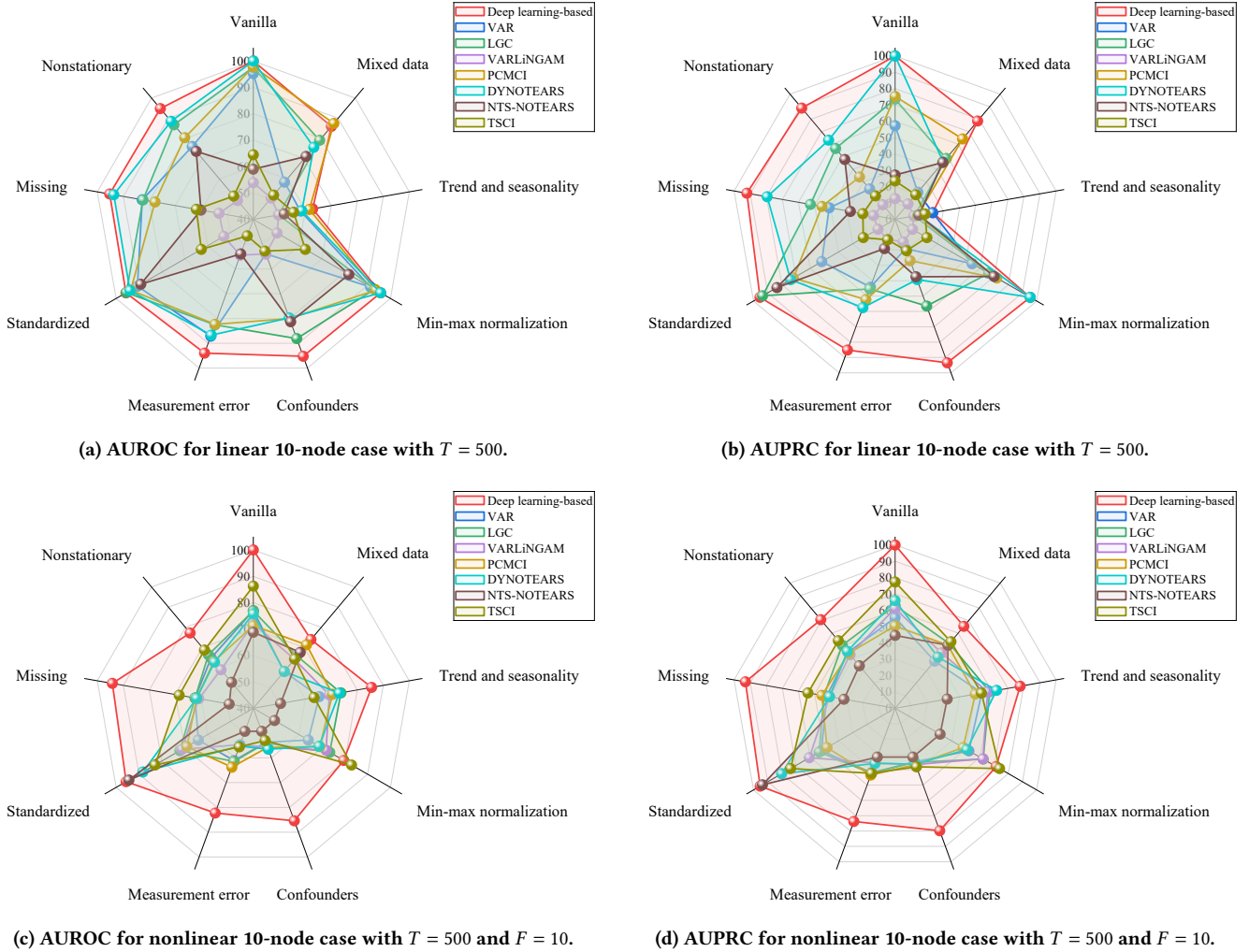


Figure 2: Experimental results under the linear and nonlinear settings across the vanilla scenario and eight assumption violation scenarios. AUROC and AUPRC (the higher the better) are evaluated over 5 trials for the 10-node case with $T = 500$. For the deep learning-based methods, we present only the optimal results.

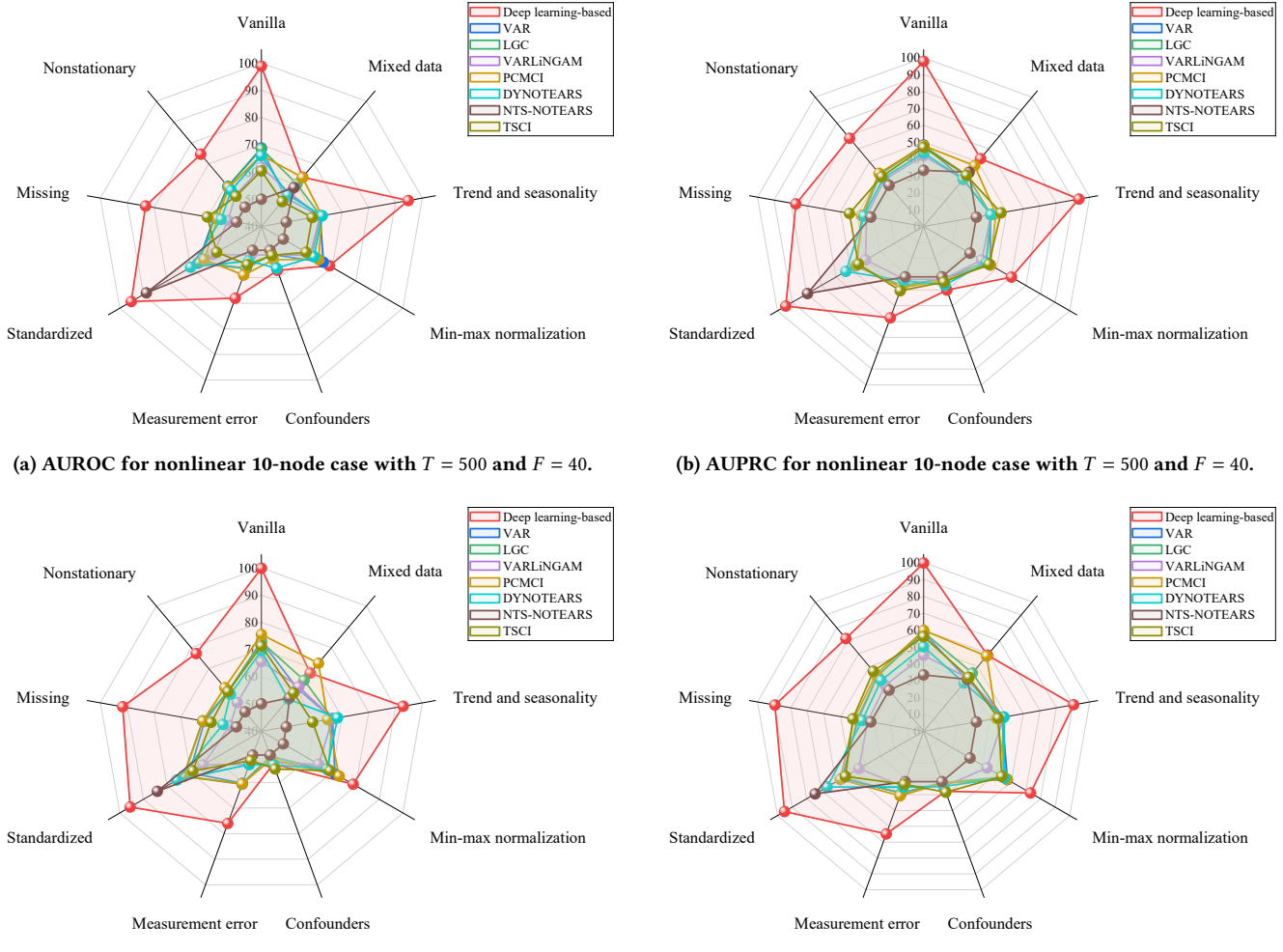


Figure 3: Experimental results under the nonlinear settings across the vanilla scenario and eight assumption violation scenarios. AUROC and AUPRC (the higher the better) are evaluated over 5 trials for the 10-node case with $F = 40$. For the deep learning-based methods, we present only the optimal results.

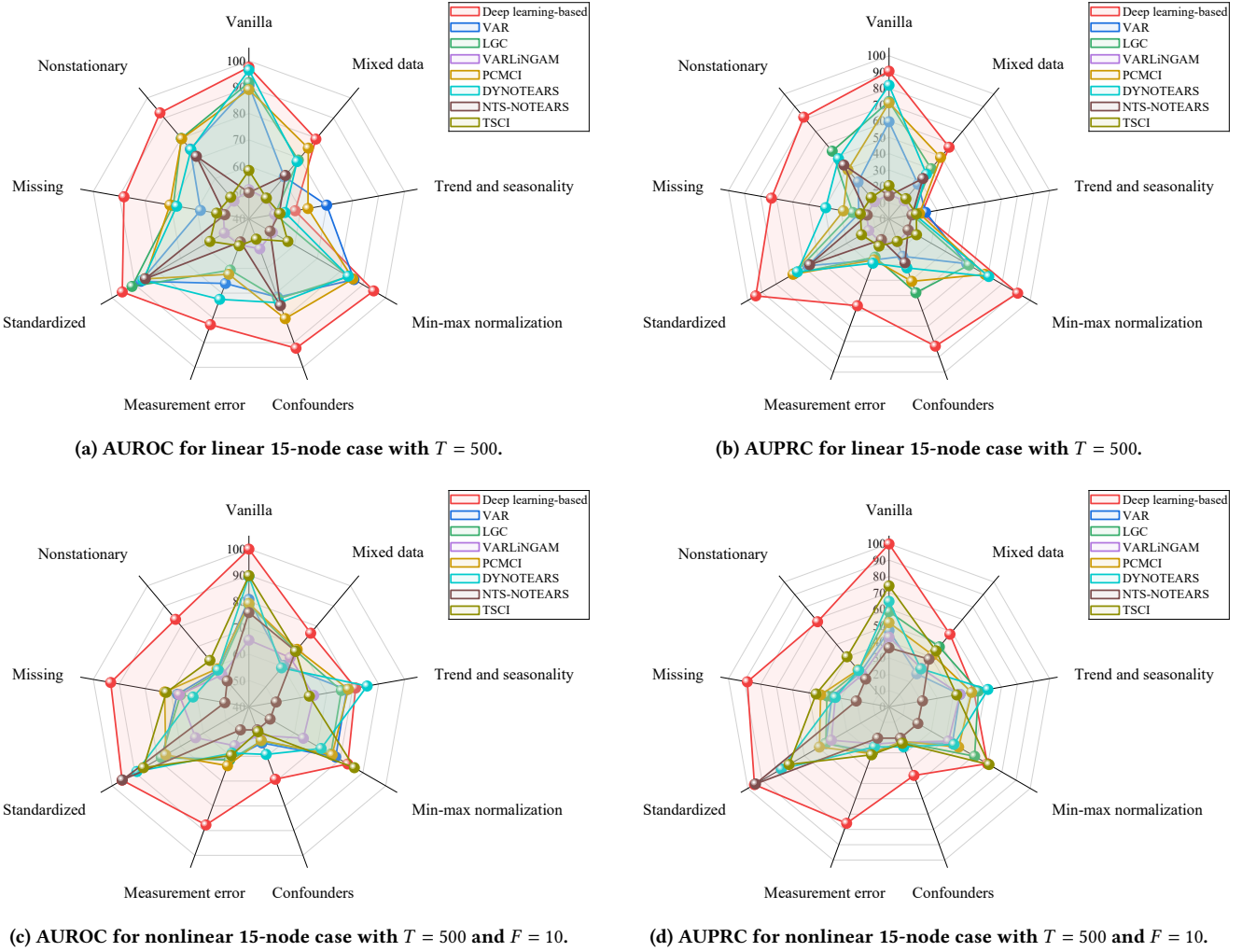


Figure 4: Experimental results under the linear and nonlinear settings across the vanilla scenario and eight assumption violation scenarios. AUROC and AUPRC (the higher the better) are evaluated over 5 trials for the 15-node case with $T = 500$. For the deep learning-based methods, we present only the optimal results.

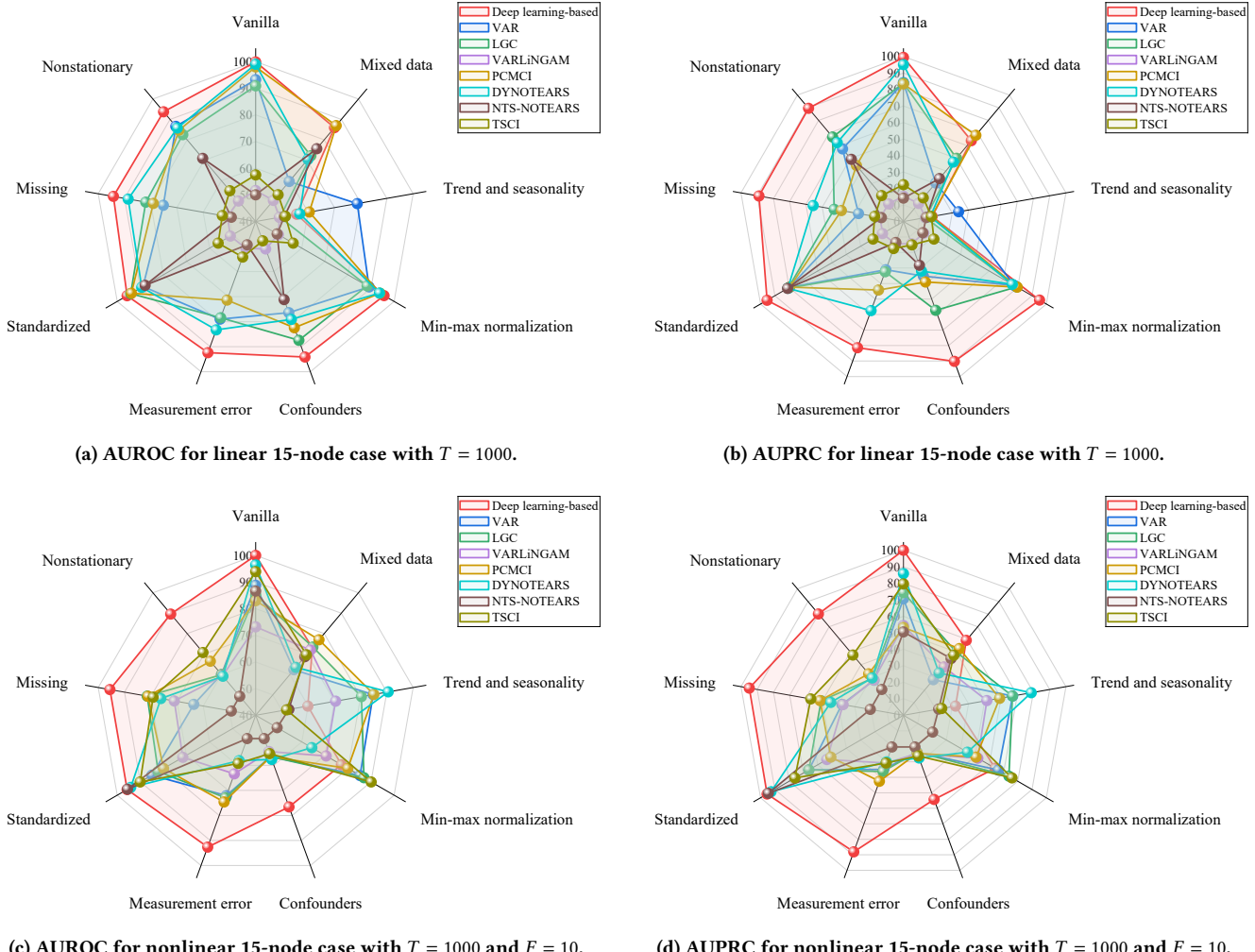


Figure 5: Experimental results under the linear and nonlinear settings across the vanilla scenario and eight assumption violation scenarios. AUROC and AUPRC (the higher the better) are evaluated over 5 trials for the 15-node case with $T = 1000$. For the deep learning-based methods, we present only the optimal results.

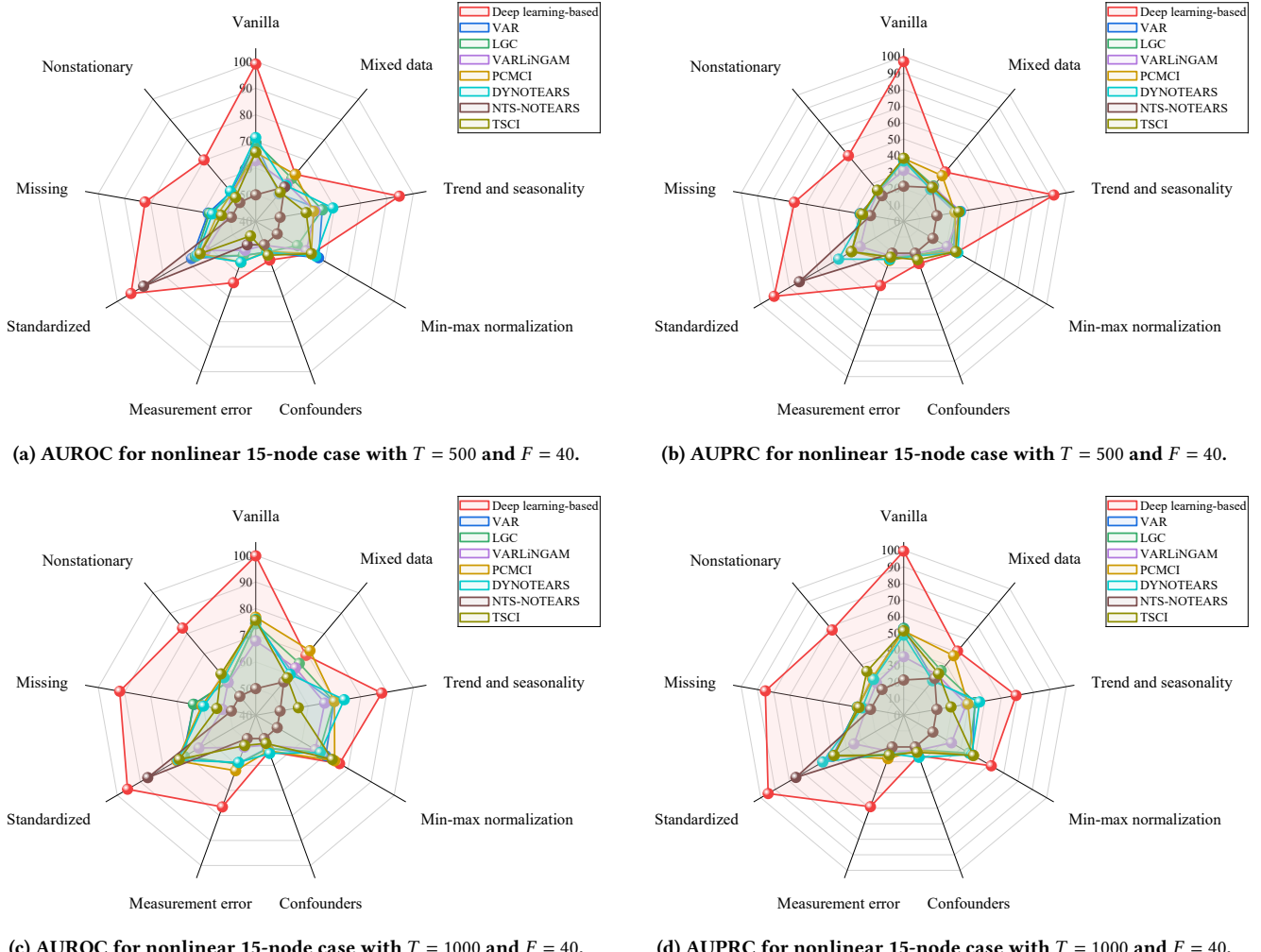


Figure 6: Experimental results under the nonlinear settings across the vanilla scenario and eight assumption violation scenarios. AUROC and AUPRC (the higher the better) are evaluated over 5 trials for the 15-node case with $F = 40$. For the deep learning-based methods, we present only the optimal results.

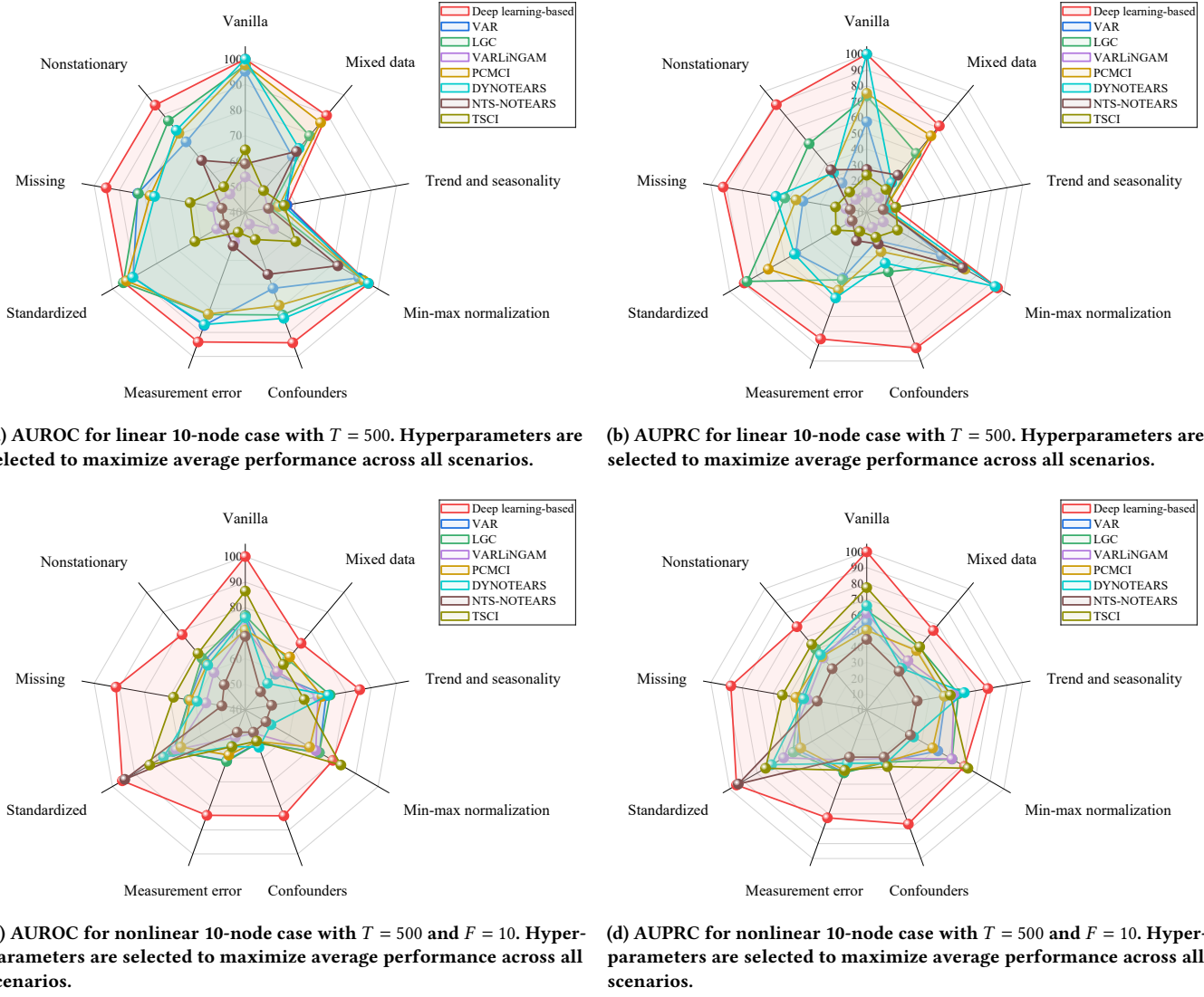


Figure 7: Experimental results under the linear and nonlinear settings across the vanilla scenario and eight assumption violation scenarios. AUROC and AUPRC (the higher the better) are evaluated over 5 trials for the 10-node case with $T = 500$. For the deep learning-based methods, we present only the optimal results. Hyperparameters are selected to maximize average performance across all scenarios.

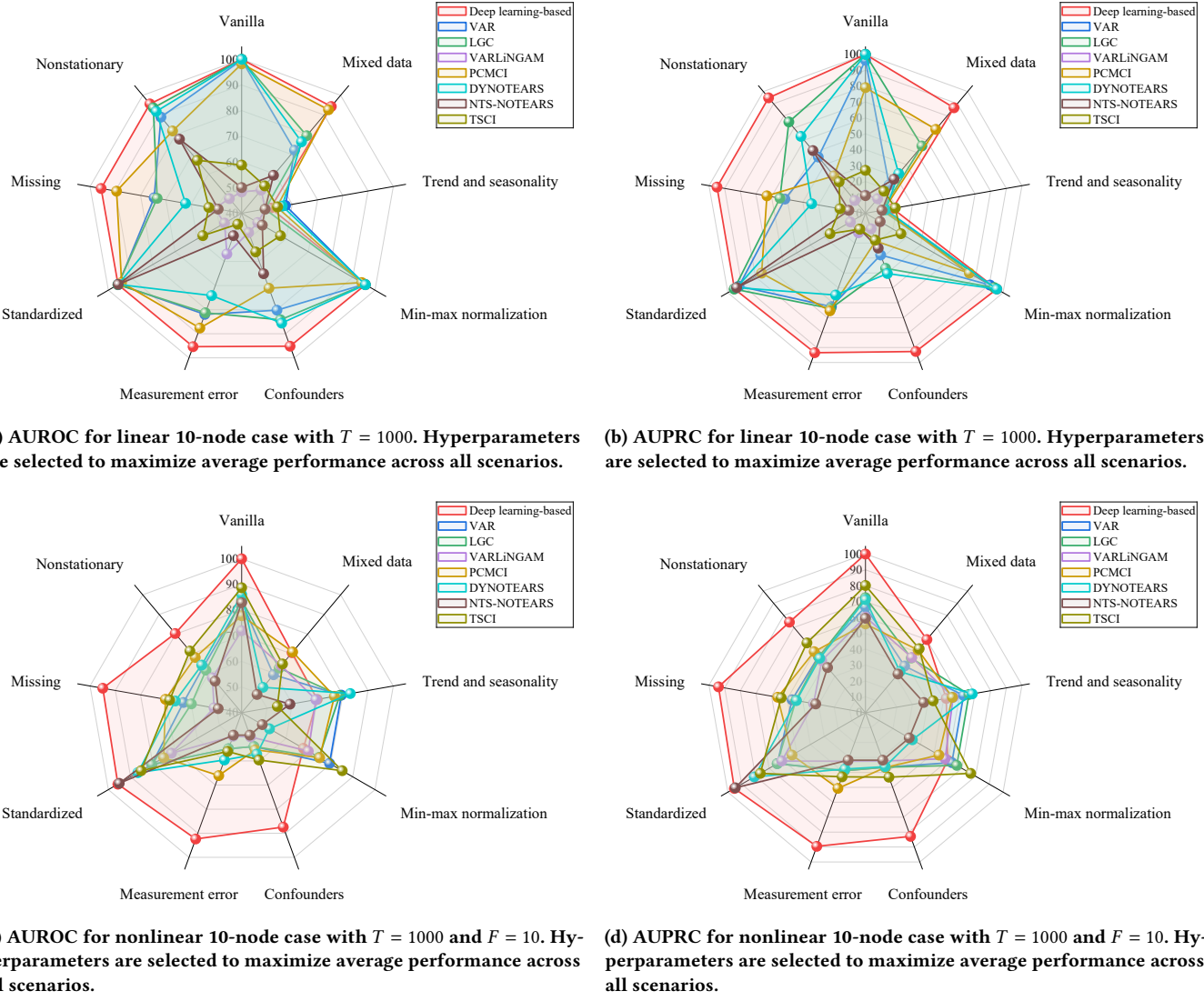
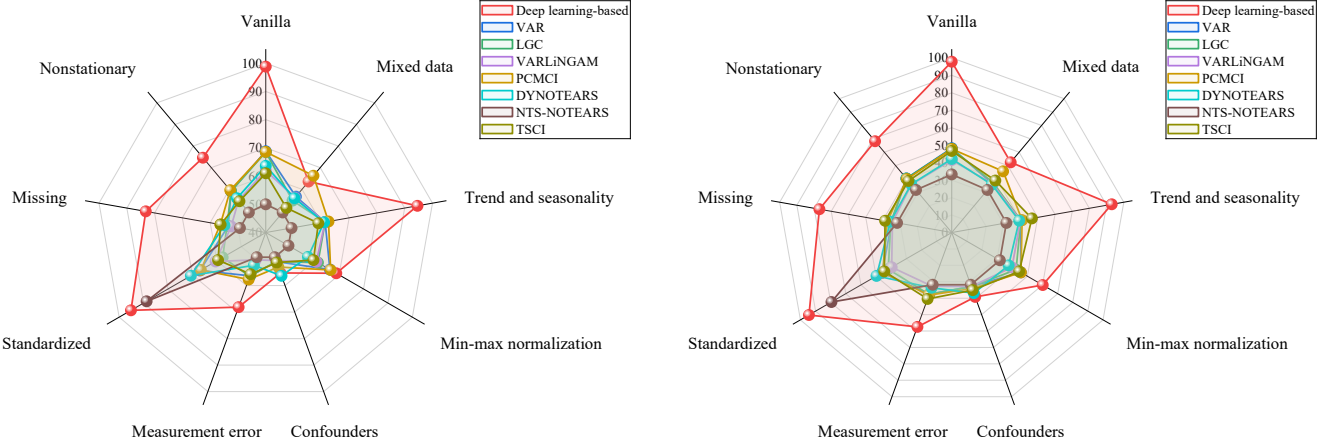
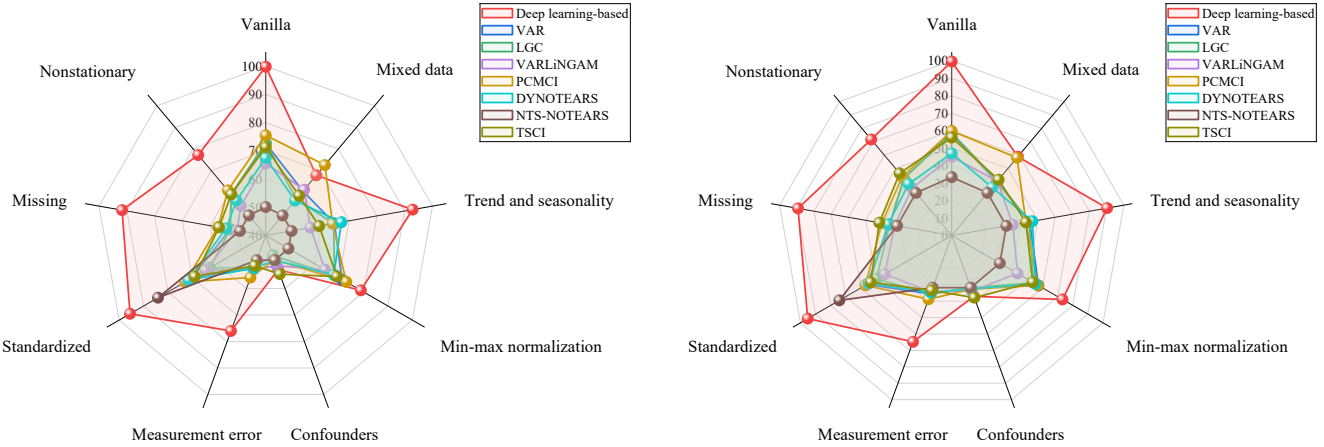


Figure 8: Experimental results under the linear and nonlinear settings across the vanilla scenario and eight assumption violation scenarios. AUROC and AUPRC (the higher the better) are evaluated over 5 trials for the 10-node case with $T = 1000$. For the deep learning-based methods, we present only the optimal results. Hyperparameters are selected to maximize average performance across all scenarios.



(a) AUROC for linear 10-node case with $T = 500$ and $F = 40$. Hyperparameters are selected to maximize average performance across all scenarios.

(b) AUPRC for linear 10-node case with $T = 500$ and $F = 40$. Hyperparameters are selected to maximize average performance across all scenarios.



(c) AUROC for nonlinear 10-node case with $T = 1000$ and $F = 40$. Hyperparameters are selected to maximize average performance across all scenarios.

(d) AUPRC for nonlinear 10-node case with $T = 1000$ and $F = 40$. Hyperparameters are selected to maximize average performance across all scenarios.

Figure 9: Experimental results under the nonlinear settings across the vanilla scenario and eight assumption violation scenarios. AUROC and AUPRC (the higher the better) are evaluated over 5 trials for the 10-node case with $F = 40$. For the deep learning-based methods, we present only the optimal results. Hyperparameters are selected to maximize average performance across all scenarios.

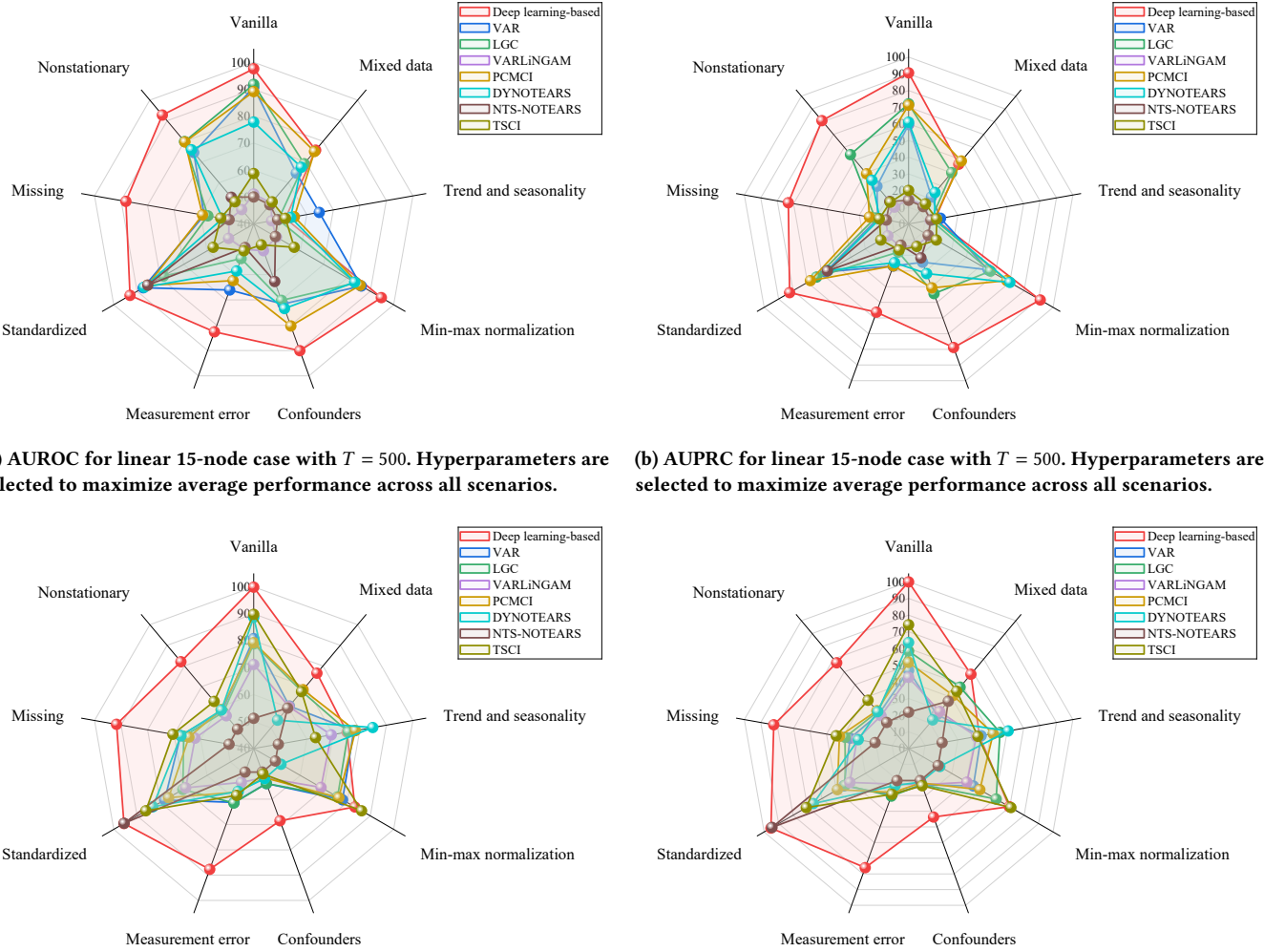
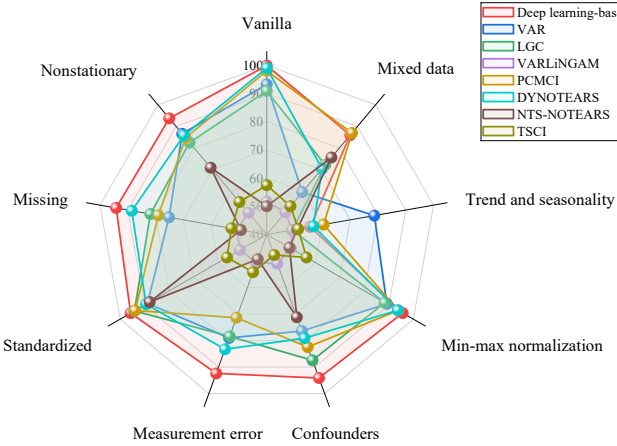
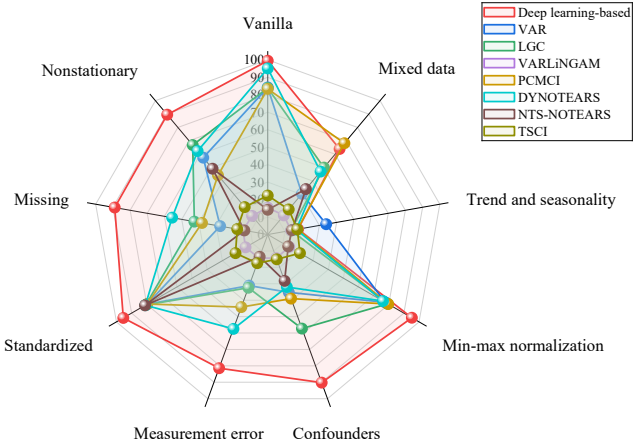


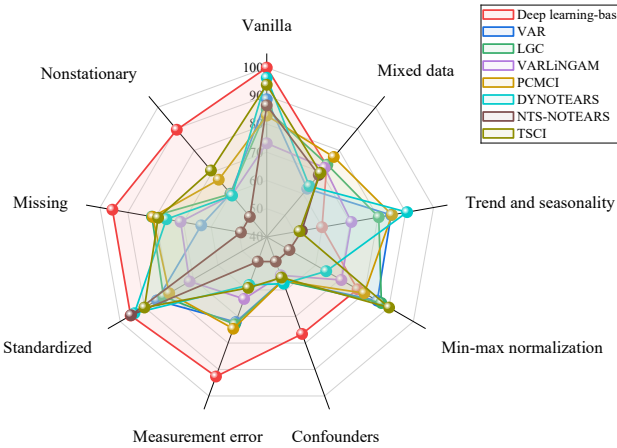
Figure 10: Experimental results under the linear and nonlinear settings across the vanilla scenario and eight assumption violation scenarios. AUROC and AUPRC (the higher the better) are evaluated over 5 trials for the 15-node case with $T = 500$. For the deep learning-based methods, we present only the optimal results. Hyperparameters are selected to maximize average performance across all scenarios.



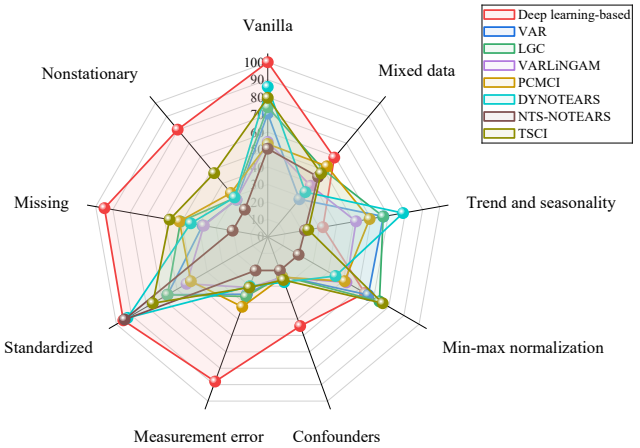
(a) AUROC for linear 15-node case with $T = 1000$. Hyperparameters are selected to maximize average performance across all scenarios.



(b) AUPRC for linear 15-node case with $T = 1000$. Hyperparameters are selected to maximize average performance across all scenarios.

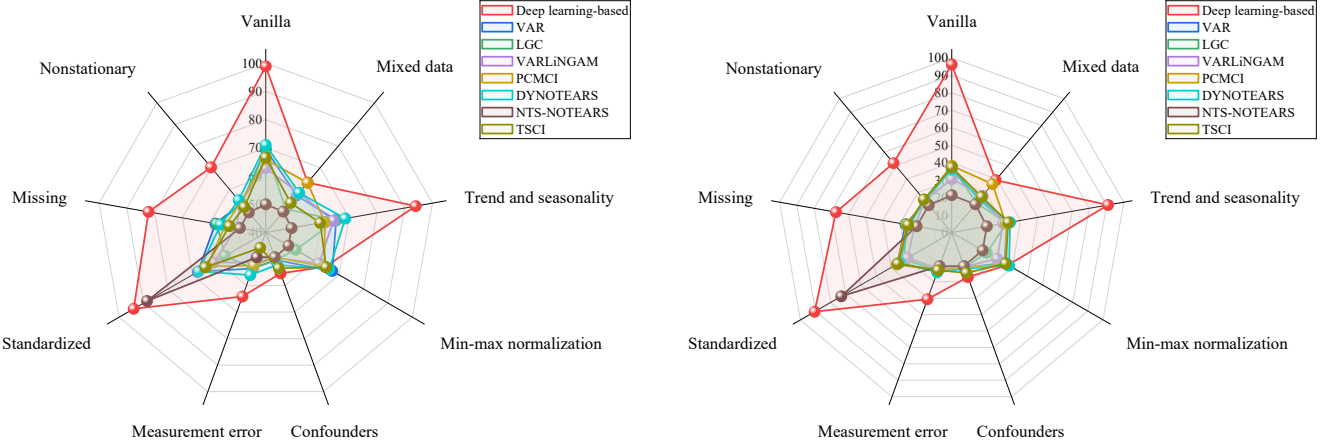


(c) AUROC for nonlinear 15-node case with $T = 1000$ and $F = 10$. Hyperparameters are selected to maximize average performance across all scenarios.



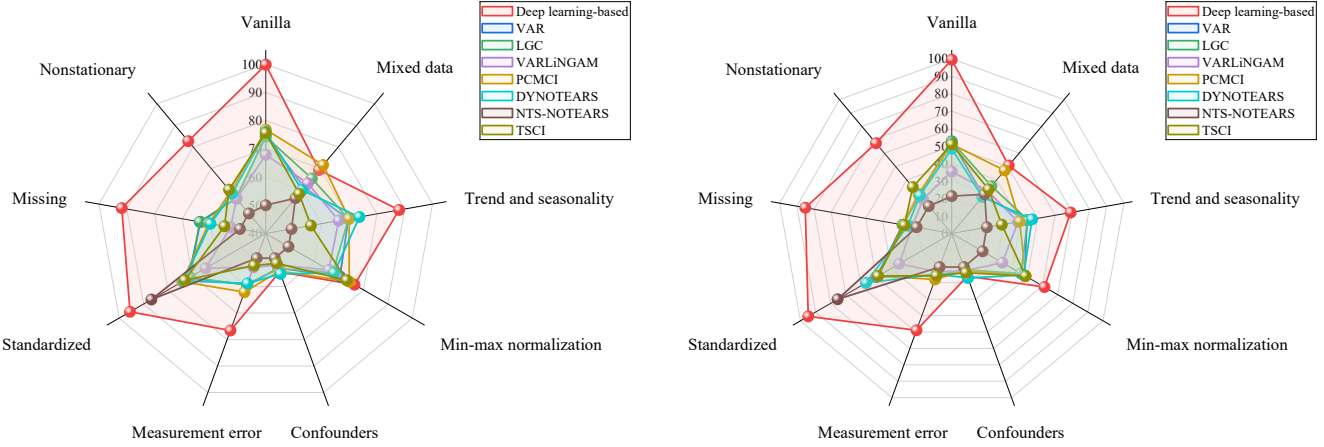
(d) AUPRC for nonlinear 15-node case with $T = 1000$ and $F = 10$. Hyperparameters are selected to maximize average performance across all scenarios.

Figure 11: Experimental results under the linear and nonlinear settings across the vanilla scenario and eight assumption violation scenarios. AUROC and AUPRC (the higher the better) are evaluated over 5 trials for the 15-node case with $T = 1000$. For the deep learning-based methods, we present only the optimal results. Hyperparameters are selected to maximize average performance across all scenarios.



(a) AUROC for nonlinear 15-node case with $T = 500$ and $F = 40$. Hyperparameters are selected to maximize average performance across all scenarios.

(b) AUPRC for nonlinear 15-node case with $T = 500$ and $F = 40$. Hyperparameters are selected to maximize average performance across all scenarios.



(c) AUROC for nonlinear 15-node case with $T = 1000$ and $F = 40$. Hyperparameters are selected to maximize average performance across all scenarios.

(d) AUPRC for nonlinear 15-node case with $T = 1000$ and $F = 40$. Hyperparameters are selected to maximize average performance across all scenarios.

Figure 12: Experimental results under the nonlinear settings across the vanilla scenario and eight assumption violation scenarios. AUROC and AUPRC (the higher the better) are evaluated over 5 trials for the 15-node case with $F = 40$. For the deep learning-based methods, we present only the optimal results. Hyperparameters are selected to maximize average performance across all scenarios.

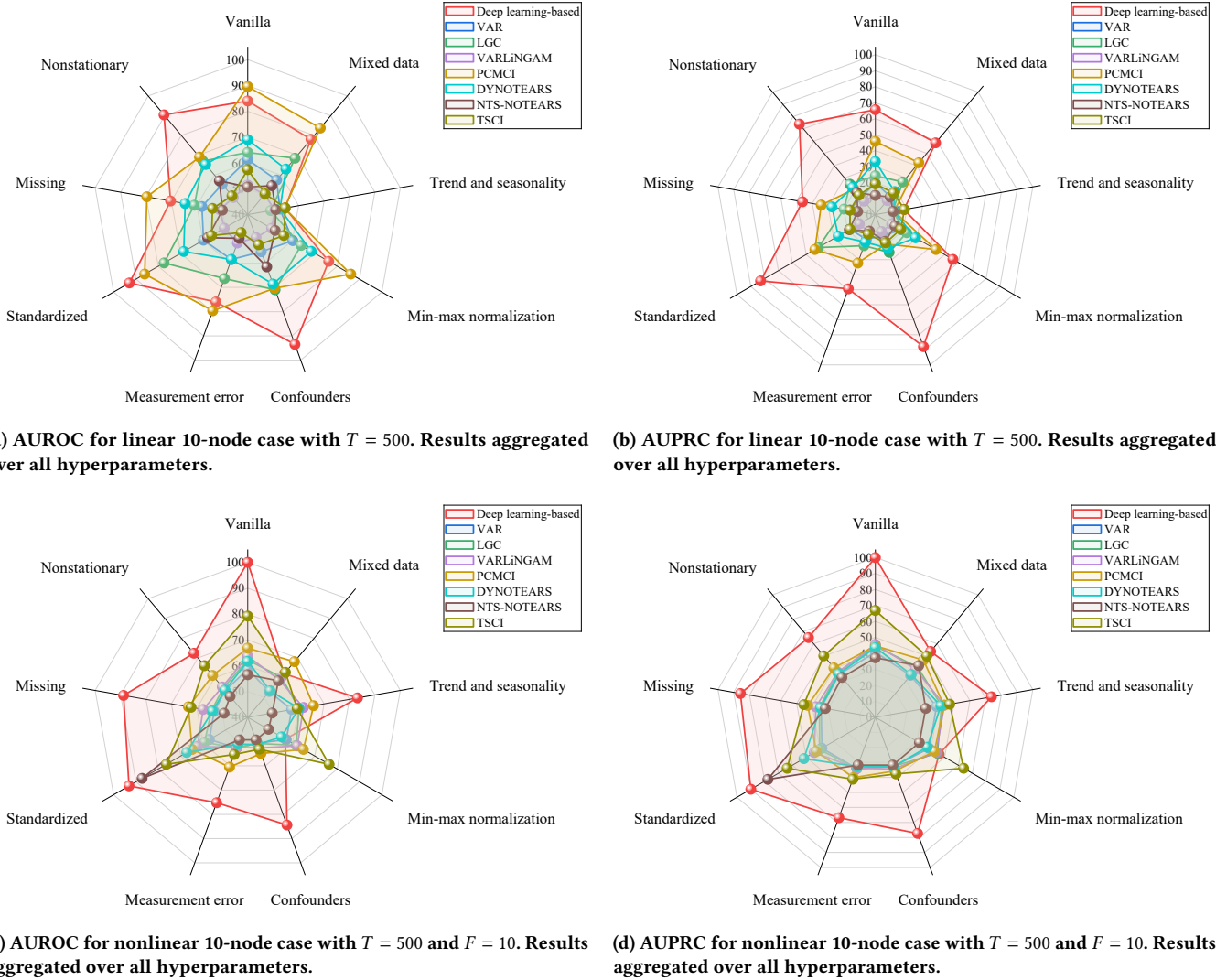


Figure 13: Experimental results under the linear and nonlinear settings across the vanilla scenario and eight assumption violation scenarios. AUROC and AUPRC (the higher the better) are evaluated over 5 trials for the 10-node case with $T = 500$. For the deep learning-based methods, we present only the optimal results. Results aggregated over all hyperparameters.

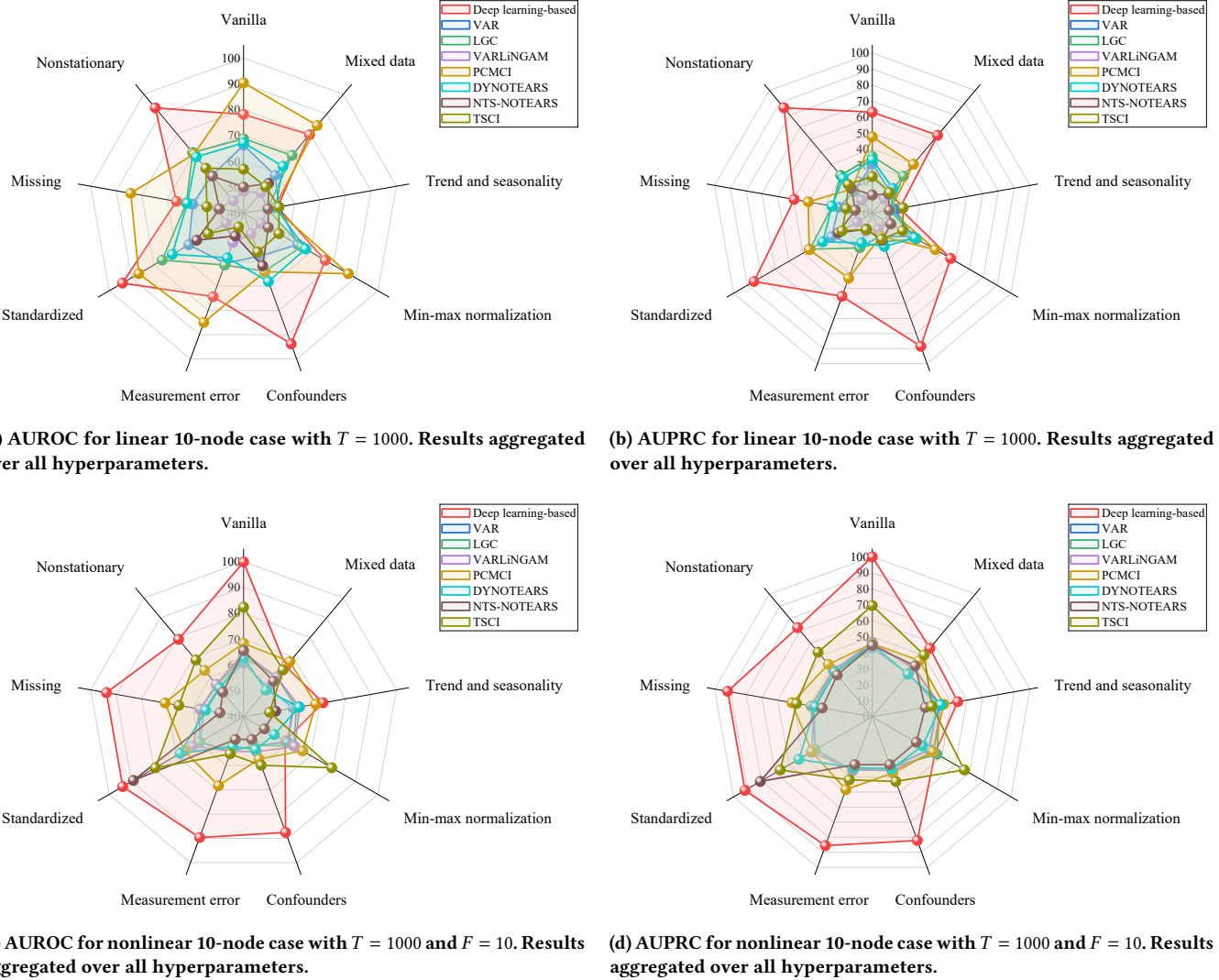
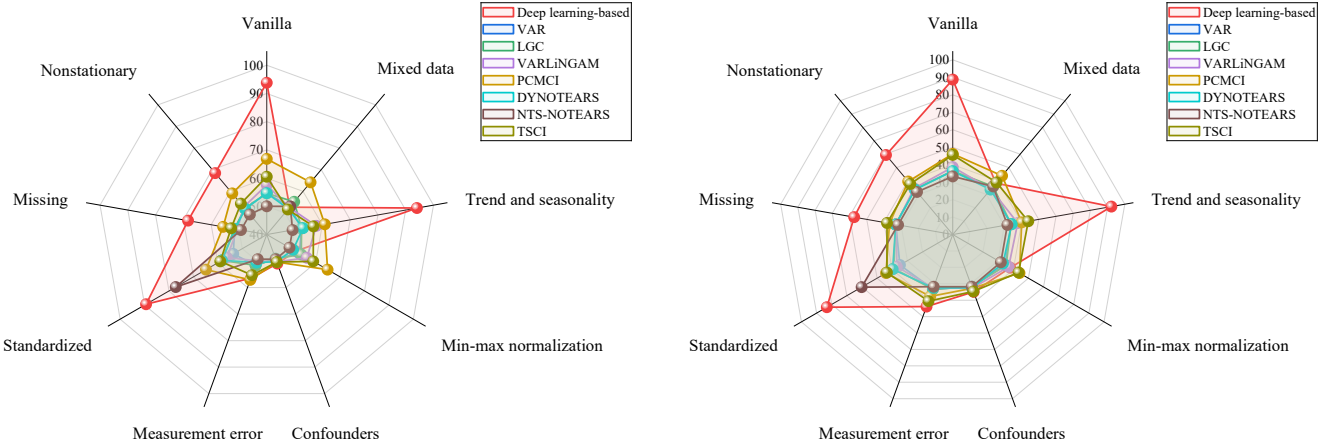
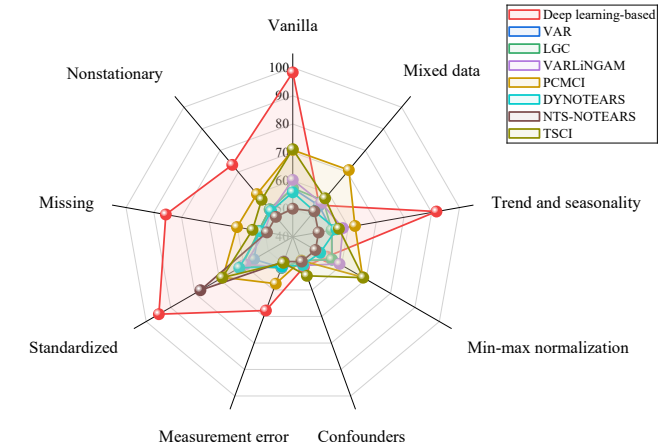


Figure 14: Experimental results under the linear and nonlinear settings across the vanilla scenario and eight assumption violation scenarios. AUROC and AUPRC (the higher the better) are evaluated over 5 trials for the 10-node case with $T = 1000$. For the deep learning-based methods, we present only the optimal results. Results aggregated over all hyperparameters.



(a) AUROC for nonlinear 10-node case with $T = 500$ and $F = 40$. Results aggregated over all hyperparameters.

(b) AUPRC for nonlinear 10-node case with $T = 500$ and $F = 40$. Results aggregated over all hyperparameters.



(c) AUROC for nonlinear 10-node case with $T = 1000$ and $F = 40$. Results aggregated over all hyperparameters.

(d) AUPRC for nonlinear 10-node case with $T = 1000$ and $F = 40$. Results aggregated over all hyperparameters.

Figure 15: Experimental results under the nonlinear settings across the vanilla scenario and eight assumption violation scenarios. AUROC and AUPRC (the higher the better) are evaluated over 5 trials for the 10-node case with $F = 40$. For the deep learning-based methods, we present only the optimal results. Results aggregated over all hyperparameters.

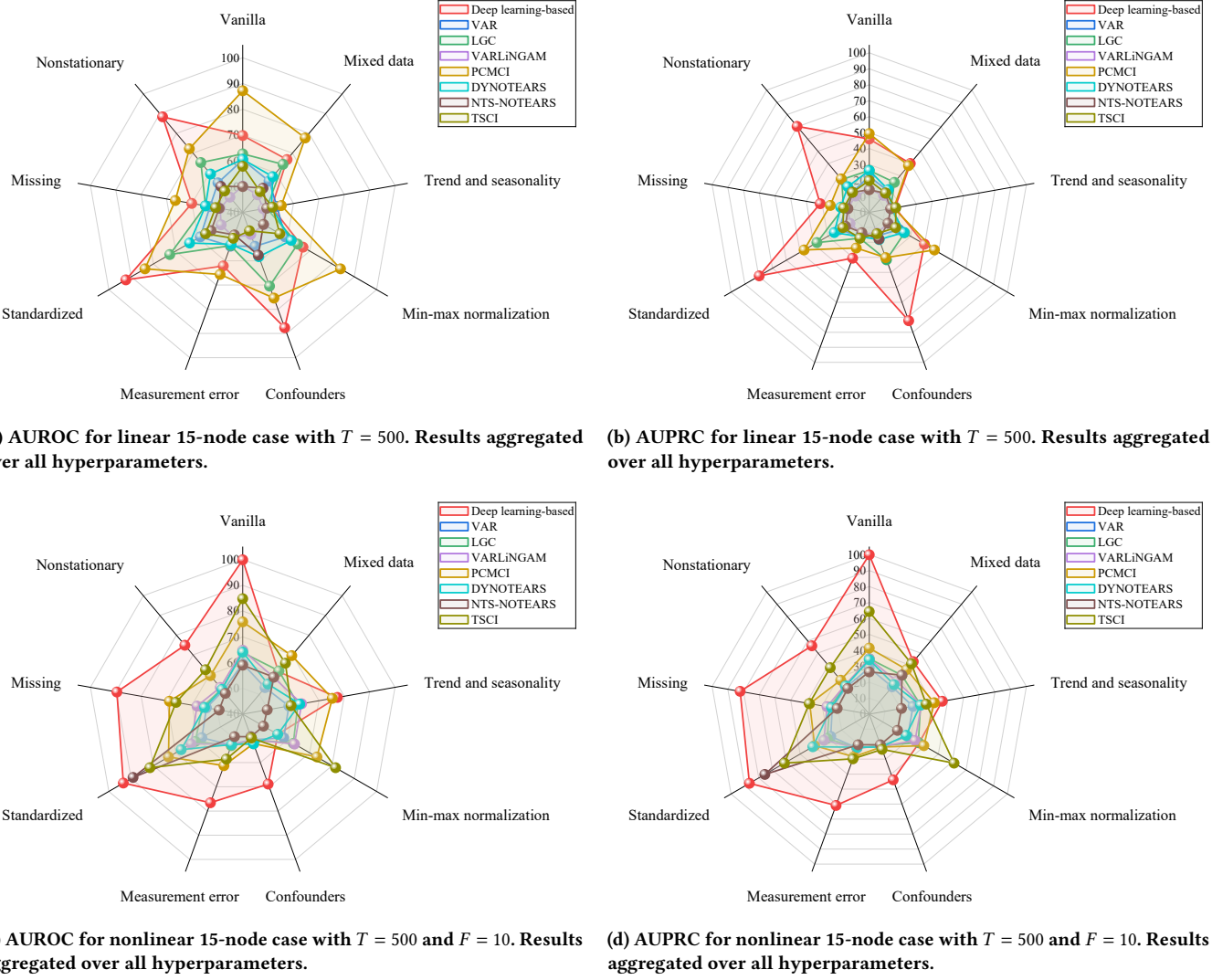


Figure 16: Experimental results under the linear and nonlinear settings across the vanilla scenario and eight assumption violation scenarios. AUROC and AUPRC (the higher the better) are evaluated over 5 trials for the 15-node case with $T = 500$. For the deep learning-based methods, we present only the optimal results. Results aggregated over all hyperparameters.

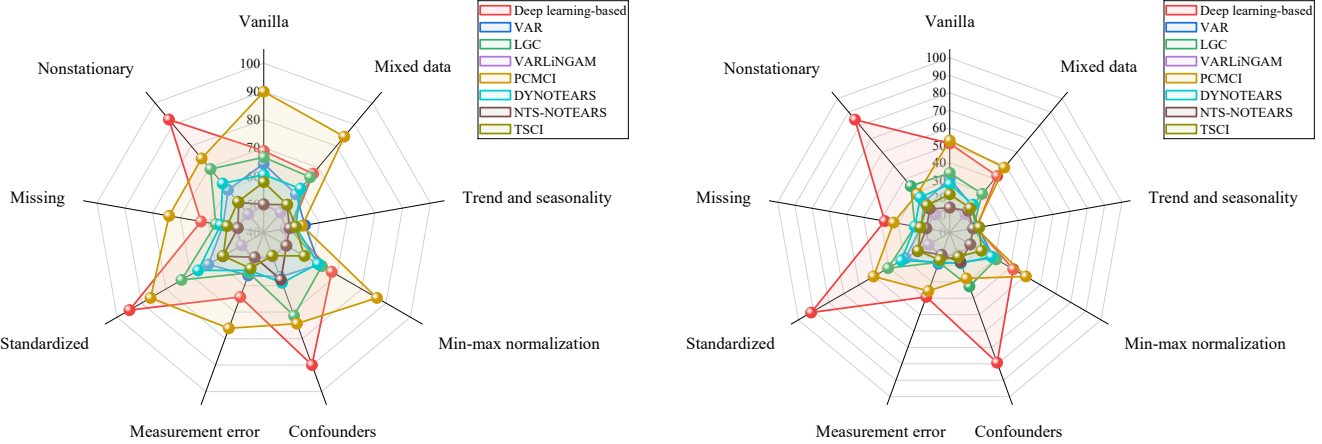
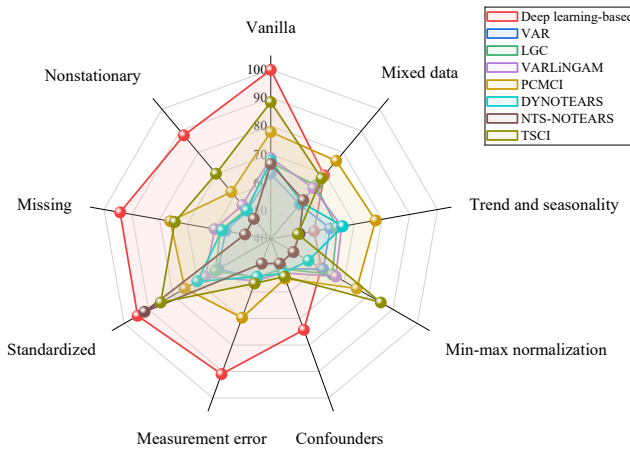
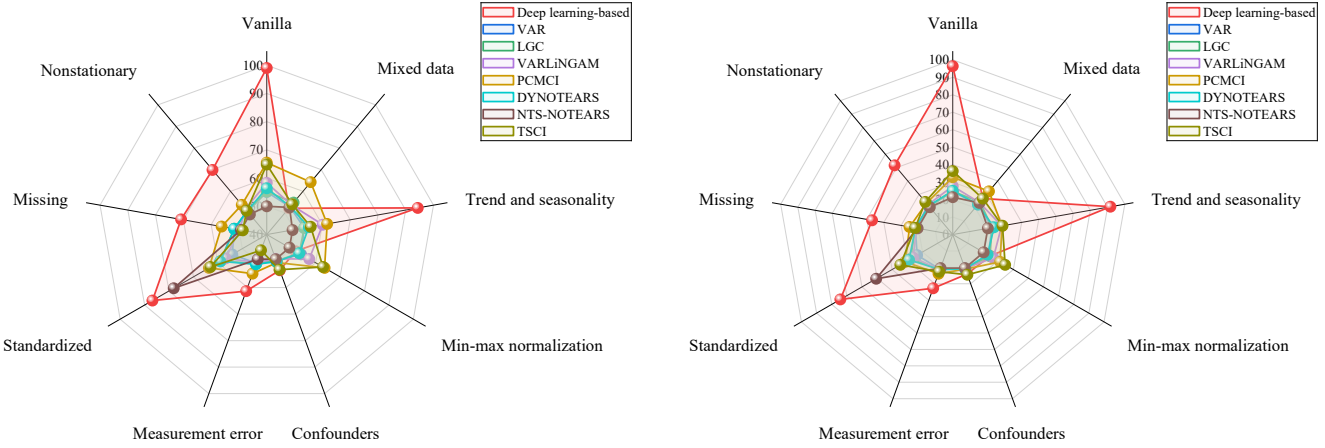
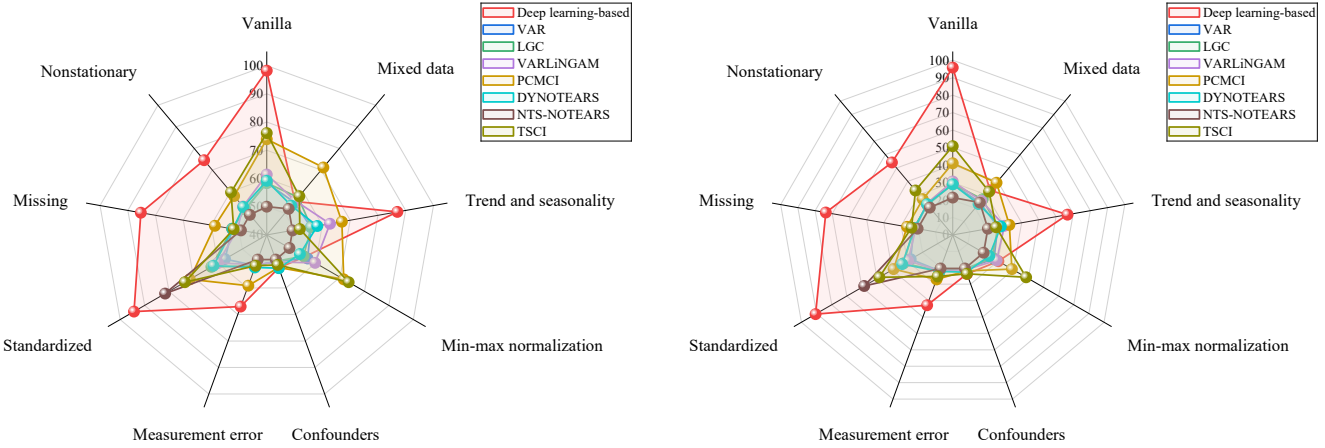
(a) AUROC for linear 15-node case with $T = 1000$. Results aggregated over all hyperparameters.(b) AUPRC for linear 15-node case with $T = 1000$. Results aggregated over all hyperparameters.(c) AUROC for nonlinear 15-node case with $T = 1000$ and $F = 10$. Results aggregated over all hyperparameters.(d) AUPRC for nonlinear 15-node case with $T = 1000$ and $F = 10$. Results aggregated over all hyperparameters.

Figure 17: Experimental results under the linear and nonlinear settings across the vanilla scenario and eight assumption violation scenarios. AUROC and AUPRC (the higher the better) are evaluated over 5 trials for the 15-node case with $T = 1000$. For the deep learning-based methods, we present only the optimal results. Results aggregated over all hyperparameters.



(a) AUROC for nonlinear 15-node case with $T = 500$ and $F = 40$. Results aggregated over all hyperparameters.

(b) AUPRC for nonlinear 15-node case with $T = 500$ and $F = 40$. Results aggregated over all hyperparameters.



(c) AUROC for nonlinear 15-node case with $T = 1000$ and $F = 40$. Results aggregated over all hyperparameters.

(d) AUPRC for nonlinear 15-node case with $T = 1000$ and $F = 40$. Results aggregated over all hyperparameters.

Figure 18: Experimental results under the nonlinear settings across the vanilla scenario and eight assumption violation scenarios. AUROC and AUPRC (the higher the better) are evaluated over 5 trials for the 15-node case with $F = 40$. For the deep learning-based methods, we present only the optimal results. Results aggregated over all hyperparameters.